INFORMATION TO USERS

This manuscript has been reproduced from the microfilm master. UMI films the text directly from the original or copy submitted. Thus, some thesis and dissertation copies are in typewriter face, while others may be from any type of computer printer.

The quality of this reproduction is dependent upon the quality of the copy submitted. Broken or indistinct print, colored or poor quality illustrations and photographs, print bleedthrough, substandard margins, and improper alignment can adversely affect reproduction.

In the unlikely event that the author did not send UMI a complete manuscript and there are missing pages, these will be noted. Also, if unauthorized copyright material had to be removed, a note will indicate the deletion.

Oversize materials (e.g., maps, drawings, charts) are reproduced by sectioning the original, beginning at the upper left-hand corner and continuing from left to right in equal sections with small overlaps.

Photographs included in the original manuscript have been reproduced xerographically in this copy. Higher quality 6" x 9" black and white photographic prints are available for any photographs or illustrations appearing in this copy for an additional charge. Contact UMI directly to order.

Bell & Howell Information and Learning
300 North Zeeb Road, Ann Arbor, MI 48106-1346 USA
800-521-0600

UMI®

Design of an Automatic Landing System for Twin Rotor Vertical Take-Off and Landing Unmanned Air Vehicle

Michael Bole

A Thesis

in

The Department

of

Mechanical Engineering

Presented in Partial Fulfilment of the Requirements
For the Degree of Master of Applied Science at
Concordia University
Montreal, Quebec, Canada

November 1999

ABSTRACT

**Design of an Automatic Landing System
for Twin Rotor Vertical Take-Off and Landing Unmanned Air Vehicle**

Michael T. Bole

With the release of Bombardier's new vertical take-off and landing unmanned air vehicle (VTOL UAV), the company's design team were interested in exploring new ideas for automatically landing the craft. Bombardier established guidelines and limitations on performance in order to ensure the safety of the craft and those individuals in its operating region. The cornerstone of the design revolved around navigation via DGPS data.

Three issues were identified as being paramount to the success of the system. First was the need for an algorithm to locate an appropriate intercept point on the intended flight profile after a position error is found after navigation system switchover from waypoint mode, using GPS, to the more precise autoland mode, which uses DGPS. With the establishment of concrete target points, a corroborative effort between two systems was required to command vehicle motion between two arbitrary points in space. The first system, a trajectory generator, provides an ideal locus of points based on a time law, paying careful attention to the craft's acceleration. The second system involved a controller using the ideal points generated by the trajectory generator to drive the craft. An easily obtainable solution for the controller was required given project scope. The evaluation tool for theory development was a simplified version of Bombardier's overall craft dynamics model for the CL-327.

ACKNOWLEDGEMENTS

The author would like to personally thank Dr. J.V. Svoboda for his guidance, light handedness, judgement, and support and honor him for his good sense of when to employ each. I would also like to thank Dr. K. Foster for his guidance and invaluable suggestions during the early stages of ht project. The author would like to thank Bombardier and their staff who gave me the opportunity to work on the project and for their continuous support. And last, but by no means least, a most sincere thank you goes out to my family, friends, and those I hold dear for their support and understanding throughout.

TABLE OF CONTENTS

LIST OF TABLES AND FIGURES

TABLES:

FIGURES:

LIST OF VARIABLES

D_A Distance covered during segment A

D_B Distance covered during segment B

D_C Distance covered during segment C

D_T Total distance between two points in space

D_{crit} Critical path distance

E_f East position of final point in space

E_I East position of initial point in space

E_{IP} East coordinate of ideal point produced by trajectory generator

E_{int} East coordinate for intercept

E_{LSP} East coordinate of landing set point (LSP)

E_{RP} East coordinate of recovery point (RP)

H_f Height of final point in space

H_I Height of initial point in space

H_{IP} Height of ideal point produced by trajectory generator

H_{int} Height of intercept

H_{LSP} Height of landing set point (LSP)

H_{RP} Height of recovery point (RP)

H_{SV} Height of SV

M Amplitude of trigonometric function

M_A Amplitude of acceleration profile for segment A

M_C Amplitude of acceleration profile for segment C

N_f North position of final point in space

N_I North position of initial point in space

N_{IP} North coordinate of ideal point produced by trajectory generator

N_{int} North coordinate for intercept

N_{LSP} North coordinate of landing set point (LSP)

N_{RP} North coordinate of recovery point (RP)

R_{SV} Radius of SV

$R_Y^{-\gamma_{GS}}$ Rotation about y-axis by angle of $-\gamma_{GS}$

$R_Z^{-\alpha_{GS}}$ Rotation about the z-axis by angle $-\alpha_{GS}$

T Period of trigonometric function

T^{RP} Transformation of RP to origin of inertial system

V_H Horizontal component of peak velocity

V_P The peak ideal, total velocity during trajectory algorithm

$V_{P,max}$ The maximum peak total velocity commanded by trajectory generator

V_V Vertical component of peak velocity

$V_{V,max}$ Maximum value for the vertical component of the peak velocity

a Ideal acceleration of craft

$a_{P,A}$ Peak acceleration reached in segment A

$a_{P,C}$ Peak acceleration reached in segment C

$a_{P,A,max}$ Maximum peak combined acceleration for segment A

d Ideal displacement of craft

d_I Ideal total displacement of craft since trajectory generation began

est_{CPT} East displacement of intercept path

h_I Ideal horizontal displacement of craft since trajectory generation began

n Scaling factor

nor_{CPT} North displacement of intercept path

r_1 Horizontal distance between the RP and the intercept (method 1)

r_3 Horizontal distance between UAV and RP (method 3)

t Instantaneous time since trajectory generation began

t_A Amount of time allotted to perform segment A

$t_{A,max}$ Maximum time allotted to complete segment A

t_B Amount of time allotted to perform segment B

t_C Amount of time allotted to perform segment C

$t_{C,max}$ Maximum time allotted to complete segment C

$t_{s,A}$ Time at which segment A begins.

$t_{s,B}$ Time at which segment B begins.

$t_{s,C}$ Time at which segment C begins.

$t_{s,D}$ Time at which segment D begins.

v Ideal velocity of craft

x X component of transformed UAV location

z Z component of transformed UAV location

y Y component of transformed UAV location

Λ $-\alpha_{GS}$

Γ $-\gamma_{GS}$

α Generalised bearing angle

α_{CPT} Bearing angle of path between initial point and intercept point

α_{GS} GS bearing angle

ϕ Angle between UAV and the plane perpendicular to GS

γ Generalised descent angle

γ_{CPT} Descent angle of path between initial point and intercept point

γ_{GS} GS descent angle

$\gamma_{GS,crit}$ Critical glideslope angle

ω Frequency of trigonometric function

ω_A Frequency of profile for segment A

LIST OF ACRONYMS AND ABBREVIATIONS

ARINC	Aeronautical Radio Incorporated
BARU	Barometric Altitude Reference Unit
AV	Air Vehicle
CAT III	Category III Instrument Landing System Conditions
CEP	Circular Error Probable
CP	Central Plane
DGPS	Differential Global Positioning System
FCS	Flight Control System
FLIR	Forward Looking Infrared
GAS	Glideslope Aligned System
GNC	Guidance Navigation and Control
GPS	Global Positioning System
GS	Glideslope
HAS	Horizon Aligned System
HP	Horsepower
ILS	Instrument Landing System
INF	Integrated Navigation Filter
IR	Infrared
LP	Landing Point
LSP	Landing Set Point
MAVUS	Marine VTOL UAV System
NCP	Navigation Co-Processor

PC	Personal Computer
RP	Recovery Point
SV	Safety Volume
SVB	Safety Volume Boundary
UAV	Unmanned Air vehicle
VTOL	Vertical Take-Off and Landing

1.0 Introduction

The capabilities of air vehicles are many and continue to increase as the years pass. Since the first man flew in a hot air balloon in 1783, humankind has used this medium of transport for various ends. At the time, there were fears that venturing into the upper atmosphere would prove fatal. To dispel these fears, the first flight was crewed by domesticated animals and so the first flight in a balloon was unmanned [1]. Since these humble beginnings, the idea of unmanned flight has come a long way. The concept became very appealing for military use. Unmanned air vehicles (UAVs) or drones as they as they are sometimes called, were seen to have great potential for reconnaissance and surveillance for military applications [2]. This was confirmed and subsequently become accepted after the experiences with UAVs in the Desert Storm Conflict proved them to be useful and beneficial [3]. Much research and development has been performed in this field because of the promise the UAVs showed. Some of the applications for which UAVs can be used in both the military and non-military environment are summarized in *table 1.1*. All these tasks and more can be performed without putting at risk the lives of personnel.

MILITARY	CIVILIAN
Increased situational awareness to scouting teams	Rescue and maintenance missions on ships and off-shore oil rigs
Surveillance	Mountain and traffic rescue operations
Targeting	Environmental investigations
Communications relay	Other life survival operations
Damage assessment	Border patrol
Mine detection	Drug enforcement operations

Table 1.1 – Uses for UAVs [2] [4] [5] [6]

Though the bulk of the work performed in the field of UAVs was done with military interests in mind, the current reduction in military budgets requires exploration of other markets. For this reason, many units are being redesigned for non-military and civil use. The civilian applications are numerous and are listed in *table 1.1*. They are designed to be safe, simple, and easy to operate [4]. During the development of these units, special emphasis is put on uncomplicated handling during the operation, the reduction of personnel, and diminishing the workload of the remaining personnel. For this reason, full automation is the manner in which to proceed [2]. Today's units must be capable of various flight modes which must include automatic unaided take-off and landing, and automatic flight control throughout the mission. More and more, mission requirements demand that the crafts be capable of vertical take-off and landings (VTOL) [5]. The performance characteristics of such craft are somewhat different as compared to fixed-wing aircraft characteristics. Most importantly, designers are challenged with such factors as the helicopter's slow speed of approach relative to head, tail, and crosswinds and the craft's ability to decelerate during final approach [7]. These are important issues which require significant attention.

This isn't to say that the construction and development of VTOL UAVs is something left only to large, resource-rich companies, in fact quite the opposite is true. University students frequently design and construct such units for use in inter-university design competitions [8] [9]. An example of this is the International Aerial Robotics Competition sponsored by the Association for Unmanned Vehicle Systems. In this competition, the craft must perform a variety of tasks including locating objects,

identification of these objects, cope with various obstructions and shields to signals, and perform all these tasks autonomously [10].

Since 1959, first Canadair and now Bombardier has been in the business of the design and production of VTOL UAVs. Many makes and models have been produced over the years and the knowledge gained from these programs has culminated in the production of the CL-327. The specifics of the craft will be explained later, but suffice it to say that this new version has been redesigned to be bigger with extended performance capabilities and range. One of the most important advancements with this new model has been the addition of GPS/DGPS to the navigation unit. Many similarities exist between this and the previous versions, but the dynamics of the craft has been changed. To accompany these changes and upgrades, Bombardier was interested in an autoland system using predominantly DGPS information and so explains the reason for this work: the design of an autoland system for the Bombardier CL-327.

1.1 Reasoning in Favor of an Autoland System

Automatic landing systems or autolands have existed for quite some time. The reasoning in favor of such a system is very convincing especially when the craft is a UAV. The critical phases of a drone mission are take-off and landing [2]. In between, the flight is quite simple and straightforward. If an automatic take-off and landing system is put in place to perform these two critical tasks, then there is no need for a pilot to be present to operate the craft. In fact, the operator acts more as a mission manager, monitoring mission progress and initiating high level commands as opposed to actually flying the craft. Some examples of these high level commands would be take-off, cruise, return home, and autoland amongst others. Automation of this level relieves the operator

from "joy stick" flying and maximizes the time available for imagery evaluation, and mission planning and execution [4]. Another important reason is that in many instances, even when a pilot is flying the vehicle, take-off and landings are performed at night and under all weather conditions [11]. As the task is predominantly dependant on visual cues, over time, this tends to overtax service personnel which can subsequently lead to errors. For a UAV to be deemed successful, the user must have a high amount of confidence in its reliable operation, especially during the take-off and landing phases [7] [11]. Given that UAV operations aim for a very high level of accuracy and safety, autoland systems are therefore a necessity. Consequently, with a robust autoland and associated systems, the vehicle can give this kind of assurances to those involved.

1.2 Other UAV offerings

Though Bombardier has a long history in the production of VTOL UAVs, they are not alone in the market. Other companies, the likes of who include Dornier, Sikorsky, and Bell Textron all have offerings which are similar to the CL-327. There are also a variety of configurations which can be used for a VTOL UAV. These configurations include the coaxial exposed rotor, the coaxial shrouded rotor, the Hiller flying platform, and tiltrotors [8]. To illustrate the variations available, the offerings from Sikorsky and Bell Textron will be overviewed.

The Sikorsky Cypher consists of a shrouded, coaxial, four bladed rotor VTOL UAV. It was the first of its kind with regards to employing shrouded rotor technology for use in a UAV and was therefore a proof-of-concept vehicle. The airframe itself is used to shroud the rotor (*figure 1.1*). Such a design is inherently safer than exposed rotor configurations by virtue of the elimination of possible contact between rotors and

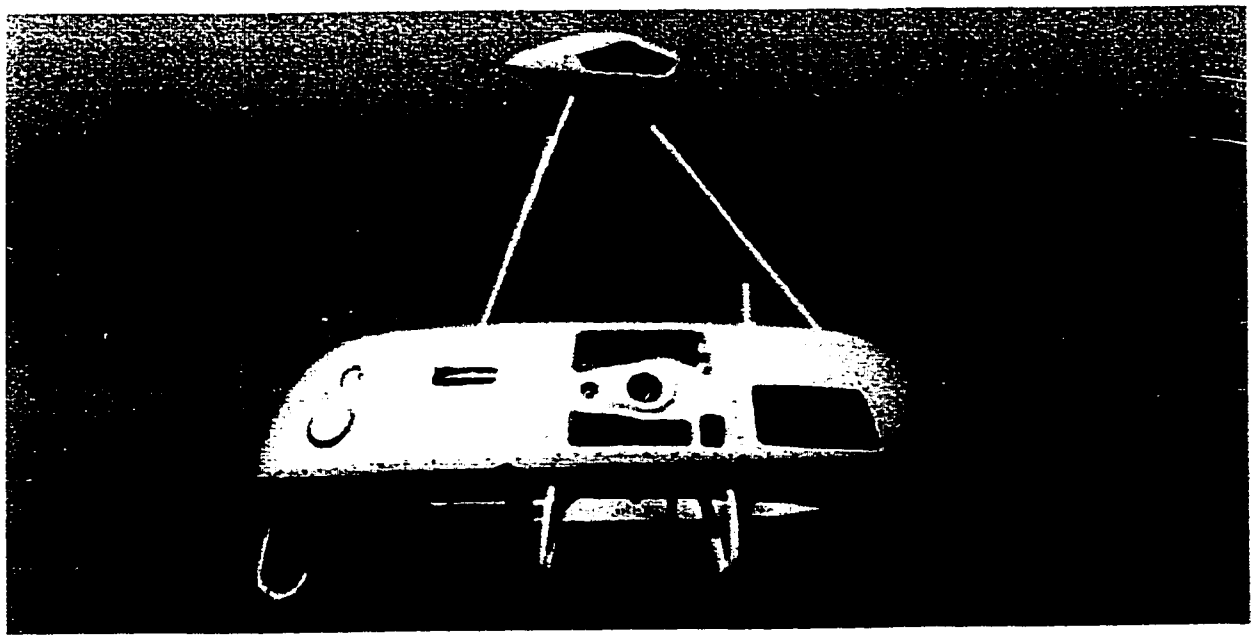

Figure 1.1 – Sikorsky Cypher [4]

obstacles or personnel. In conjunction with this, the chance of blade strikes in confined areas is also reduced. By virtue of the craft being a coaxial counter rotating system, torque equilibrium and a means of directional control are intrinsic. It is portable and requires no special launch or recovery equipment. In addition to this, at 6.5 feet in diameter, its compact size provides a low observable signature or footprint for increased aircraft survivability in high threat environments [12]. The payloads it carries include electro-optic, infrared, and electronic countermeasures equipment. Command and control systems consist of a ground control station, data uplink for transmission of control commands, and downlink from transmission of vehicle status and payload information to the ground station. It is capable of performing missions autonomously to further reduce operator input requirements and of transitioning between various flight modes. It is also important to note that the vehicle does use GPS/DGPS technology to some extent in navigation [4].

The Bell Textron Eagle Eye was designed for the Navy. It required a VTOL vehicle which had the capacity to be launched and recovered form the decks of small ships. What makes this vehicle different is that it uses a tiltrotor approach to perform such tasks [3]. Its intrinsic capacity to fly fast, the advantage of wing-born lift to drag ratios for the endurance segment, and the relative ease with which low speed maneuvers and recovery can be accomplished are all advantages of this design [13]. The propulsion system for the vehicle consists of two three bladed gimballed rotors, mounted on wingtip tilting pylons (*figure 1.2*). The pylons have a range of 0° (airplane mode) to 93° which represents the maximum aft tilt during helicopter mode. In airplane mode, the rotor

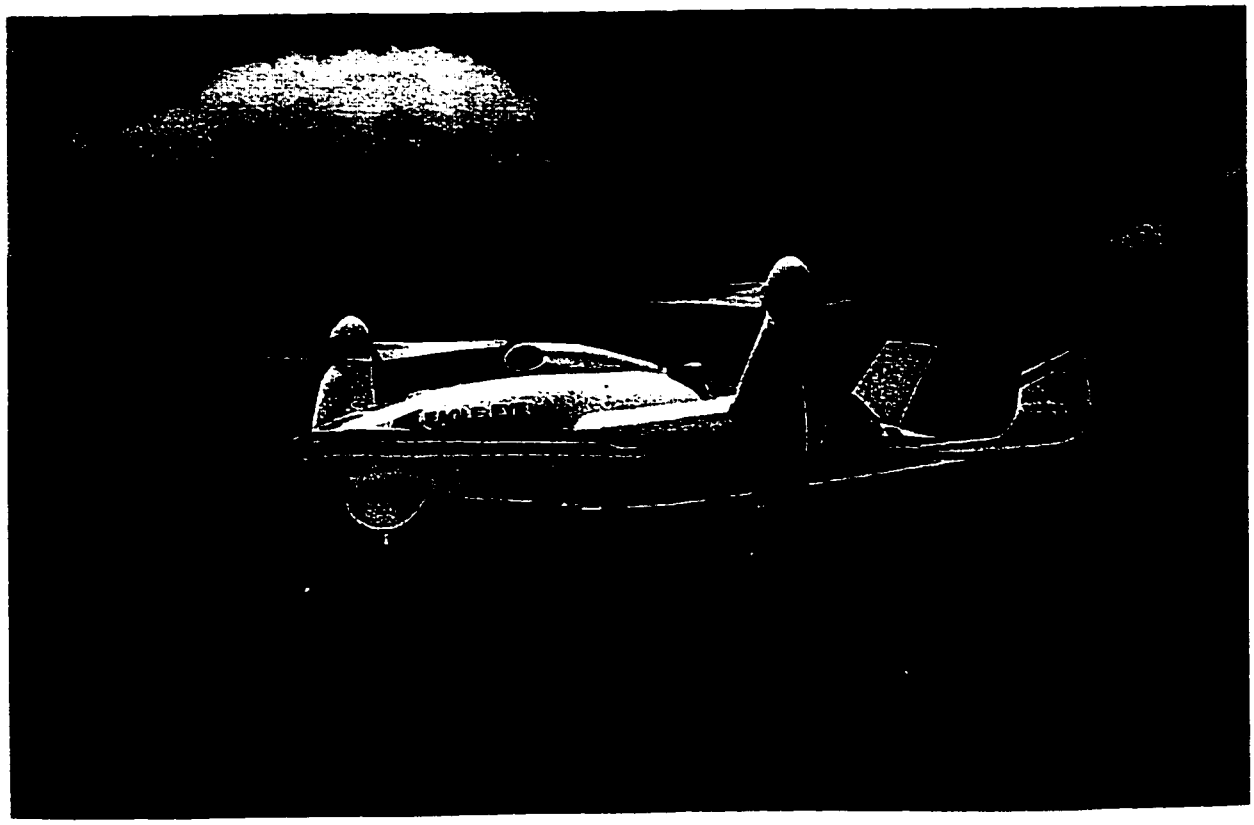

Figure 1.2 – Bell Textron Eagle Eye [3]

speed can be reduced from 100% to 80% output to improve rotor blade efficiency and reduce aerodynamic loads in forward flight, thus providing further fuel saving. As with the offering from Sikorsky, the Eagle Eye tiltrotor craft also uses GPS in its navigation system [3].

1.3 Early UAVs from Bombardier

Bombardier has been involved in the creation of VTOL UAVs since 1959. In that time they have gained much knowledge and expertise in the field. Throughout the years, it has been determined that drones using a coaxial helicopter arrangement provide the best solution for landing on small platforms or enclosed spaces [2]. The VTOL platform is maneuverable, controllable, and efficient in hover [4]. The use of contra-rotating propellers allows for rapid yaw control as well as canceling torque problems inherent with a single fan design [8]. These facts and findings only solidify the design concept which Bombardier has been using for years in its program. A brief history of the various stages of the Bombardier program will be detailed here from its inception in 1959 through to the CL-227, the predecessor to the CL-327.

The Dynacopter was the first system designed. It was begun after a section chief was asked to critique a coaxial, counter rotating, tethered vehicle which the Canadian military was considering. He made some suggestions and improvements and Canadair, now part of Bombardier, subsequently came up with their own vehicle, the Dynacopter. The vehicle's design phase lasted from 1965-67. Its concept was based on a very small, exposed coaxial rotor, lifting platform equipped with real time sensors to meet surveillance needs of ground personnel. It could cover a frontage of 19 km to a penetration depth into enemy territory of 13 km. It was the first of its kind which could

operate untethered. The final version of the craft stood 5 feet 8 inches high and tipped the scales at 140 lbs. It was composed of four sections which in descending order included the engine (15 HP), lift/control section, electrical, and the sensor section which was comprised of a television camera, stabilized platform, and data transmitter. Refinements of the craft led to new studies in vehicle configurations. The final version of the craft is shown in *figure 1.3* [14].

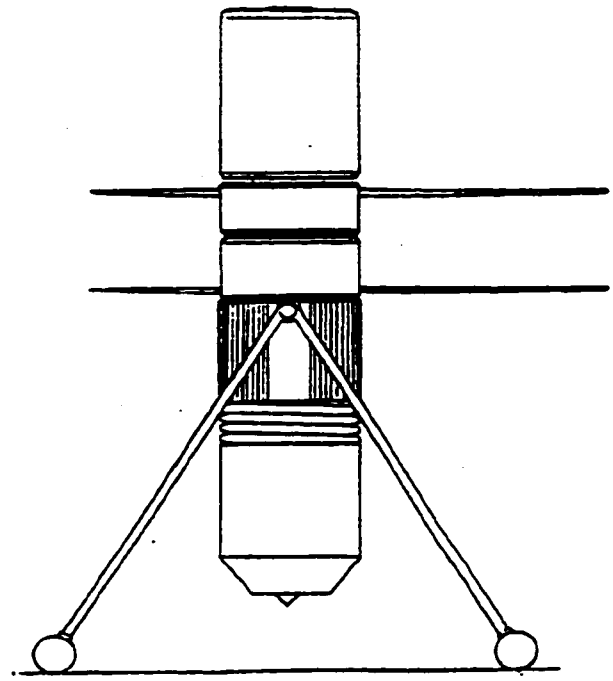

Figure 1.3 – Dynacopter (1965-67) [14]

The CL-265 was the craft which succeeded the Dynacopter in the Canadair stables. It was designed and spent most of its life being tested in the windtunnel at the National Aeronautical Establishment in Ottawa. It was in this model that the configuration changed from two bladed to three bladed. This craft was essentially used as a feasibility study which led to the CL-227 [14].

The CL-227 is the predecessor to the CL-327. It went through several stages before a final version was decided upon. First there was proof-of-concept, then the surveillance and target acquisition phase, and finally the establishment of stability and flight maneuver envelopes. Initially it used parts retrieved from the CL-265 program [14]. Several engines were tested including a 20 HP Wankel rotary before a 32 HP gas turbine was decided upon. The engine was mounted with the shaft axis vertical which allowed for the air intake to be located on the bottom and the exhaust on the top. This provided a significant reduction to craft's IR signature. Like the previous versions, it used two counter-rotating exposed rotors and maintained the three blades per rotor that was used with the CL-265 [15].

The CL-227 was the first model to use three interchangeable modules. These consisted of power, propeller, and the payload interface module (*figure 1.4*). They were designed to have quick interchangeability to suit mission or maintenance requirements. The upper sphere contained the engine and fuel tank. The waist of the craft held the

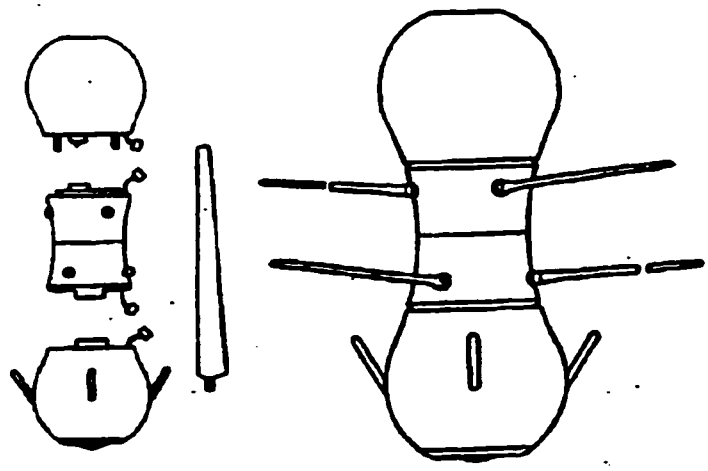

Figure 1.4 – CL-227 Phase I: Modular concept [14]

computers and control mechanisms for the rotors and propeller blades while the lower sphere housed the payload, elements of the command and control data link system, and avionics and power support systems. There were a variety of payloads which could be interchanged into the air vehicle as a function of a tactical mission. Amongst other things, it could include Texas Instruments' forward looking infrared (FLIR) sensor which allowed for day or night operations, real time video systems, radio communications relay, electronic warfare jamming, and decoy packages [14] [15].

The CL-227 made extensive use of composite materials and this in conjunction with its shape, made it one of the first uses of stealth design. The first Phase I tethered flight took place in August of 1978 while the first free flight was conducted in March 1980. In the early 1990's, program MAVUS was established which stood for maritime

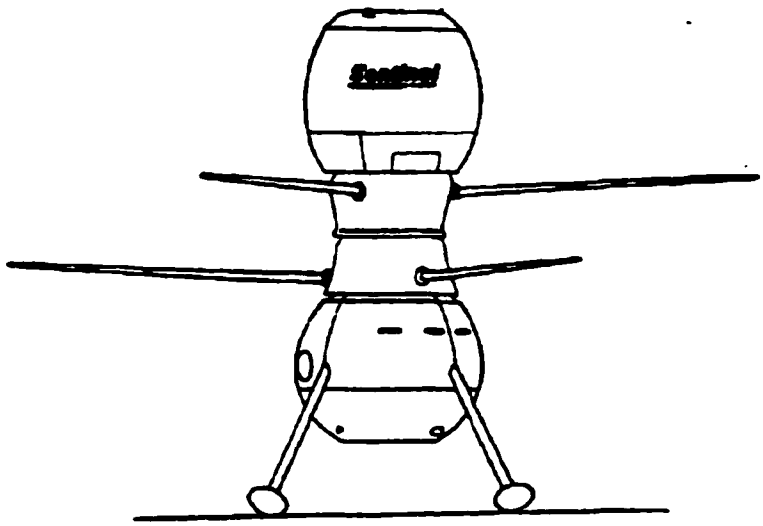

Figure 1.5 – CL-227 Phase III: General arrangement [15]

VTOL UAV system. By the time Phase III was complete (*figure 1.5*), many new system components including a mission planning and control station (MPCS), antenna, and data link. New payloads included a revised communication relay, EW package, FLIR, and daylight television. It was then decided that a new more modern version of the craft needed to be created. After all, the 227 was first conceived back in 1977. This was the reason for the creation of a new, more modern vehicle for the new millennium. This craft is the CL-327 [14] [15].

1.4 Bombardier CL-327

It is evident from this and the previous section that UAV projects were almost uniquely funded though military budgets. These vast sums of money allowed for the use of the most elaborate materials and equipment. However, after the fall of the Berlin Wall and the subsequent end of the Cold War, global military budgets were slashed. When Bombardier created the CL-327, it did so to fulfil both military and civilian needs. The next section briefly explains the general make-up of the craft, its performance capabilities, and its guidance and control functions.

1.4.1 General Overview

The CL-327 Guardian is a robust and reconfigurable system based on the 227 (*figure 1.6*) [16]. Its first flight was performed in November 1997 at the Fort Sill Test Facility in Lawton, Oklahoma [17]. The 327 air vehicle VTOL characteristics allow for launches and recoveries from confined areas typically 10 x 10 meters. The guidance, navigation, and control (GNC) functions provide a high level of automation

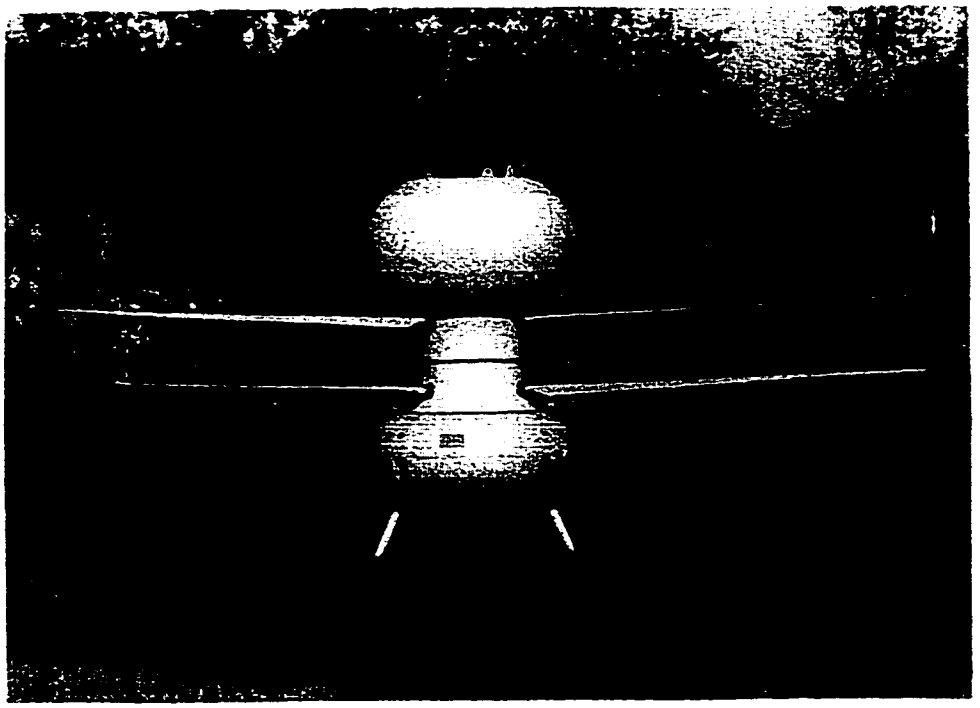

Figure 1.6 – Cl-327: General arrangement [6]

that reduces operator workload [16]. The 327 has the ability to carry out a pre-programmed mission with or without intervention from the surface element. The 327 will be offered world-wide to customers seeking an affordable unmanned surveillance vehicle that will be able to operate from ships and in rugged land environments which lack infrastructure [17]. It has been designed to satisfy emerging market requirements as is evident with the control laws which are custom designed to fit customer requirements [7].

The 327, like the 227 before it, makes use of counter-rotating propellers (*figure 1.6*) for propulsion as the arrangement also allows for rapid yaw control as well as eliminating torque problems associated with a single fan design [8] [16]. At 6 feet tall and with a 13 foot rotor diameter, the size and shape of the vehicle is such that it inherently minimizes infrared (IR), acoustic, and radar signatures. The IR signature is

low as the engine is mounted similar to that in the 227 with the exhaust at the top of the craft. The engine, similar to its predecessor, is turbine style, though the output has been increased substantially to 100 HP and uses a variety of heavy fuels. The fuel capacity is large at 180 liters with the volume split up into two tanks of 130 liters and 50 liters located in the top sphere and bottom sphere respectively. Also a carry over from the previous model is the division of the craft into three distinct modules, the upper sphere encases the engine and transmission, the middle contains the propeller and associated hardware, and the lower sphere houses avionics, landing struts, fuel distribution system, and the sensor package [16].

The performance characteristics for this vehicle is where the craft distinguishes itself from its predecessor. With the added volume of the fuel tanks, the endurance of the vehicle is much improved. *Figure 1.7* provides on station endurance as a function of range for a sea level take-off, a cruise altitude of 3,000 m (9,800 ft) and loiter altitudes of 2,000 m (6,500 ft). Also counted is a fuel reserve based on a 30 minute recovery point hover at 50 m (165 ft). The mission is performed with a 50 kg (110 lbs) payload [16]. *Table 1.2* [6] demonstrates some other major performance improvements over the 227. In horizontal flight, the 327 has a dash true airspeed of 157 $^{km}/_{hr}$ (85 kts). It also has hover capacity up to a density altitude of 2,740 m (9,000 feet). As for the weight of the craft, it has a maximum gross vehicle take-off mass set to 350 kg (770 lbs). As for craft maneuverability and agility, for pitch, roll, and yaw, an adaptive gain ensures that the response remains the same under all ambient mass and engine speed conditions. This being said, the 327 is not designed for maneuver performance. The only benefit maneuver performance brings to a craft of this sort is to reduce turn radius for more

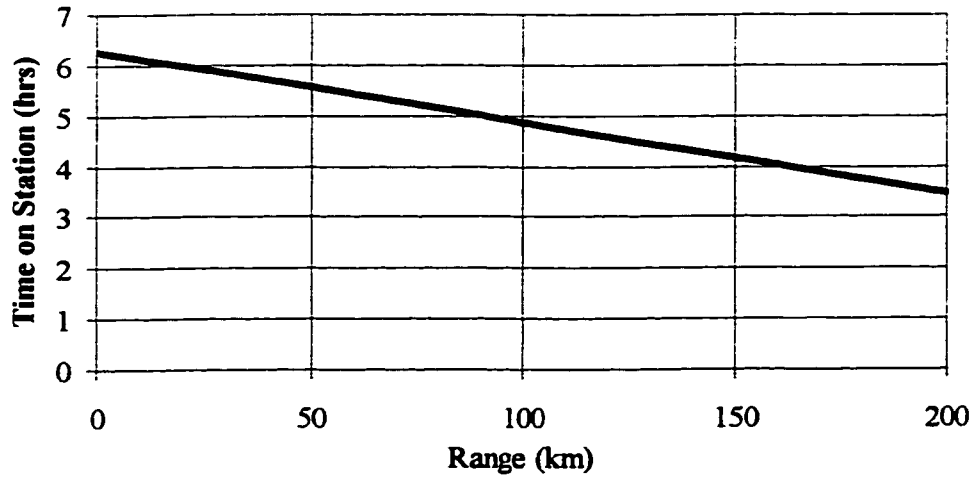

Figure 1.7 – CI-327 on station endurance [16]

	CL-327	CL-227
ceiling	5,500 m	3,000 m
	18,000 feet	9,800 feet
payload carrying capacity	100 kg	25 kg
	220 lbs	55 lbs
climb and descent rates	-5 to +7.6 $^{m}/_{s}$	-1.5 to +2.0 $^{m}/_{s}$
	-980 to +1500 $^{ft}/_{min}$	-300 to +400 $^{ft}/_{min}$

Table 1.2 – Changes in performance between CL-327 and CL-227 [14] [15] [16]

flexibility in target tracking. With the CL-327, the payload (i.e. cameras) perform this task independent of craft orientation or ability to change directions. Therefore the craft requires only enough maneuverability performance to enable changes in flight state and direction [16].

1.4.2 Guidance, Navigation, and Control

The advanced guidance, navigation, and control (GNC) function for the 327 has had some modifications performed to it. It includes GPS/DGPS aided flight, waypoint navigation, automatic vertical take-off and autonomous flight without intervention from the surface. The combination of the GNC functions with different communication modes give rise to advanced capabilities such as automatic and autonomous flight as well as automatic take-off and landings. The general schematic for GNC is shown in *figure 1.8*. What follows is a simplified explanation of how these pieces fit together and how they will effect the development of the autoland system.

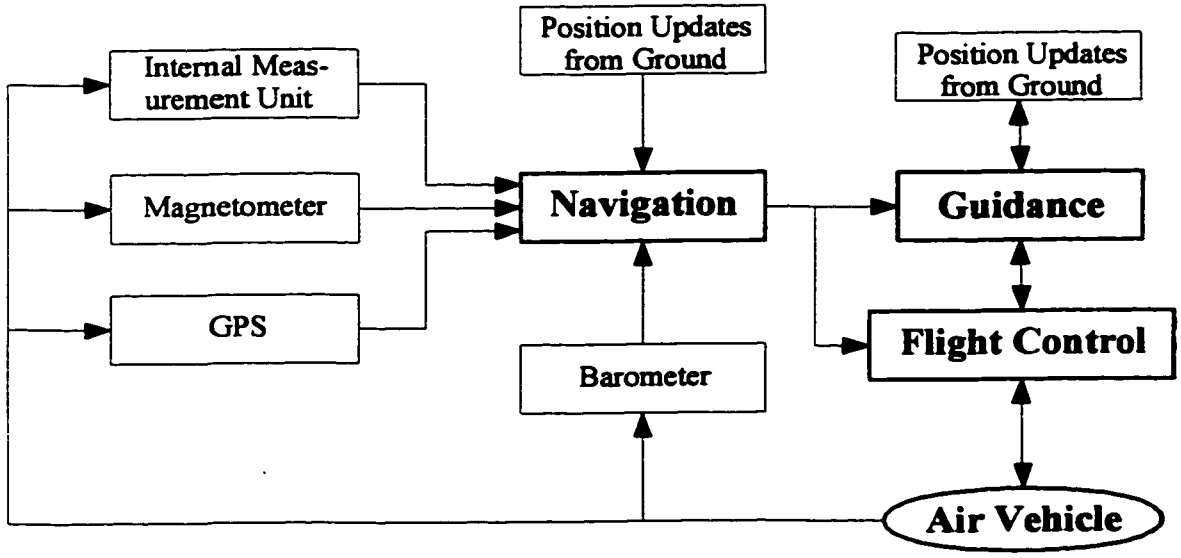

Figure 1.8 – High-level architecture of GNC functions [16]

The navigation functions provide estimates of the AV translational and angular position and velocity to both the guidance and flight control functions. The manner in which this is done is that navigation function is actually provided by the navigation control processor (NCP) which receives data from different sensors. The integrated

navigation filter (INF) automatically selects the best navigation mode based on sensor availability and uses Kalman filtering to compute accurate position and velocity estimates. The NCP gives significant improvement to the accuracy and reliability of the various measured values especially that for height. For the horizontal, the most accurate individual source for measurement is the DGPS. For vertical navigation, 3-D position and velocity updates are integrated with the barometric altitude reference unit (BARU), derived altitude, and inertial measurements [16]. This integration of various navigation system's data is an accepted and accurate approach [19].

The guidance function elaborates high level commands to make the AV follow a flight path. These commands are automatically converted into low level commands which are then implemented by the flight control system (FCS) which is the entity responsible for stabilizing the AV in flight. The FCS architecture is illustrated in *figure*

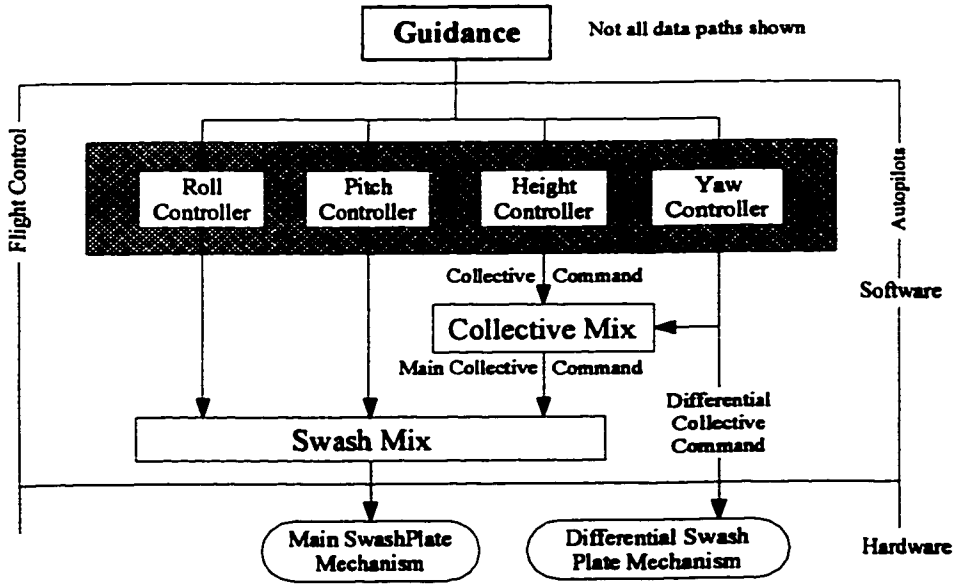

Figure 1.9 – High-level architecture of FCS [16]

1.9. The guidance commands for height, yaw, and horizontal or ground velocity (i.e. tilt and tilt heading) are transmitted to the FCS. These commands are first converted into equivalent roll, pitch, and yaw commands for the corresponding roll, pitch, and yaw autopilots. Motion feedback is provided by the navigation function. The guidance function of the 327 allows the AV to follow a flight path which is either pre-defined (automatic guidance) or controlled manually by an operator from the ground using a joystick (manual guidance). In automatic guidance, the flight path is defined with a series of waypoints in between which the AV will follow straight lines. The maximum number of points which the craft can be programmed to intercept is 255 [16].

The CL-327 is not just a 227 with some cosmetic changes. It is undeniably a craft capable of carrying bigger payloads, at higher altitudes, for a longer period of time than its forerunner. The craft's increased overall size is representative of this change. The one change which will most influence how the craft navigates and is critical to the development of the autoland is the incorporation of GPS technology. This will add a great deal of accuracy especially when in DGPS mode. The reasons behind its addition to the AV's navigation system will be briefly explored.

1.5 Navigation Methods and GPS

For a UAV to be a competitor in today's market, it must be able to provide itself with high navigation accuracy [2]. In the past, helicopters and UAVs used such methods as weather radar, microwave technologies, lasers, or stereo-vision and recognition software to determine distances [2] [20] [21] [22]. These proved to be either not accurate enough or for the most part, extremely expensive. Automation requires the application of recent technologies and this is especially true when discussing UAVs [2]. There are

many methods and associated hardware which give excellent navigation information, but this increased accuracy comes at a price. With the opening of the market to civilian users, the AVs must now become affordable. A cost effective and powerful means of navigation is provided using GPS and DGPS navigation [21] [23]. Depending on the quality of the unit installed, the craft can be provided with accuracy down to less than 0.5 m with the DGPS system activated [24]. Preliminary performance analysis has shown that some differential signals are capable of meeting CAT III accuracy requirements for fixed wing craft [25]. These findings would indicate that DGPS would be capable of safely landing UAVs in inhabited areas as well. Thus this technology is both cost effective and efficient as a means of navigation. For an explanation of how GPS/DGPS works, please refer to Appendix A.

UAV design is a dynamic field at the moment. Not only are aerospace giants involved, but also university programs have been set up to explore the field. As microprocessors and electronics continue to evolve, those who employ these products are the beneficiaries. UAV payload equipment has become very sophisticated over the years and the new models continue this trend. The payload equipment isn't the only system effected. The GNC functions have made great strides lately, so much so that autonomous flight and automatic take-off and landing systems are the norm in the industry. The key now is to make these military vehicles available to the non-military and civil market. This means a very high level of automation must be provided at a low cost. To these ends, an automatic landing system using GPS and DGPS is the right choice. The next chapter will look at what is required of the autoland algorithms, what tools are given, and the limitations set forth to create the system.

2.0 Problem Description

The production of drone type rotocraft has been going on in Canada for quite some time. First Canadair and now Bombardier have designed and manufactured such crafts. The problems faced are similar from one generation of craft to the next. Similar, but not the same. How should the controller be designed? Can the package's ability to withstand disturbances be enhanced? These and many others are questions which must be dealt with and their answers are invariably different from those found to work for its predecessor. In this section, the problem background will be developed and then the major issues, concerning what is required of the craft, will be assessed.

2.1 Landing Profile

Landing a UAV is stressful and tiring work for the operator. With the implementation of an autoland system, the intricacies of such a maneuver will be left to the onboard computer. The computer can then monitor the craft's performance and execute the required landing profile as instructed by the various algorithms. The landing profile itself is to be common to any instance where the autoland is used. The first section will effectively explain the form of the landing profile and the terminology used to describe it. Then the profile will be split into three separate portions which will define the various phases of the autoland.

2.1.1 Components and Structure

The landing profile is comprised of the final three points the craft must rejoin for a given mission. These points are described using an inertial based Cartesian coordinate

system. The three axes for this system are east, north, and height and depict the standard x, y, and z system respectively. The three points, in the order they occur are the recovery point (RP), the landing set point (LSP), and the landing point (LP). The RP is the final point which the craft endeavors to obtain while using GPS fed navigation. The LSP and the LP only differ in the vertical components of their coordinates. The LP is at ground level and indicates the touch-down point. The LSP lies directly above the LP by some 20-50 meters. The key to the landing profile lies in the line that connects the RP and the LSP. It is termed the glideslope (GS). *Figure 2.1* illustrates the scenario.

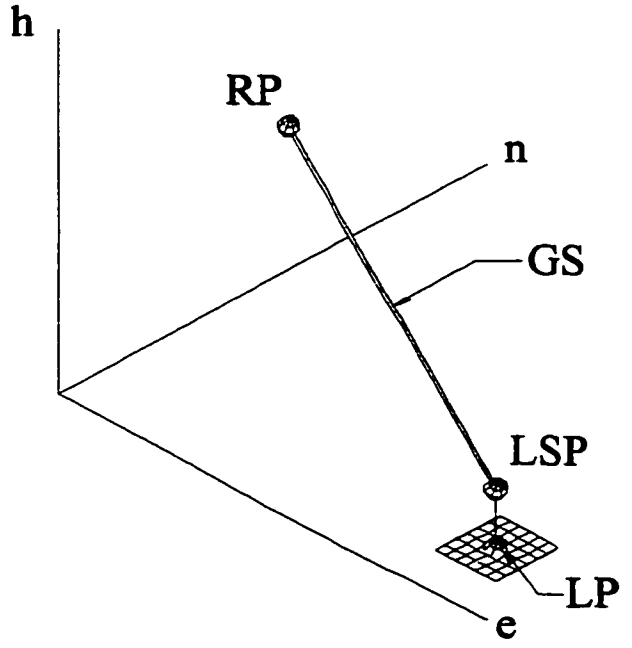

Figure 2.1 – Generalized landing profile

The GS is the center of the problem. It defines the path which is to be taken between the RP and the LSP. It is important to realize that the GS has a specific direction as it begins at the RP and ends at the LSP. The GS demonstrates what the craft must do to put itself in a position to land. The geometry of this path is critical to decision making.

The two major geometrical indicators for the GS are its direction or bearing angle and its descent angle. The bearing angle (α_{GS}) is the angle that the GS makes from the east and is always taken with the RP indicating the origin (*figure 2.2*). The bearing angle takes into account only the horizontal components of the GS and is therefore seen best when viewed from above. The aircraft heading range of ±180° (*figure 2.3*) is used in lieu of a range which spans from 0° to 360° because of binary bit allocation convention in the bus which transports electronic information throughout the craft. This an ARINC-629 standard and is observed in this vehicle [26]. The descent angle (γ_{GS}) is the acute angle the GS makes with the horizontal. As was the case with α_{GS}, γ_{GS} is also dependant on GS orientation. This allows for α_{GS} to always be acute. The true angle is seen when looking perpendicular to the GS. Two examples are given in *figure 2.4* showing how γ_{GS} is always acute. Though computational devices will calculate both α_{GS}, and γ_{GS} in radians, the angles will be referred to throughout this work in degrees.

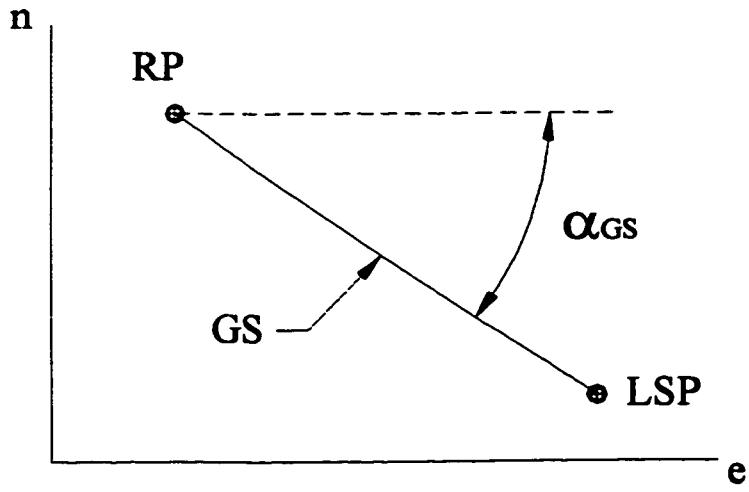

Figure 2.2 – Example of bearing angle (plan view)

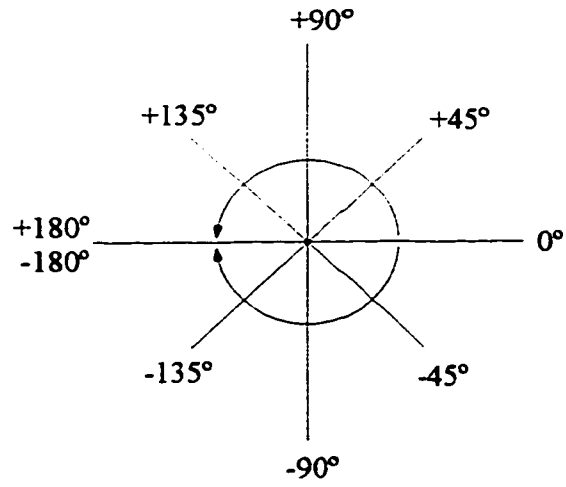

Figure 2.3 – Bearing angle orientation

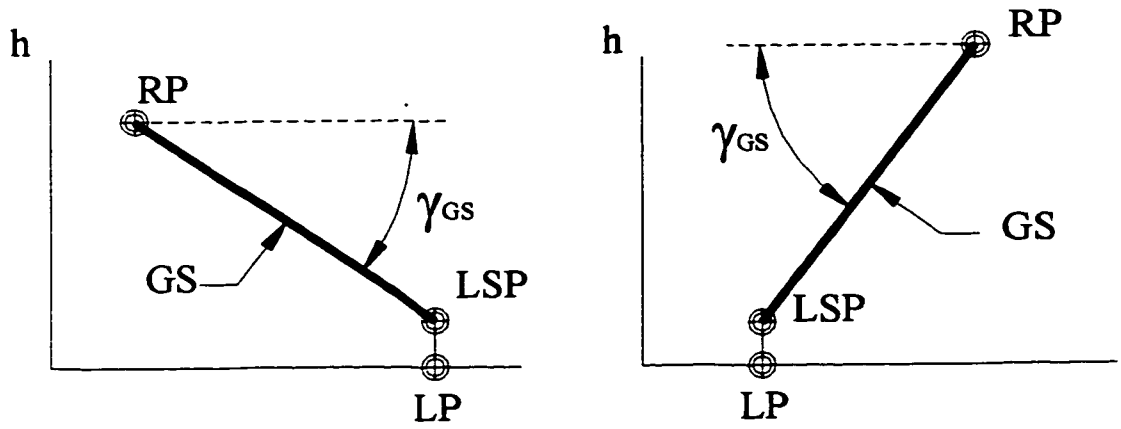

Figure 2.4 – Two examples of descent angle configuration

The manner in which these two indices are calculated are simple and similar. Both depend solely on the coordinates for the RP and the LSP. The horizontal components combine to form α_{GS} as shown in *eqn. 2.1*. As for γ_{GS}, it uses all six coordinates as it requires the differential distance in each direction (*eqn. 2.2*). It must be stressed here that though at times negative angles are formed, the computational devices will handle these with the same ease as it would positive values.

$$\alpha_{GS} = \tan^{-1}\left(\frac{N_{LSP} - N_{RP}}{E_{LSP} - E_{RP}}\right) \tag{2.1}$$

$$\gamma_{GS} = \tan^{-1}\left(\frac{H_{LSP} - H_{RP}}{\sqrt{\left(N_{LSP} - N_{RP}\right)^2 + \left(E_{LSP} - E_{RP}\right)^2}}\right) \tag{2.2}$$

where,

N_{RP} = North coordinate of recovery point (RP)

E_{RP} = East coordinate of recovery point (RP)

H_{RP} = Height of recovery point (RP)

N_{LSP} = North coordinate of landing set point (LSP)

E_{LSP} = East coordinate of landing set point (LSP)

H_{LSP} = Height of landing set point (LSP)

2.1.2 Autoland Segments

The autoland process is broken into three specific portions or segments. The two final segments follow the landing profile as described in the previous section. The first of the three segments, the GS intercept, makes replication of the landing profile possible. When it reaches the recovery point, it is using GPS to navigate. As discussed before, this is not accurate enough to provide adequate safety for both the craft and ground crew. In order to achieve the required accuracy, the craft switches from GPS to DGPS using differential information provided by the ground station. With this newly acquired accuracy, the craft almost certainly discovers that it is not where it thought it was and that some position error exists. The craft could proceed to its original target, that being the

RP, or it could find another place somewhere else along the GS to intercept its desired line of travel. Which is better remains to be seen.

The second phase is the glideslope descent portion. After the craft has chosen and arrived at an appropriate intercept point on the glideslope, the craft then switches over to this other algorithm to proceed with the next phase. The craft is to proceed from the intercept point, along the glideslope to the LSP. It is to follow the GS religiously as the GS itself has been carefully chosen to be clear of obstacles.

The third phase, entitled the final descent, is the final portion of the landing profile and subsequently the last of the autoland process. This section defines the path between the LSP and the point on the ground which is the LP. The craft is to descend this path until it reaches the ground where impact sensors in the landing gear of the unit will terminate the descent phase and shut down the craft as a whole. It is to be noted that as compared to the other two sections, where the craft commands both horizontal and vertical motion, the final descent portion contains only commanded vertical velocity. This is because, as specified previously, the LSP and the LP will both have the same horizontal co-ordinates. In other words, the final descent path will always be vertical.

2.1.3 Safety Volume

The safety volume (SV) is a space around the RP which is designated free of obstacles. It must be devoid of any object, whether it be movable or immovable, which could interfere with the vehicle. Every RP must have a safe volume enveloping it. This is a major condition which must be met when selecting a possible RP. The size and shape of the SV is dependant on the accuracy of the navigation unit in use at the time. Given that

the autoland system uses two methods of navigation, the reasoning behind using the accuracy of the GPS unit upon which to create the SV will also be explained. In finishing, the form which the SV takes will be addressed.

The size and form of the region is dependant on the accuracy of the navigation device. The safety volume represents the accuracy of a navigation unit about a given point. If for example, the horizontal accuracy of the unit is ±200 meters, this would mean that the craft could lie anywhere within this region. The size of the SV would have to be of equal size as the inaccuracy to provide safe passage for the craft. With respect to the UAV location within this space, it is for all intents and purposes chance that dictates where it will end up. The SV allows for this aspect of chance.

There are two navigation devices which operate in the region about the RP. First the GPS unit brings the craft from the last waypoint to the RP. Second, the DGPS corrects for the error in the GPS driven results, intercepts the GS, and is used from this point forward. The size of the SV is dependant on the accuracy of the coarsest of the two units. In this instance, it's the GPS unit. The reason behind the region's dimensions being dependant on the least accurate of the two navigation methods is intuitive. If the SV was any smaller than the accuracy provided by the GPS unit, there is a very real chance that the craft would fall outside the cleared zone. This could prove catastrophic.

The shape of the region is a cylinder. Its proportions will vary depending on the accuracy of, in this instance, the GPS unit. The circular planes of the cylinder are parallel with the ground. A typical SV is illustrated in *figure 2.5* with an accompanying landing scenario. The reason it resembles a cylinder is due to the horizontal error of the unit

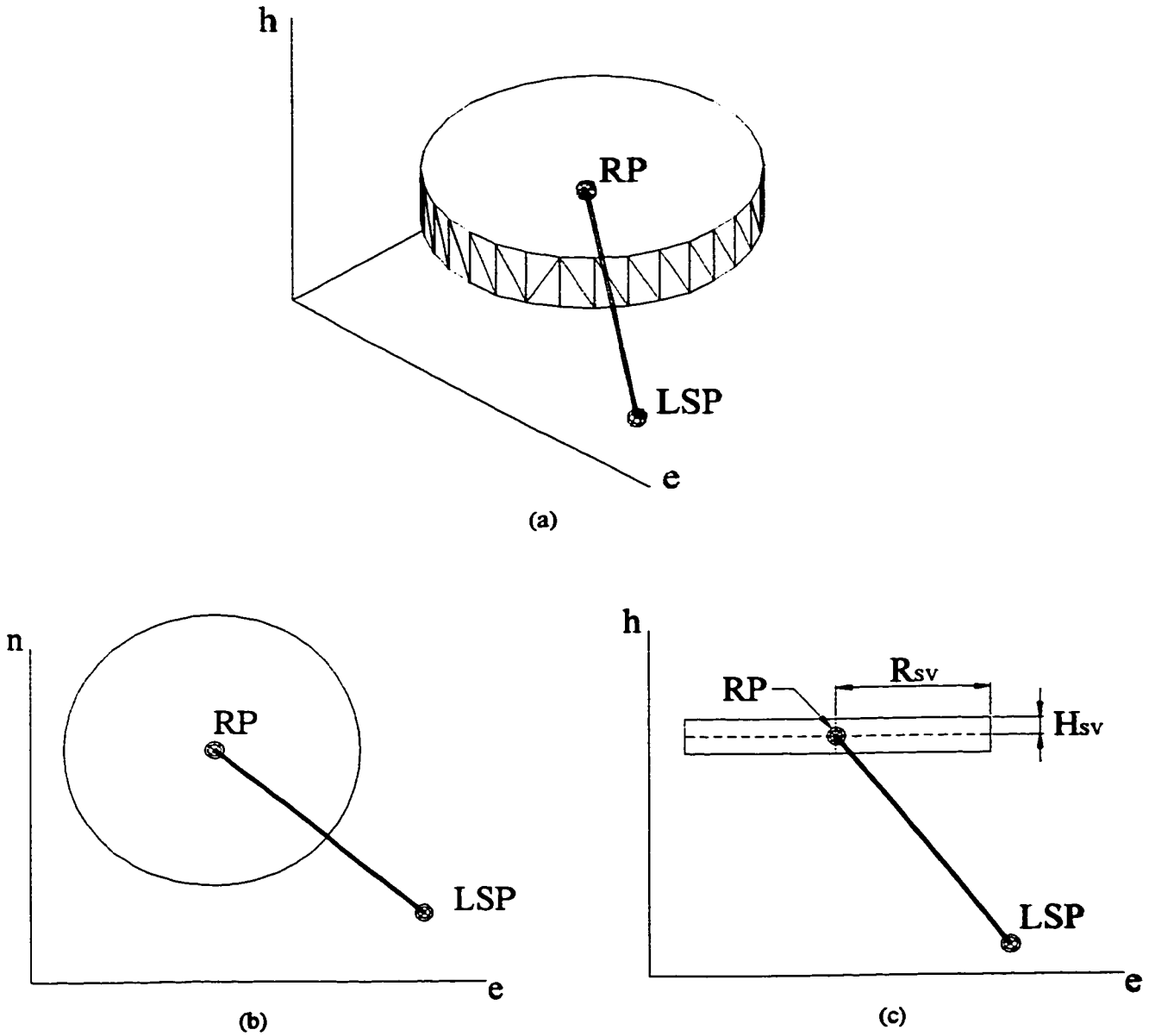

Figure 2.5 – SV figures

being defined as Circular Error Probable (CEP). There are two directions which make up the horizontal, north and east. An error will exist in both these directions. Thus a the description of the error in the horizontal as a radius (R_{SV}). As for the vertical, there is only one dimensional error, thus the height error just stretches the circular horizontal error

over a given height interval above and below the RP (H_{SV}). These variables are illustrated in *figure 2.5c*.

This region is a safe zone where the craft will not come in contact with any object. It is large enough that wherever the GPS system guides the craft, the SV will provide a RP such that no obstacles will lie between the craft and the GS. With this the case, the craft is to reach the GS before it leaves this zone. This allows for a much safer process for all concerned.

2.2 CL-327 Model Overview

System models are invaluable to a designer. With an established model in place, a designer need only produce an idea in code form, incorporate it into the existing model, and run some simulations. This vastly reduces development time before an idea either comes to fruition or before it is scrapped. For this reason, a system model for the craft was designed and constructed to simulate the CL-327's systems and how they interact with one another. A brief and general overview of this model will include its inputs and outputs, plane specific performance characteristics, and a brief explanation of model scope. This section will explain the model in so much as how it will effect the basic design of the autoland algorithms and controllers.

2.2.1 Inputs and Outputs

The inputs and outputs of this model are what the flight control algorithms may use to fly the craft. Although they may not appear in this specific form in a conventional helicopter, they are essentially the same core data which a pilot would use to fly a VTOL vehicle. It is important to note that the inputs for the model are desired quantities, while

the outputs from the model represent actual values. This is generally the case with most of today's fly-by-wire and fly-by-light aircraft systems.

The inputs used to command all craft movements differ from plane to plane. In the horizontal, the command values are desired aircraft tilt, while its counterpart in the vertical is the desired rate of climb or descent. Though the inputs for the horizontal and vertical seem to differ, they in fact both relate to velocities. This is because the desired horizontal tilt of the vehicle is directly related to the horizontal velocity of the craft. The tilt in the horizontal is actually split into two components, that for the east and that for the north. This provides an input which is in a ready to use form as the velocity is already split into its fundamental components. The input to the vertical controller is comprised of the desired vertical velocity and is straightforward. As both inputs relate themselves to rate of change in their respective planes, this describes a velocity controlled system.

The outputs depict what resulting motion is created when the input values are filtered through the model or in real life, given to the craft. For the horizontal, the actual values provided by the model are horizontal position and velocity of the craft. For the vertical profile, the outputs are similar to the horizontal in that actual vertical position and velocity are produced. In the real world, these values described as model outputs are the actual position and velocity which results from the commanded inputs. Seeing as they are the actual values for the craft, they will in fact be provided by the navigation system.

2.2.2 Plane Specific Flight Performance Characteristics

The performance characteristics for the model is varied depending on whether the horizontal or vertical plane is being discussed. This differing of performance is attributed

to the manner in which displacement is achieved. Also, the craft's physical properties play a role in the plane-to-plane flight performance discrepancies.

In the horizontal, as was already mentioned, the controller uses desired tilt to command the motion of the craft. In reality, a tilt is produced by an altering of the cyclic pitch in such a way as to pitch the whole unit towards the desired heading. The tilting of the craft relocates the trust vector such that there is both a horizontal and a vertical component. It is this horizontal component which creates the desired velocity for the craft. This rotating of the craft's mass to produce tilt takes some time to materialize. Moreover the velocity is reached only after the tilt has been achieved. In addition to this, momentum, once created, takes an equal effort to dissipate. For this reason, harsh limiters are employed to prevent unstable conditions.

For the vertical, the aforementioned vertical rate of ascent or decent is used by the controller as the primary input. The physical method in which this takes place aboard the craft is that an adjustment is made to the pitch angle of all rotor blades. Another way of describing this process is that the collective pitch or simply the collective is adjusted. It is intuitive that it will take longer to produce a climb as opposed to a descent of the same speed since in the prior, the desired command is to fly against gravity, while in the latter, it can utilize the earth's gravitational pull.

The changing of the collective is a very rapid type of adjustment as the blade pitch is quite easy to regulate. It is then understood that the thrust change would also be very quick and hence the velocity control of the craft. The same cannot be said of the horizontal control. Thus even when comparing a climb in the vertical, the worst of the two options in that orientation, it is still a considerably quicker response than one in the

horizontal axis for the same speed. This is illustrated in *figure 2.6* where the open loop response has been plotted for both the horizontal and vertical models. For a more detailed description of the fundamentals of helicopter flight and maneuvering, see reference [27].

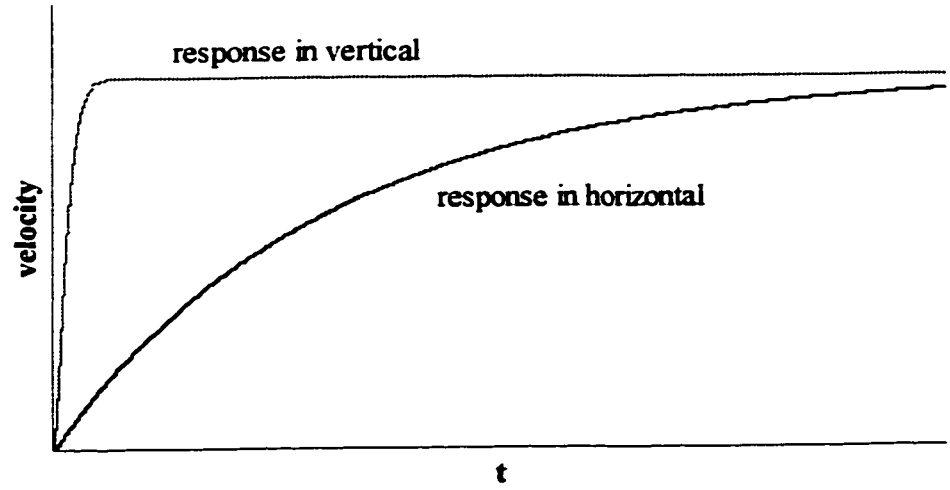

Figure 2.6 – Response to step velocity input for vertical as opposed to horizontal

2.2.3 Model Scope

The model used is an in-house produced program which has been developed over the past decade. It takes into account most any phenomenon that exists within the craft and its environs. It is sufficiently accurate and approximates the real craft quite well. With this being said, it is important to note that the model is not a full model of the system as it is understood. Many aspects of the system have been omitted to allow for a system which can be managed on a normal PC. A full model exists, but must be run on a high power computational unit and is located at the Bombardier's CL-327 design center. Realistically though, the simplified version is satisfactory for initial design purposes. Its results are meaningful and its limits are well within the scope of this project.

2.3 Autoland System Requirements

The autoland process described in this chapter has outlined the background material related to the problem. This section will detail what is expected of the vehicle throughout the course of the events beginning with the navigation switchover through to touchdown. More than discussing the fundamentals of what should be done, the intricate concerns relevant to how the task is accomplished will be outlined. The general requirements of the autoland system are landing profile execution, path geometry, and control accuracy. In addition to these, craft limitations, the usage of the DGPS navigation system, and the overall system disturbance rejection will also be discussed.

2.3.1 Landing Profile Execution

The autoland system takes control of the rotocraft as soon as it switches over from GPS to DGPS. This was described at the beginning of the autoland sequence. The basic task which is required of the autoland process is to fly the craft from the point where it is found after the navigation system switchover, to the GS, and along the profile to the ground. This is the fundamental task of the algorithms which will make up the autoland process. Thus it must carry out the GS intercept, the GS descent, and the final descent portions. Moreover, when carrying out the GS intersect, the SV must be incorporated and utilized to assure safety.

2.3.2 Path Geometry Concerns

The GS is the last technical flying the craft will do before it is slowly maneuvered to the ground in the final vertical section. It is also the heart of the landing profile as it is the portion which allows for profile variability. Hence the glideslope must be able to be

oriented in any direction and can have a descent angle of anywhere from horizontal to vertical. In addition to this, the algorithm directing flight during the GS descent must be able to accept any length of GS. This criteria allows for a full range of motion for the vehicle which is important in avoiding obstacles and enhancing craft versatility.

2.3.3 Control Accuracy

The craft will have well thought out and accurate algorithms to create the environment for the fully adjustable glideslope. A navigation system may be assembled of all the finest devices on the market and arranged in a manner to provide outstanding accuracy. However, all this will be a waste if the system is not equipped with a well designed controller. The controller will keep the craft flying with sharp response, but yet not overly harsh thereby restricting the possibility of craft instability. There is a very fine line between these two states especially when large unpredictable disturbances such as wind and reference data noise are encountered. The ideal path, irrespective of the specific portion must be adhered to with sufficient accuracy.

2.3.4 Craft Limitations

There are certain performance limitations which were alluded to earlier. Thus limiters are put in place to prevent conditions which will lead to instabilities. A pitch and roll limiter is installed to keep the craft from "cartwheeling" due to excess momentum. This could happen while executing a commanded acceleration or deceleration. The total velocity and the vertical velocity are also limited to reduce the chance of over speeding and to keep the vehicle closer to its prescribed track. The velocity limitation for the landing sequence is justifiable, for with the proximity of the ground, any errors could be

catastrophic. Also, since the distance the craft must travel in this sequence is small in comparison to the mission, a reduction in speed will cost little in overall time penalties.

2.3.5 Use of GPS & DGPS

The UAV approaches the RP using GPS provided navigation data. It then undertakes the switchover to DGPS which provides a one hundred-fold increase in accuracy. For the switchover to occur, the ship must open a communication link with the ground station. This is the first communication between the craft and the ground station since the vehicle departed on its mission. This link now exposes the location of not only the craft, but also the ground station. Up to this point, the craft had limited its various signatures. Both thermal and acoustic were minimal as the engines exhaust was pointed upwards and the rotor speed was low. The radar signature was equally small. With the communications link, the veil has effectively been lifted. The controller will use both position and velocity provided by the DGPS to guide the craft through the autoland. This will be the case for both the horizontal and vertical controllers. With this information to guide the vehicle, the craft is to execute a quick and accurate landing enabling a speedy departure of craft and crew from the landing area if need be.

2.3.6 Disturbance Rejection Handling

When dealing with a system without disturbances, there is much more leniency with respect to controller design, and the basic control algorithms. The craft can be pushed somewhat harder, the controller can approach neutral stability considerably closer, and the choice of control algorithms is more varied. Limitations and major changes must be made to a system with the introduction of disturbances. In this case, the primary

disturbances are the noise of the navigation data (position and velocity) and most importantly - *wind*. The craft may be stationed behind an escarpment and then asked to fly over it. The wind shear here would be tremendous and without an adaptable system, the helicopter may be lost. Overall system ability to withstand internal and external disturbances must be of the highest order if the autoland sequence is to be successful.

3.0 Design Concept

The concepts set forth in this section give an overall view of what will be involved in the design of the autoland system. Ideas are to be brought forth and addressed so that they can be revisited in the future. It is important to understand that this section, like this work in general, is not a "how to" manual in autoland design, but rather presents some key factors which must be considered. This chapter introduces these topics with a philosophical and problem solving approach so that the actual calculations and topic development can be performed with a conscious understanding of how the various topics are co-dependent and how they individually effect the autoland system as a whole.

3.1 GS Intercept

When the craft switches from GPS to DGPS, the autoland process is initiated. With the increased precision of the new navigation data system, there will certainly exist some amount of position error between where the craft was aiming for and where it ended up. It is understood that the unit embarking on an uncleared path is a dangerous affair. It is to intercept the GS in timely fashion and do so according to the criteria laid out in the problem description section.

The easiest manner in which to accomplish the task of intercepting the GS is to go to its original target, the RP. In some instances, this would be the best idea, but not in all cases. The reason stems from the knowledge that the GS descent is the next phase to be undertaken. It is known which direction the flight will take in this section and it is known that it will in all but the rarest case, be descending. It makes sense that an educated short-

cut could be taken. For example if the craft lies below the RP after switchover, it would be counterproductive to fly up to the RP only to fly down to and past the same altitude where the craft was found originally. It must be ensured that the craft always travels within the safety volume whenever it is choosing these alternative intercepts. Other decisions could be taken to economize craft movement depending on where it is found after navigation system switchover. The only knowledge required is where the unit lies relative to the flight profile.

The flight profile, described in *chapter 2*, is central to the autoland process. Once the craft intersects the GS, it will not leave this trace until it completes its mission. It is similar to a localizer used in conventional ILS approach. This being said, it is evident that this profile can be of great use in determining the intercept. In other words, where the craft lies about the profile can be used to distinguish where the craft could be sent during the intercept portion to avoid unnecessary travel. The craft location is known in inertial co-ordinates as are the points which make up the flight profile. It therefore makes sense conceptually that the AV can be located relative to the flight profile, thus allowing for a point to be selected which would economize on distance traveled. The manner of figuring out the exact method of craft location relative to the profile remains to be seen.

The GS intercept portion is a makeshift phase to rectify the error brought on by the navigation system. To choose the RP as the intercept is a simple method of doing things, but by no means refined. By looking forward and being proactive, time and energy can be saved at no cost. The only information required is to know where the UAV lies relative to the flight profile. With this, unnecessary travel can be eliminated and the process as a whole can become sounder and quicker.

3.2 Trajectory Generator

When the vehicle embarks upon a mission, it is passing between various non-arbitrary co-ordinates in space. During normal flight, these points are called waypoints. For the autoland process, the UAV is always looking to achieve its final goal of reaching its landing point. To do this, the craft first intercepts the GS, flies to the LSP, and finally to the LP. This is again a case of hopping from point to point. The system is using these intermediate points to guide the ship to its final goal of the LP. The major difference between the waypoint navigation and autolanding being that the latter must be performed with greater precision due to the proximity of obstacles.

The controller will be used to drive the system. To do this, it will require an error signal comprised of the position tracking error, the velocity tracking error, or something related to the two. Tracking error refers to the difference between the desired input to the plant and the plant's output [27]. The plant's output is the information provided by the DGPS unit and so is readily accessible. The desired position must be provided in one way or another. It can be obtained from the path itself where the target point of where the craft is aiming for is used as the ideal position. This creates a very large range which the position error may span. This large range means the controller must be tuned to accommodate this large error. With this, the craft will undergo a very harsh command when it is a great distance from its target while it will react sluggishly when close to its target, if it reacts at all. This is a tried and true recipe for instability. Therefore to avoid this situation, the position error must be kept small [2].

Position error reduction can be performed in a variety of ways. One method is to create more fixed points along the flight path. This means creating points which are

equally spaced between the two points in question. There are two problems with this solution. First, the memory required to hold these points must increase which can pose problems [17]. Second, when the craft is slowing down at arrival at the each point, the position error will be the same as when it is at its maximum speed when between the two points. This would pose a problem. However, a second method exists to create target points which are dependant on time. Knowing the time which has elapsed since a given phase began, the craft knows where it is supposed to be. For the second method, the target point for an instant in time is calculated on the spot. This requires no added memory and the distance between the points can be varied depending on how quickly it is desired that the craft travel. With this fed to the controller, the craft can effectively be pulled along like a rabbit following a carrot. What has been described here is a trajectory generator [30].

The controller is the beneficiary of this trajectory generation. It receives the ideal position for the craft and can check it against the actual craft position and use the discrepancy to drive the unit [30]. The question remains however, how small should the error range be? This is dependant on a few factors. First is the iteration rate of the trajectory generator. The closer the points are, the less the error range. Ideally the time step between iterations would approach zero, but this would overload the craft's microprocessor with calculations. A more realistic number would be the sampling rate at which the unit's navigation system runs. Here, for every instance the actual craft position is verified, a new ideal point is calculated. Another factor effecting the error range is how quickly "the carrot is moved ahead of the rabbit." If the ideal points are spaced at too great a distance, the problem of large position error range reoccurs [2]. If they are too

close, poor performance exists. A happy medium must be achieved. This can be adjusted depending on the trajectory profile chosen. A final factor is the presence of winds. If gusting winds knock the craft off its path, the vehicle may become unstable trying to realign itself with the ideal position. For this reason, the trajectory generator must, like the controller, be tuned to allow for disturbances.

A trajectory generator would be a strong component of the autoland process. Correctly configured, it would effectively remove the threat of instability through position error range reduction. It would be dependant on time which is a variable independent of outside disturbances. Moreover it would provide the ideal position of the craft to the controller which would make the two of them codependent [30]. The trajectory generator would also be versatile in that it could be used for navigation between any two points in space, irrespective of their locations.

3.3 Controller

The controller is the heart of the autoland system. It takes in navigation signals and based on these values, gives output commands to the various flight hardware actuators. These actuators will then modify the flight surfaces to alter the immediate performance of the craft [29]. The navigation unit will take a new sample of various inertial and non inertial parameters and provide data reporting what are the craft's inertial reference data values for that given instant in time [17]. This information will be read by the controller and it will determine what adjustments should be given to the control surface actuators at the given moment. This process happens many times a second. Due

to the high accuracy of all components involved, the craft's performance has the potential for exceptionality.

The overall requirements of the system are straightforward. The control unit as a whole must be flexible in its ability to handle disturbances. These will come predominantly from winds and navigation data signal noise. They will be large at times and have varying frequencies. The craft must be provided with a large stability envelope to withstand such conditions. In addition to this, the position error between ideal and actual values must be small. Seeing as the craft is on its final descent earthward, the consequences for deviation from the prescribed path, or transcending stability limitations are severe. Finally the controller structure must be uncomplicated.

How the controller makes its decisions is based on two factors, what kind of controller is being used and what are the input signals. With regards to which input signals are to be used, the supply is limited. In fact, since this autoland is being designed for a GPS navigation system in mind, there are only two signals available, position and velocity. How these signals are to be used remains to be seen. Contingencies exist for error signals to be calculated between ideal and actual position and velocity values, with the navigation unit in the AV supplying the actual data and the trajectory generator supplying the ideal data.

The form which the controller will take could be a boundless undertaking. The controller will work on feedback concepts to drive the craft, but as to how this is done is a study unto itself. The design and synthesis of a specialized or even unique controller is not the goal of this project. The controller is an important piece of the system, but a piece nonetheless. The scope of this project requires a controller which will conform to the

conditions set forth previously in this section, will be easy to use, and easy to adjust. To this end, it will be a unit which is well known and requires no fundamental development.

3.4 Summary

The chapter has introduced the major issues which are pertinent to the design of the autoland system for the Bombardier CL-327. First there is the algorithm designed to save time and travel depending on the location of the AV after navigation system switchover. Then there is the idea of a program which will customize travel between two points in space to the users performance requirements and limitations. Finally there is the system which controls the craft's ability to respond to disturbances and remain in close proximity to the ideal path being provided. In the first portion of the autoland profile, between the navigation system switchover location and where the AV intercepts the GS, all three of these processes will be required. Only the latter two will be needed while negotiating the GS and between the LSP and the LP, only the controller will be required. So if the first portion of the autoland profile is deemed the model section, as it incorporates all three topics discussed here, the first task performed in this portion would be to determine where the craft should meet up with the GS. This process is known as the GS intercept portion.

4.0 Glideslope Intercept Algorithm

The UAV has just arrived at the RP. It has been flying for two-and-three-quarter hours. It has performed its mission using GPS and is in the process of communicating with the ground system to engage the switchover to DGPS. The craft now becomes aware that it's not where it thought it was. The higher precision DGPS system has exposed a potentially substantial position error which must be dealt with. It now must decide what to do. The intercept algorithm begins its job determining where the craft is to go next. The intercept algorithm surveys the situation and produces a well thought out target point which will allow the craft to intercept the GS. This is the first decided step in the autoland process. The algorithm has options available to it as to which location is best suited to act as the intercept point on the GS. It could proceed to its original target, the RP, to the LSP, or to any point on the line that is formed by these two points. Any of these options could be undertaken, but the best option is yet to be seen. If the UAV is to be predictable and rational, guidelines must be set as to what options are available when the intercept selection process is undertaken.

4.1 Conditions of the Glideslope Intercept Algorithm

To give a basic outline of what must be considered in the development of the intercept algorithm, basic conditions and restrictions must be set forth. They will mold the development process to create a well thought out solution. The areas in which specific concerns are prevalent include system foresight, safety of the craft and personnel, and considerations with respect to path geometry.

The premise for design of this autoland system revolves around adherence to efficient operating procedures. In accordance with this, the basic conditions for the intercept algorithm correspond to simple logical parameters. One of the most important individual condition is the avoidance of flight command contradictions. The conflict involves what the craft is told to do during this portion and what it will be told to do in the next. The present task is to intercept the GS, while the next is to fly down the GS. The direction of flight along the GS is known, so the object is to select an intercept point which is in harmony with the glideslope descent portion. The general rule is don't fly in one direction in the glideslope intercept portion only to fly in the other direction moments later in the glideslope descent portion. Similarly, don't fly up only to go down. This provides for conservation of movement between the two portions of the autoland process as well as demonstrating a well thought out plan of action.

Another important condition touches on the issue of safety. This applies to the craft, personnel, and bystanders through confinement of the flight envelope. As was stated earlier, the choices available to the rotorcraft are plenty. If no limits were placed on its intercept selection, the options available were to fly to the RP, the LSP, or any point in between. This scenario of using the LSP as a viable intercept point would be valid if the craft was being used in a flat desert environment or on a calm sea. However, this assumption is unrealistic in all but the rarest of cases. This vehicle is to be used in diverse milieus. Moreover, the vehicle must respect the SV. Recall that the SV is set forth to provide an obstruction free zone in which the craft may fly to intercept the GS. This must be stringently adhered to so as to ensure a safe mission. Having said this, it is apparent that the craft could not make up its own path and choose the LSP as a realistic

target point for the capture of the GS. In fact the lowest altitude which the craft may intersect the GS is where the GS crosses the perimeter of the SV. Close adherence to these provisos will ensure this portion of the autoland will be safe.

As for possible path geometry between the craft location and that of its intercept, the algorithm must be capable of dealing with anything which is asked of it. It must be as capable of choosing a target point on the GS which could be located as far as 200 meters away. Conversely, it could also be directly on top of the GS thus resulting in very little if any travel required. This last case would result in an omission of the glideslope intercept portion altogether. Together with varying distance, the vehicle could be located anywhere about the RP. This means that even though it could be 50 meters from the RP, the difference between being above the GS as opposed to below the GS makes all the difference with respect to the selected intercept point.

The conditions set out in this section will be incorporated into the basic foundation of the algorithm. It is to take into account and respect these topics, while putting together a product which will actively allow for dynamic performance and decision-making. To take the first step in determining what is the best plan of action as to which point the craft should be sent, the location of the vehicle relative to its original target, the RP, would be of great interest. This is the primary reason behind the topic of the next section, the central plane.

4.2 Approaches to Intercept Selection

The intercept is merely a target point which the craft endeavors to obtain. The intercept will always be located along the GS, but which point would be optimum? A single point could be chosen to which the craft will be sent regardless of it's location

about the RP, but this would be an overly simplified approach. Instead, a method will be developed which will take into account where the craft lies relative to the RP and flight profile. This section will first describe the motivation for the use of the central plane as it simplifies the problem significantly by reducing it from three dimensions to two. The subsection describing the spatial nomenclature will then describe a two dimensional space about the RP and break it down further into manageable zones. The last part of this section will, with the knowledge gained from the spatial nomenclature, explain which intercept selection method will be chosen. This last subsection will explain the philosophies behind the various target point selection methods.

4.2.1 Rationale Behind Central Plane (CP)

The first step in finding an appropriate point which intercepts the GS, is to locate where the craft is in relation to the RP. The RP is chosen as the central point as it was where the craft was aiming for originally and also because it is the first point on the GS, thereby making it the first available target point. The decision must be made on some universal fixed criteria to account for the diversity of possible locations for the agent. To complicate matters, the GS can be oriented in any direction and can be at any descent angle (γ_{GS}) ranging from horizontal or 0° (*figure 4.1a*) to vertical or -90° (*figure 4.1b*).

The concept of this ideal or central plane (CP), one which is central to the flight plan, designates the first step to coherently assess the relation between the UAV's position and its designated mission. This CP would, as mentioned previously, be equivalent to the localizer on a fixed wing ILS. If the point designating the landing point (LP) and the line which comprises the GS are combined to form a plane, this plane then

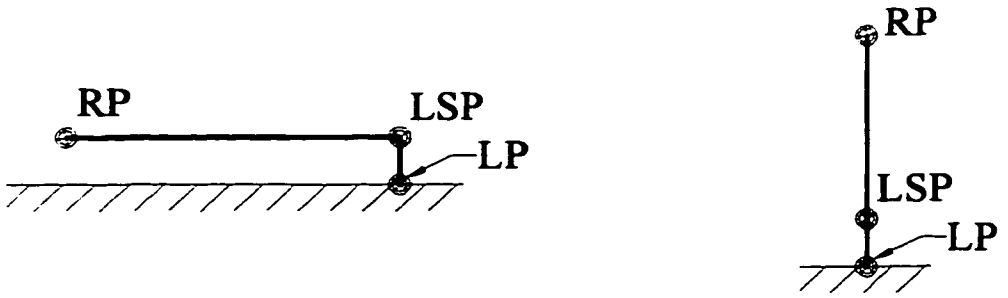

(a) (b)

Figure 4.1 – Examples of the two extremes for γ_{GS}

represents the ideal plane of travel. In other words, once the craft intercepts the GS, it would ideally never travel out of this plane until it reached the ground.

The most important advantage to using the CP is that it acts as a plane of symmetry for the space about the RP. Looking down the GS from the point of view of the RP, the CP splits the space into one to the right of the GS and one to the left. This is illustrated in *figure 4.2a*. Now by viewing the problem perpendicular to the CP, the problem is reduced from three dimensions to two (*figure 4.2b*). The conditions related to this algorithm revolve around conservation of motion parallel to what has now been described as the CP. Corrections perpendicular to this plane are not of issue when choosing an intercept point and are therefore ignored. Thus the views perpendicular to the CP give all which is required by the conditions to select an intercept. This allows for a two dimensional analysis to solve the problem. Side views of the CP will be frequently referred to throughout this work. Two dimensional analysis will be the focus from this point forward unless otherwise stated.

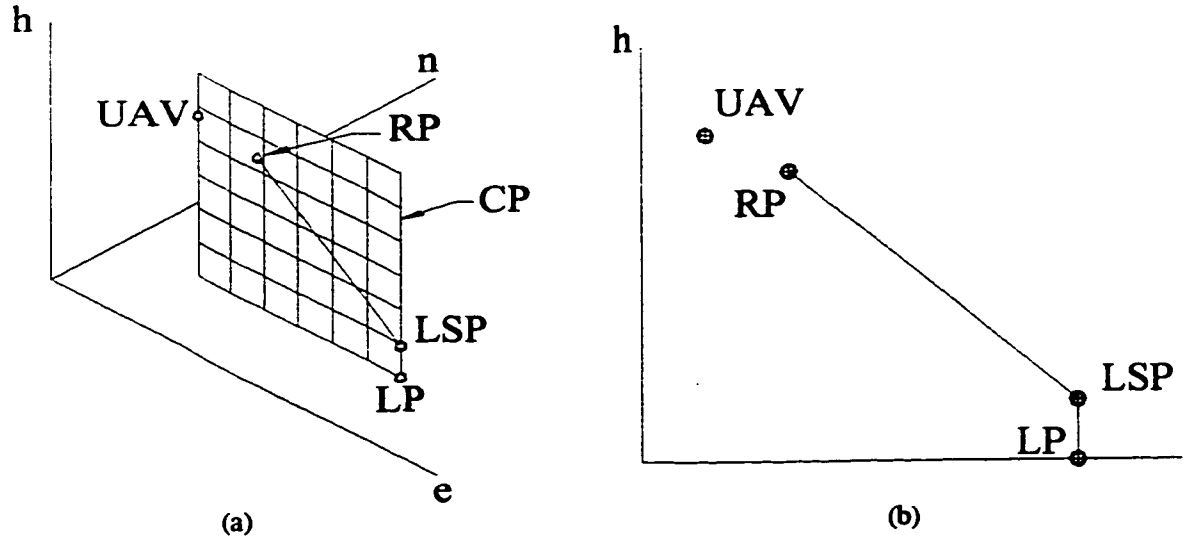

Figure 4.2 – Depiction of CP

4.2.2 Spatial Nomenclature

Spatial Nomenclature is used to further describe the position of the UAV in the vicinity of the RP. Not only does this nomenclature directly relate to the process that is undergone in the algorithm, but it also doubles as a highly effective illustration tool. To simplify matters, the problem will be reduced from three to two dimensions by employing the CP. That which remains will be separated further to define where the UAV resides with respect to known entities of the path.

Firstly, the problem is reduced from three dimensions to two dimensions. This is accomplished by employing the CP. The view perpendicular to the CP allows for easy recognition of where the UAV is situated relative to the GS and RP. This facilitates the induction of terminology which will describe the craft's position relative to the RP. It is important to understand that the CP splits the space about the RP in two. If when visualized from the RP and looking down the GS, there is a space to the right and one to

the left. The fact that the craft may lie to the left or right of this plane is of no concern to the algorithm. Thus little interest need be provided to this fact.

The identification of the UAV's position in the vertical is given with respect to the origin of this relative space, the RP. If the UAV is at an altitude higher than that of the RP, it is said to be above the RP or above for short. The reverse holds true in that if the craft lies beneath the RP, it is said to be below (*figure 4.3*). Seeing as the RP was the target point leading up to the autoland sequence and that it is the first point on the GS, it is the point at the highest available altitude for selection as an intercept. It is reasonable that this point be used as a reference datum in the vertical.

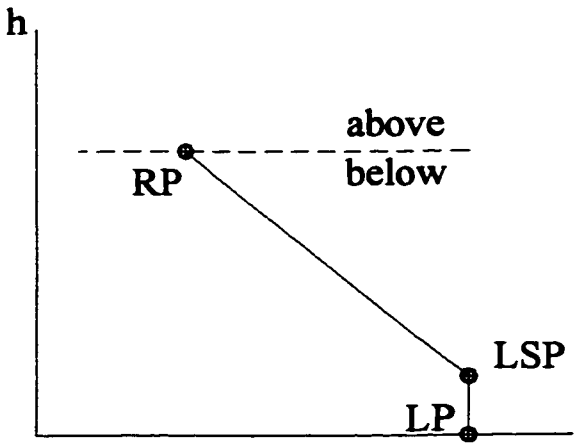

Figure 4.3 – Regions designated above and below

When the scenario is viewed perpendicular to the CP, it can be distinguished if the craft lies ahead or behind the GS. It must be clarified that in this case, the GS also includes a supplemental vertical extension to allow for the nomenclature to extend above the RP since the GS only exists below this point (*figure 4.4*). The denomination of ahead and behind depends on the direction of the GS. The direction that the GS points is in fact that of the bearing angle. A couple of examples of how the GS direction effects the

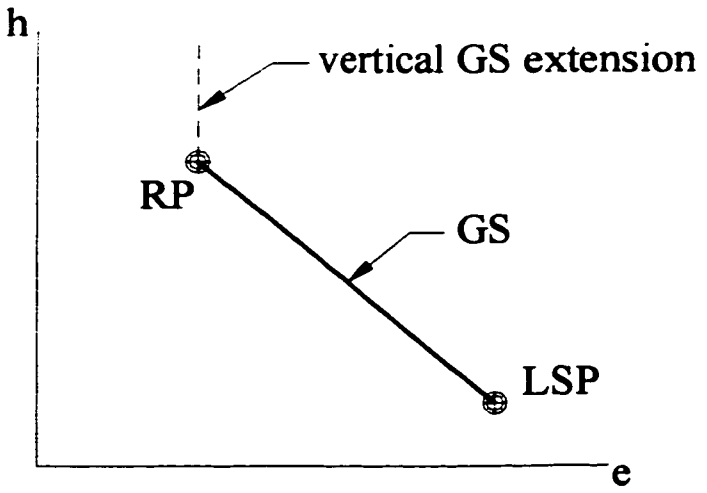

Figure 4.4 – GS vertical extension

location of the craft in this relative system are shown in *figures 4.5a & b.* Ahead is described as the sector in front of the GS and behind is the region aft of the GS.

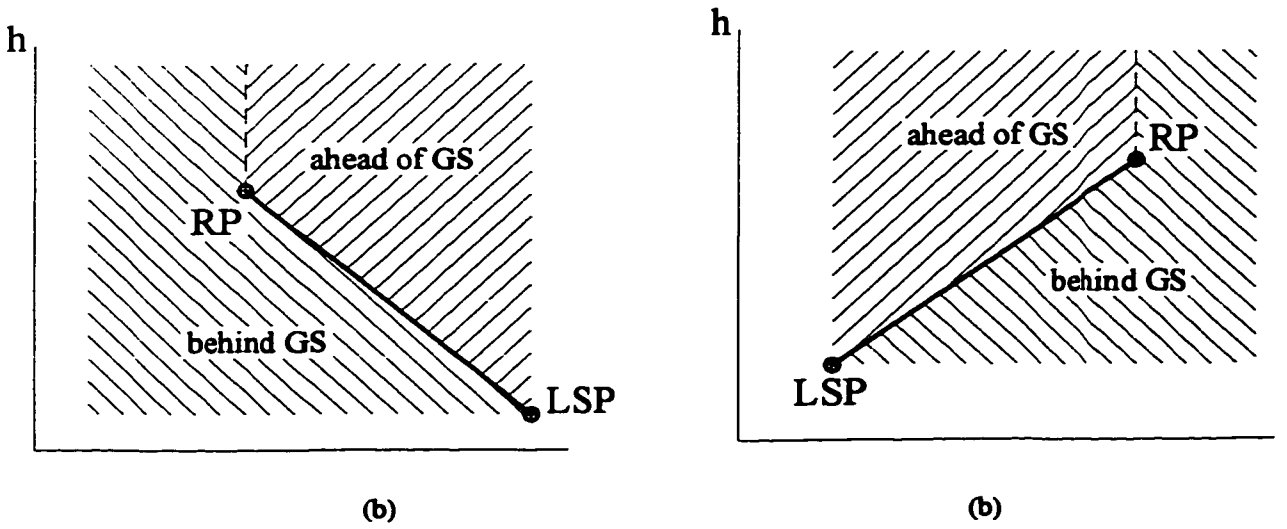

Figure 4.5 – Regions designated above and below

The spatial nomenclature gives a definitive explanation of the problem. It covers the entire region about the RP and is summarized by *figure 4.6*. Though in reality eight zones exist, recall that the CP is a plane of symmetry, only four of the eight are distinct, as described by *figure 4.6*. The criteria describing the spatial nomenclature is such that it can be applied for any length, direction, and gradient of GS or any location of RP. This information will now be used to describe what will be the plan of action when the craft location is determined.

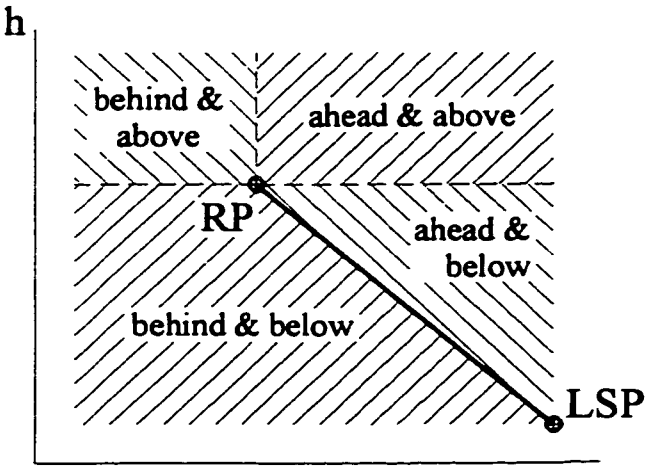

Figure 4.6 – Summary of spatial nomenclature

4.2.3 Intercept Philosophies for the Ideal System

The ideal system describes a specific manner in which the space about the RP is divided. Its three dimensional form is depicted in *figure 4.7a* while that in the more useful form, viewed perpendicular to the CP, is shown in *figure 4.7b*. The space is split into three distinct zones according to the location of the RP and the GS geometry. In essence the ideal system replicates that which was described by the spatial nomenclature. The sole difference is that the two ahead regions are amalgamated into a single zone. In

figure 4.7b, a number identifies each zone. The zone 1 describes the sector behind the GS and below the RP. Zone 2 identifies the region behind the GS, but above the RP while zone 3 describes the entire area ahead of the GS. In the following paragraphs, the philosophies associated with the intercept selection method for each of these distinct zones will be explained.

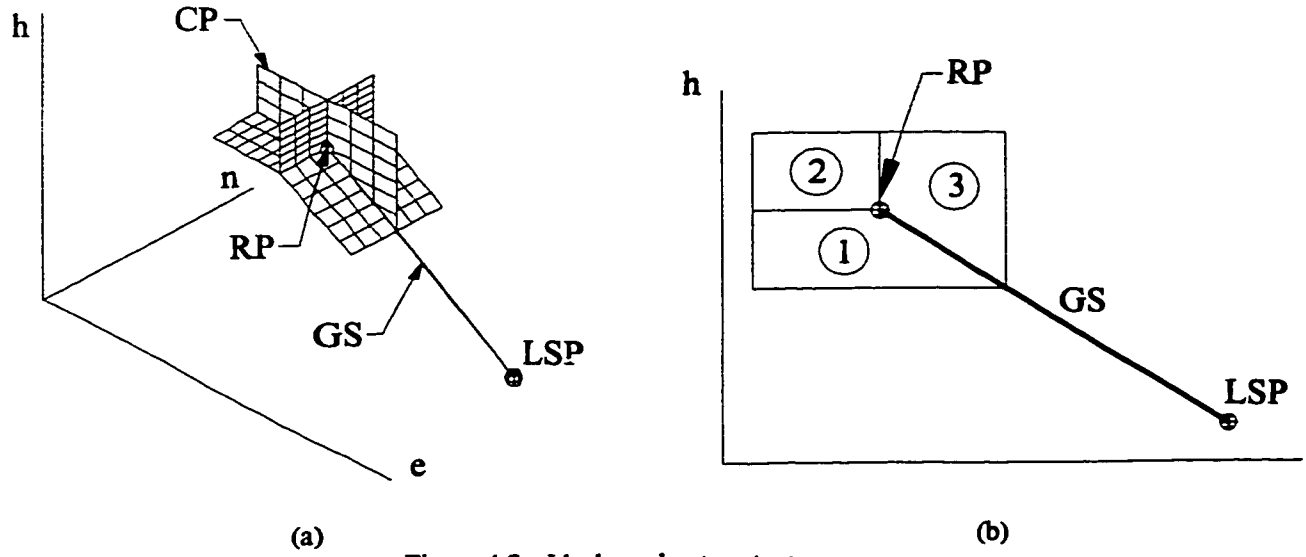

Figure 4.7 – Ideal quadrant system

Zone 1 describes the region in the relative space below and behind. The idea driving the intercept selection for this zone is for the craft to fly horizontally. In other words, wherever the craft is found after the switchover, it should intercept the GS at the point which is described by the same altitude as the craft. The reasoning here is that any increase in altitude during the intercept portion would be counterproductive since it would just have to fly back down the GS during the glideslope descent portion of the autoland process. To chose a point below the given altitude of the UAV would reduce the overall distance covered during the autoland process, but would lead to increased deviation from the defined path. This is potentially dangerous behavior as increased

deviation from the defined path leads to increased probability for collision. An important fact is that the intercept for zone 1 and the path taken to engage the intercept will always fall within the safety volume. By definition the craft is to be located within the SV after the navigation system switchover. Since the craft is to fly horizontally to its intercept with the GS, the intercept is guaranteed to fall within the confines of the SV. For these reasons, the fly horizontal approach was deemed a good option.

Zone 2 is the region behind and above as described by *figure 4.7b*. When found in this zone, the craft is to fly to the RP. The motivation behind sending the craft to the RP revolves around adherence to the ideal path. By sending it to the RP, the craft is sent to rendezvous the GS at the first available point. The RP describes the highest most altitude to which the GS in its literal sense extends to. If it was sent to an intercept point at an altitude less than that of the RP, the craft would be creating its own path in a region where a safe path already exists. Thus by choosing the RP, the craft is adhering to the GS as closely as possible. In addition to this, the method described for zone 2 will always create an intercept and a path to the intercept which is within the SV. This means that this method is quick and safe for all possible UAV positions within zone 2.

Zone 3 involves the region ahead of the GS when below the RP or ahead of the vertical extension of the GS when speaking of the region above the RP. This zone involves using two separate methods to intercept the GS depending on where the craft lies relative to the RP. The first method used to determine an intercept is given the title of the cylinder radius method. In a nutshell, this method involves dropping the UAV down to the GS with minimal travel along the GS. The avoidance of forward travel in this region is key as it is already located ahead of the GS. The idea to bring it down as

quickly as possible seems the most appropriate for this region. If the craft was to fly horizontally back to the GS, it would subsequently violate the flight commands contradiction condition. This is because the next portion of the autoland, the glideslope descent, would send the craft back on a heading similar from whence it came. If the craft was found above the RP, the craft would fly back to the RP in the intercept portion, only to fly forward in the GS portion. A double contradiction would be the case if the vehicle lay beneath the RP as it would not only have to fly back to the RP, but it would also have to fly up. The GS portion would reverse both these actions. Therefore a predominantly vertical descent with lateral corrections is the best possible option.

Though this method is exact, it has a drawback in that the intercept may fall outside the SV if the craft lies sufficiently far ahead of the RP. If this is the case, another method will be employed. This supplemental method will calculate the point where the GS and the perimeter of the SV, the safety volume boundary (SVB), will meet. This will be the alternative intercept if the first method provides an intercept which falls outside the SV. By calculating the intersection of the GS with the SVB, the last valid intercept is found. Last meaning it is the furthest from the RP and the lowest altitude possible while still falling within the SV. This method provides an alternative to the cylinder radius method.

To date, the problem has been reduced from three dimensions to two. Also, the region around the RP has been broken down into different zones. The logic behind where to send the craft for each zone has also been described. The final step in intercept calculation is to give an exact explanation for the calculations involved in each of these

methods. The calculations for these four methods will be fully explained in the following section.

4.3 Target Point Calculations

The UAV is looking to be directed after it has switched over to the higher precision navigation system. Through this entire process described as the intercept algorithm, the goal is to find a point on the GS from which the UAV can proceed with the last two segments of the autoland process. The sticking point is adhering to the basic conditions outlined previously, particularly the avoidance of conflicting flight commands and staying within the SV. However, the craft must endeavor to adhere as closely as possible to the outlined flight path as designated by the GS. With predominantly these factors in mind, logic was developed to allow for direct attainment of the glideslope yet respect the conditions concerning flight commands conflicts. Four basic methods were worked out. They are, fly horizontal to the GS, fly to the RP, what will be named the cylinder radius approach, and to fly to the intersection of the GS and SVB. These commands are issued dependent upon where the craft is in the space about the RP. So it goes that the decision to use a given method it dependent solely on where the craft is located in relation to the RP and has no bearing on one method being superior to another.

4.3.1 Method 1: Fly Horizontal

The fly horizontal method is employed when the craft is below and behind as illustrated in the ideal system's zone 1 (*figure 4.7*). The idea here is that any increase in altitude during the intercept portion would be counterproductive since it would just have to fly back down the GS during the glideslope descent section of the autoland process.

The calculations required to determine the intercept point using this method are quite simple. Since the unit will be flying horizontal, the vertical coordinate of the intercept point is the same as that of the craft at the instant the intercept algorithm starts. Subtracting this value from the height of the RP gives the differential height between the UAV and its original target point. The differential height can be used to determine the horizontal distance between the RP and the intercept. This is accomplished using the glideslope descent angle (*eqn. 4.1*). To find the horizontal components of the intercept point, the horizontal distance between the RP and the intercept is used in combination with the glideslope bearing angle to determine the differential distance between the intercept point and the RP. When the differential values are summed with the coordinates for the RP, the result is the coordinates for the intercept point (*eqns. 4.2-4.4*). The vertical coordinate of the intercept is the same as that for the initial position for the craft when the intercept algorithm is activated.

$$r_1 = \frac{H_{RP} - H_{UAV}}{\tan \gamma_{GS}} \tag{4.1}$$

$$N_{\text{int}} = N_{RP} + r_1 \sin \alpha_{GS} \tag{4.2}$$

$$E_{\text{int}} = E_{RP} + r_1 \cos \alpha_{GS} \tag{4.3}$$

$$H_{\text{int}} = H_{UAV} \tag{4.4}$$

where,

r_1 = Horizontal distance between the RP and the intercept (method 1)

γ_{GS} = GS descent angle

N_{int} = North coordinate for intercept

α_{GS} = GS bearing angle

E_{int} = East coordinate for intercept

H_{int} = Height of intercept

Of course contingencies must be made to avoid using this method when γ_{GS} is small. When the descent angle to the GS is shallow, the fly horizontal method may put the craft beyond the LSP, thus putting it in peril. To avoid this occurrence, the distance between the RP and the intercept must be compared with the length of the GS itself. If the prior exceeds the latter, there is a problem with the current choice of intercept as the craft will overshoot the LSP. In the interest of safety, to avoid overshoot, a new intercept should be chosen. For simplicity's sake, it should be one of the ends of the GS. The best choice of intercept would then be the RP. This point is preferred over the LSP as reaching the RP does not require flight through space which has not been cleared of obstacles. An alternate approach is method 4.

4.3.2 Method 2: Fly to RP

The fly to the RP method is used when the craft is found to be above the RP and behind the vertical extension to the GS. The aforementioned location in the ideal system is depicted by zone 2 in *figure 4.7b*. Of the three possible methods of determining a target point, this is the easiest since there is no calculation involved. The intercept is the RP, so the values for the intercept coordinates are simply as follows.

$$N_{int} = N_{RP} \tag{4.5}$$

$$E_{int} = E_{RP} \tag{4.6}$$

$$H_{int} = H_{RP} \tag{4.7}$$

The intercept algorithm benefits from this method's ability to produce harmonious flight commands between the intercept portion and the GS descent portion. Moreover, it requires no calculation time. This absence of calculations is of great importance as it improves the overall performance and response of the craft.

4.3.3 Method 3: Cylinder Radius Method

The cylinder radius method is one of the methods used when the craft is located in zone 3. It is used when the craft is located ahead of the GS regardless of the craft's relative vertical position. The method involves dropping the UAV down to the GS with very little travel in the direction of the LSP. The avoidance of forward travel in this region is key since it is already ahead of the GS.

The concept to calculate this intercept revolves around using the craft's horizontal position information to find where is the best intercept for the given situation. The horizontal distance is calculated between the RP and the UAV. If the RP is considered the datum for this method, the distance becomes a radius with the central point being the RP. This is the same idea as in method 1 only the radius is taken from the UAV position unlike that performed in the other method where the horizontal radius was taken between the intercept and the RP. If only the horizontal plane is considered and the apparent radius is rotated about the RP, it can't help but intersect the GS at some point (*figure 4.8a*). This figure depicts the plan view of the three dimensional problem, thus ignoring

the height of the two entities. If the height aspect is reintroduced and the arc created by the rotating of the radius about the RP is given some depth of height, it resembles a section of a cylinder (*figure 4.8b*). The point where the apparent cylinder crosses the GS is the intercept point hence the term cylinder radius method. As is evident from *figure 4.8a*, the amount of forward flight is quite small.

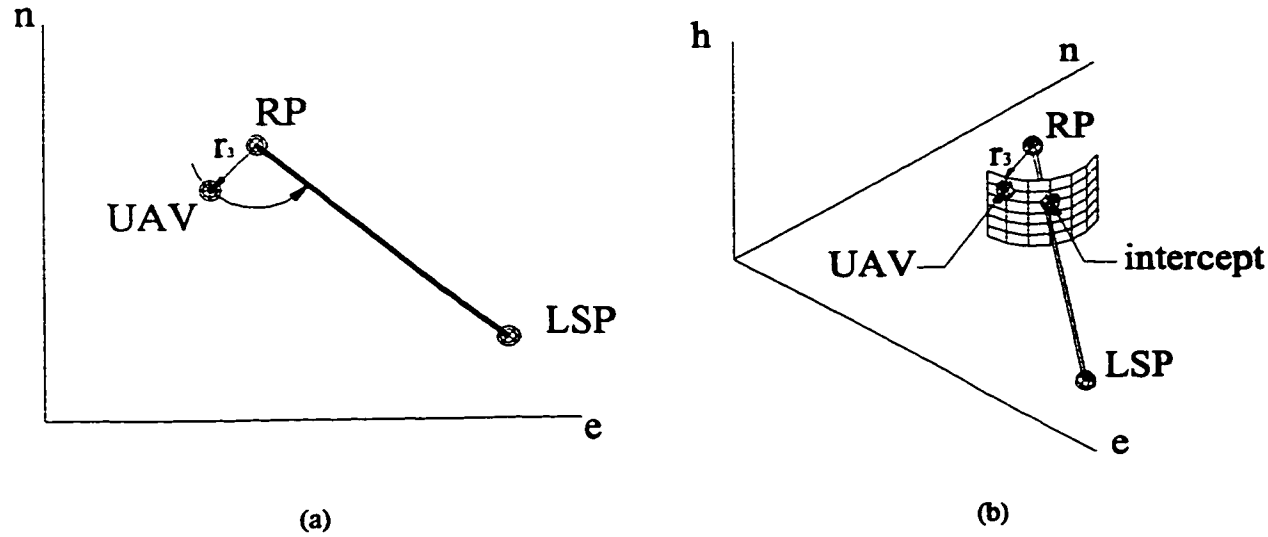

Figure 4.8 – Visualization of cylinder radius method

The manner in which this method calculates the intersect point resembles the first method somewhat. It starts with determining the horizontal distance between the RP and the UAV. This means that the altitude of the craft relative to the RP is of no concern (*eqn. 4.8*).

$$r_3 = \sqrt{\left(N_{UAV} - N_{RP}\right)^2 + \left(E_{UAV} - E_{RP}\right)^2} \qquad (4.8)$$

where,

r_3 = Horizontal distance between UAV and RP (method 3)

This effective radius when combined with the known geometry of the GS produces the intercept point. The GS geometry variables α_{GS} and γ_{GS} are employed in conjunction with the RP coordinates to determine the intercept point (*eqns.4.9-4.11*)

$$H_{\text{int}} = H_{RP} + r_3 \tan\gamma_{GS} \tag{4.9}$$

$$N_{\text{int}} = N_{RP} + r_3 \sin\alpha_{GS} \tag{4.10}$$

$$E_{\text{int}} = E_{RP} + r_3 \cos\alpha_{GS} \tag{4.11}$$

Similar to the fly horizontal method, the cylinder radius method runs into problems when the UAV lies some distance from the RP or when γ_{GS} becomes exceedingly large. If either of these conditions exist, the greater the chance that the intersect will fall outside the SV. To prevent this, the height differential between the RP and the intercept is compared against the height of the SV (H_{SV}). If the prior is greater than the latter, an overshoot problem exists.

4.3.4 Method 4: Intersection of GS and SVB

The previous method illustrates one manner of choosing a target point for the ahead spectrum. This method works very well when the craft is close to the RP and the horizontal distance between the RP and the UAV is small. If the craft lies some distance away, the intercept may fall outside the SV. If method 3 was used in this case, the craft would create its own path, one which is through unfamiliar territory. The SV, up to and including the SVB, represents the area which the intercept must fall within. By calculating the intersection of the GS with the SVB, the intercept the furthest from the RP while still within the confines of the SV is found. Examples which illustrate scenarios

where the craft lies too far from the RP (*figure 4.9a*) and a GS which is overly steep (*figure 4.9b*) are depicted.

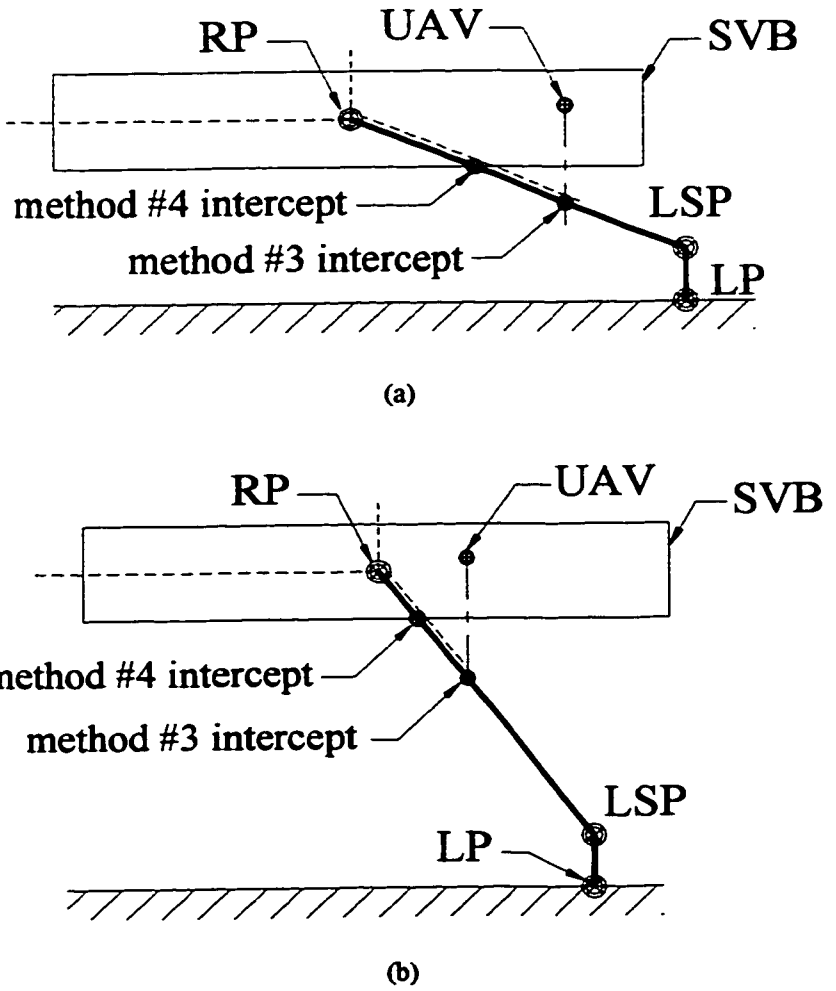

Figure 4.9 – Examples where method 3 breaks down

To calculate the intersection point of the SVB with the GS, the only values required are those which describe the geometry of the GS and that of the SV. Since the method requires no data relating to the UAV position, the coordinates for this intercept method can be calculated prior to the switchover from the GPS to DGPS. This ability to prepare prior to the actual time at which the intercept is required, reduces demand on the microprocessor during this crucial period thereby accelerating the process as a whole.

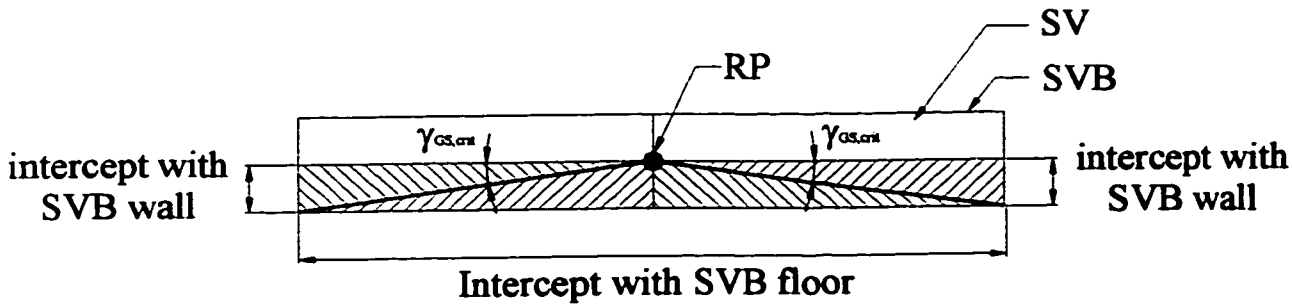

Figure 4.10 – Method 4

The possibilities exist that the intercept point could be with the wall of the SVB or more likely its floor (*figure 4.10*). To determine the intercept with the floor, it is known that the change in altitude is exactly equal to half the height of the SV. From this, the geometry of the GS, and the RP coordinates, the intercept can be found. The coordinate of the vertical can be found as simply as subtracting the height of the SVB from that of the RP (*eqn. 4.12*).

$$H_{int} = H_{RP} - H_{SV} \qquad (4.12)$$

where,

H_{SV}= Height of the safety volume

To find the horizontal coordinates of the intercept, again the horizontal distance between the intersection point and the RP is required (*eqn. 4.13*). Using this horizontal distance, the horizontal coordinates are easily calculated (*eqns. 4.14* and *4.15*).

$$r_4 = \frac{H_{SV}}{\tan \gamma_{GS}} \qquad (4.13)$$

$$N_{int} = N_{RP} + r_4 \sin \alpha_{GS} \qquad (4.14)$$

$$E_{int} = E_{RP} + r_4 \cos \alpha_{GS} \qquad (4.15)$$

In the event that the intersection of the GS is with the wall of the SVB, calculations the same as those used in the cylinder radius method are used. Seeing as the wall of the SVB is a known horizontal distance away, this gives the horizontal radius. The vertical coordinate is derived from this horizontal radius and γ_{GS} similar to *eqn. 4.9*. The horizontal coordinates are calculated in the same way as *eqns. 4.10* and *4.11* save for the fact that r_4 is replaced by the radius of the SV (R_{SV}).

The methods to find the intercept point, when the SVB is the limiting factor, is a very simple process mathematically. The points themselves involve only a basic test of geometry. The two cases are also mutually exclusive. Either the GS intercepts the floor or the wall of the SV, so the distinction must be made as to which method to pursue. The solution to this is also an exercise in simple geometry. Since the dimensions of the SV and γ_{GS} are known previously, it can be easily solved using γ_{GS} and the SV dimensions The GS angle which indicates the switchover from floor intercept to wall intercept is known as the critical GS descent angle ($\gamma_{GS,crit}$) (*figure 4.10*). This angle is found using the height and radius of the SV (*eqn. 4.16*). Knowing $\gamma_{GS,crit}$, the specifics as to a wall or floor intercept is a matter of comparing $\gamma_{GS,crit}$ and γ_{GS}. If the latter is greater or equal to the prior, then the intercept between the GS and the SVB will be with the floor. Otherwise the intercept will be with the wall.

$$\gamma_{GS,crit} = \tan^{-1}\frac{H_{SV}}{R_{SV}} \qquad (4.16)$$

where,

$\gamma_{GS,crit}$ = Critical glideslope angle

R_{SV} = Radius of the safety volume

Again a contingency must be made if the length of the line connecting the RP with the intercept is longer than the GS. This would mean that the LSP rests within the SV itself. This is possible when the γ_{GS} is low and the GS short. The distances of interest here are between the RP and the intercept and that between the RP and the LSP. With these known, the craft can be told to carry on with the original intercept, or rather go to the LSP. The second of the two options would result in a skip of the glideslope following portion entirely and reconvening the autoland process with the final descent segment. It should be said that the chance of this sort of occurrence where the LSP lies within the SV is slight. The concept behind the glideslope is that it has a significant amount of vertical travel thus allowing for a tighter and safer path to follow in landing. This last occurrence would be considered out of the ordinary.

This concludes what is to be done with the craft once it is found where it lies relative to the RP. All regions of the ideal system have been covered and for some, multiple methods have been presented. The final order of business is to determine exactly where the craft lies relative to the RP. This will be the topic of concern for the remaining sections.

4.4 Cartesian System as a Base for the Ideal System

The ideal system is the framework upon which the intercept selection methods are based. It is therefore this system which must be replicated in one manner or another. The fact that the planes used to describe the ideal system are not perpendicular is a major issue. To replicate the ideal system as a system of planes in space would be very involved. Then the craft location would have to be determined within this system of planes in space. Again a difficult task. A simpler approach is introduced in the utilization of the standard Cartesian axis system as a base system of planes to replicate the ideal system. With the location of the craft determined within this simple grid, useful knowledge as to craft location about the RP would be known.

The Cartesian system of planes is the most widely used reference system. It consists of three planes all perpendicular to one another. Its use in this application is to place the origin of the Cartesian system at the RP and to orient the system such that it is as accommodating as possible to relative craft location calculations. The inertial coordinate system is also based on a Cartesian system. It is no coincidence that the system centered at the RP was selected to be a Cartesian system as well. The two will be used in conjunction with one another to determine the position of the craft first about RP centered system, but ultimately about the ideal system. A complete discussion of this topic will be left for later.

The major drawback to the Cartesian system is that since its planes are all perpendicular to one another, they will never correspond directly to the ideal system. Thus to replicate the ideal system exactly, supplemental calculations must be made to

provide for the ideal system. Even with this drawback, using the Cartesian system of planes as a base from which to work is the simplest method.

The orientation of the Cartesian system itself has not been addressed. It is understood that the origin will be located at the RP, but that is all that has been decided. To finalize the coordinate system definition, other factors must be considered especially the manner of determining how the craft will be located within the Cartesian arrangement. To explain this, Appendix B gives a quick overview of the homogeneous matrix transformations which will be used to manipulate the relative system such that pin-pointing of the craft will be a simple affair [30] [31]. The remaining question is what will be the orientation of the base system? All that has been determined is that it will be centered at the RP. Two orientations will be described in the following section.

4.5 Ideal System Implementation Methods

The previous section has called for the Cartesian system origin and the RP to become one and the same, but how should the RP centered system be oriented? The end result is to find a simple manner in which to replicate the ideal system. To do this, a combination of the Cartesian system and supplemental calculations must be employed. The arrangement demonstrating the best results will be the one used for the autoland. It must be reiterated that the solution will be one where the quadrant system works harmoniously with the UAV locating method. They must complement one another. Two orientations of systems will be explored. The first will be the glideslope aligned system followed by the horizon aligned system.

4.5.1 Glideslope Aligned System

The first quadrant configuration considered is the one illustrated in *figure 4.11a & b*, and is termed the glideslope aligned system (GAS). The origin for the system is the RP and the CP is used to designate the ideal path of travel. This plane will determine if the UAV is found to the left or the right of the GS. The second of the three planes runs along the GS and is perpendicular to the CP. The third plane contains the RP and is perpendicular to the other two planes. To superimpose the ideal system onto this orientation of the Cartesian arrangement and to look perpendicular to the CP (*figure 4.12*), shows the ideal arrangement dividing two separate Cartesian quadrants. Contingencies will have to be made to account for this.

This system is oriented along the GS, but is located in a region of space dependant on the RP location. Using translation and rotation transformations, a simple, reliable solution is obtainable to determine where the craft lies. Using transformations, the whole

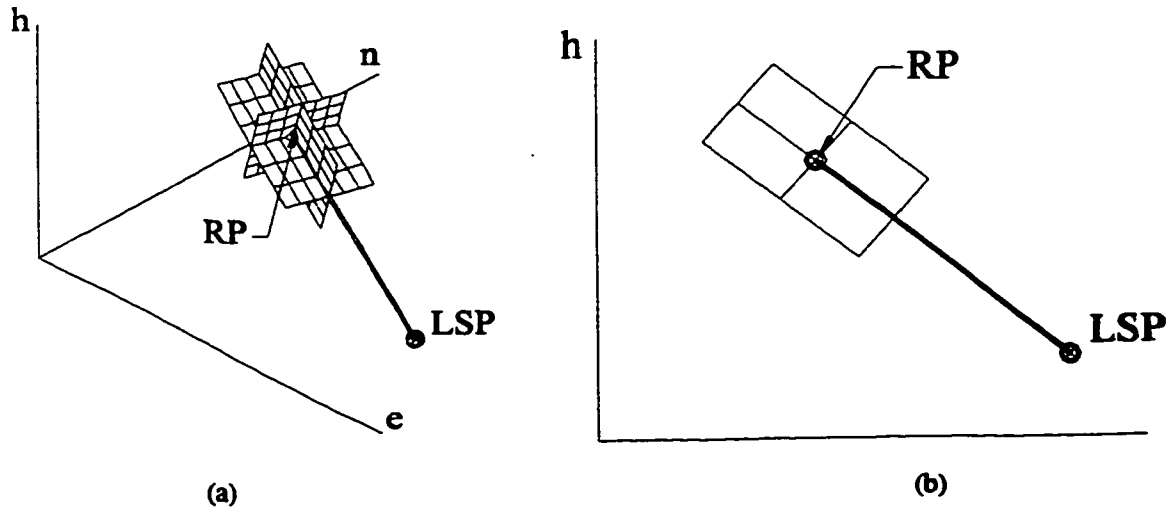

Figure 4.11 – GAS

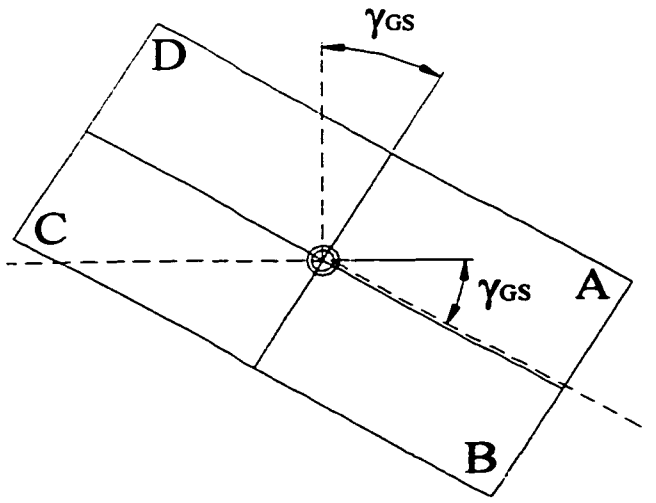

Figure 4.12 – Ideal system overlaid upon GAS

RP centered system can be moved and rotated such that the three perpendicular planes of the GAS align directly with the north, east, and height axes of the inertial axis system. Knowing these steps, the same transformations can be performed on the UAV coordinate, thereby making the pinpointing of the craft, for the most part, a simple two dimensional task of verification of signs of the transformed UAV coordinates. This is the rationale behind using a Cartesian form as a base for the ideal system.

For the sake of simplicity, the inertial axis system, which has been characterized by the designation of north, east and height, will be renamed for the transformation portion. This is in the interest of confusion avoidance for when the axes X, Y, and Z are indicated, this implies that the coordinates have been or are in the process of being transformed. It also clarifies which transformation is used as the rotational transformations are described in terms of rotations about the conventional X, Y, and Z axes. In this case, east will be known as the X-axis, north will be named the Y-axis, and the height axis will become the Z-axis. It is important to point out that the angles

describing the bearing and descent angle of the GS can be used throughout the transformation process. They will prove very useful. Through the rest of this section, the emphasis will be put on transforming the RP centered system about the newly designated X, Y, and Z inertial based system. In reality, when these procedures are incorporated into the autoland, the only object to be transformed will be the UAV. Describing the transformation of the system is for illustration and comprehension purposes only.

The first transformation made is the translation of the RP to the origin of the newly entitled X, Y, and Z axis system. As the origin of the base system is (0,0,0) and the origin of the RP centered system is just as its name describes, the RP, the transformation is accomplished by adding the negative coordinates of the RP to the system as a whole. Consequently, the transformation is that given by *eqn. 4.17*. *Figure 4.13* illustrates the progression of the transformations of the RP centered system will undergo. *Figure 4.13a* shows a typical location for a flight profile, while *figure 4.13b* shows the result of the translation just described. Notice that the RP now coincides with the origin of the inertial system.

$$T^{RP} = \begin{bmatrix} 1 & 0 & 0 & 0 \\ 0 & 1 & 0 & 0 \\ 0 & 0 & 1 & 0 \\ -N_{RP} & -E_{RP} & -H_{RP} & 1 \end{bmatrix} \qquad (4.17)$$

where,

T^{RP} = Transformation of RP to origin of inertial system

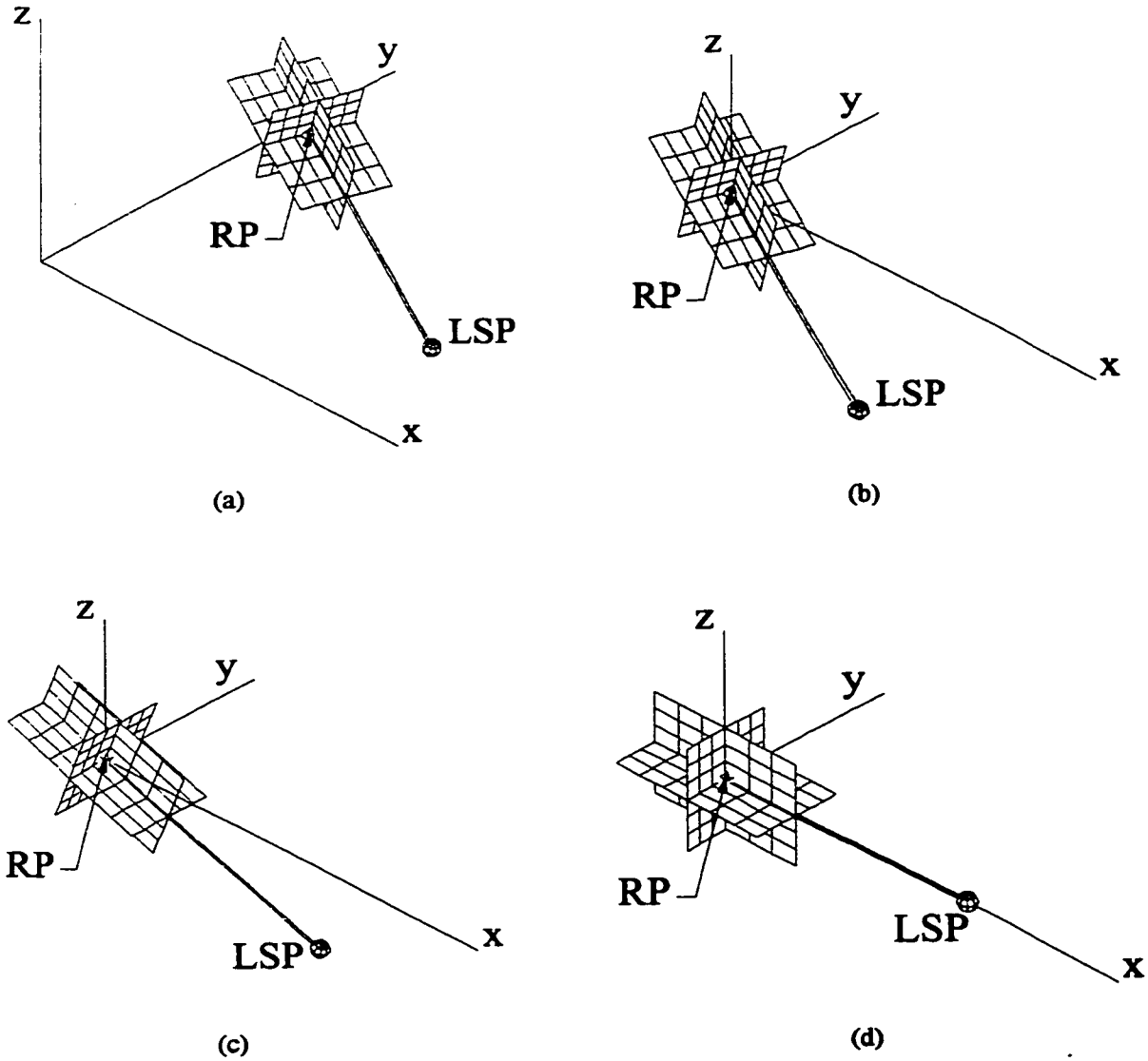

Figure 4.13 – Step by step transformations of RP based GAS

The next transformation is rotating the translated system about the Z-axis. The desired amount of rotation is such that the two planes which intersected on the GS should lie directly beneath the X-axis (*figure 4.13c*). The GS bearing angle (α_{GS}) is given from the east which conforms to the X-axis in the transformed system. Since α_{GS} is calculated directly from the original position coordinates, it is still valid. It goes that the angle of rotation is to be enough to counter that of the GS bearing angle to rotate the system back

in alignment with the X-axis. The rotation of the quadrant system about the Z-axis by $-\alpha_{GS}$ is given by (*eqn. 4.18*).

$$R_Z^{-\alpha_{GS}} = \begin{bmatrix} \cos\Lambda & \sin\Lambda & 0 & 0 \\ -\sin\Lambda & \cos\Lambda & 0 & 0 \\ 0 & 0 & 1 & 0 \\ 0 & 0 & 0 & 1 \end{bmatrix} \qquad (4.18)$$

where,

$\Lambda = -\alpha_{GS}$

$R_Z^{-\alpha_{GS}}$ = Rotation about the Z-axis by angle $-\alpha_{GS}$

The third and final rotation required to align the GAS with the origin of the X, Y, and Z-axis system is a rotation about the Y-axis. This transformation rotates the system so that what used to be the line which described the GS will align itself directly along the X-axis (*figure 4.13d*). The GS is always oriented between the horizontal and pointed straight downwards, so therefore, the rotation itself is always in the same direction. This means that the amount of rotation is equal to that of the descent angle (γ_{GS}). It therefore comes down to rotating the transformed system up to the horizontal which is now known as the X-axis. The angle of rotation must counter the original angle of the GS, therefore the transformation must be for $-\gamma_{GS}$. Thus the transformation matrix will resemble the following (*eqn. 4.19*)

$$R_Y^{-\gamma_{GS}} = \begin{bmatrix} \cos\Gamma & 0 & -\sin\Gamma & 0 \\ 0 & 1 & 0 & 0 \\ \sin\Gamma & 0 & \cos\Gamma & 0 \\ 0 & 0 & 0 & 1 \end{bmatrix} \qquad (4.19)$$

where,

$\Gamma = -\gamma_{GS}$

$R_Y^{-\gamma_{GS}}$ = Rotation about Y-axis by angle of $-\gamma_{GS}$

To determine the transformed position of the UAV, its homogeneous position can be multiplied by each of the matrices separately. A simpler method is to create a concatenated matrix. A concatenated matrix is one where all the transformation matrices are multiplied together to form one matrix which the UAV coordinate in homogeneous form can then be multiplied by. The concatenated matrix from this method is shown in *eqn. 4.20*. As was described previously, the fact of whether the craft lies to the right or left of the plane of symmetry is of no interest. It has no bearing on the decisions being made. The CP which was the plane of symmetry has been transformed such that in the transformed system, plane XZ is the symmetrical plane. Consequently, the information concerning the Y position of the UAV after transformation is of no interest. Similarly, no scaling is to be performed so the fourth column of the concatenated matrix is not required. Only the X and Z components of the transformed UAV position are of use. Therefore, to remove unnecessary calculations, the concatenated matrix in *eqn 4.20* can be reduced to that of *eqn. 4.21*.

$$T_{TOTAL}^{GAS} = \begin{bmatrix} \cos\Lambda\cos\Gamma & \sin\Lambda & -\cos\Lambda\sin\Gamma & 0 \\ -\sin\Lambda\cos\Gamma & \cos\Lambda & \sin\Lambda\sin\Gamma & 0 \\ \sin\Gamma & 0 & co\Gamma & 0 \\ \cos\Gamma\{-E_{RP}\cos\Lambda + N_{RP}\sin\Lambda\} - H_{RP}\sin\Gamma & -E_{RP}\sin\Lambda & -\sin\Gamma\{-E_{RP}\cos\Lambda + N_{RP}\sin\Lambda\} - H_{RP}\cos\Gamma & 1 \end{bmatrix} \quad (4.20)$$

where,

$\Lambda = -\alpha_{GS}$

$\Gamma = -\gamma_{GS}$

$$T_{TOTAL,RED}^{GAS} = \begin{bmatrix} \cos\Lambda\cos\Gamma & -\cos\Lambda\sin\Gamma \\ -\sin\Lambda\cos\Gamma & \sin\Lambda\sin\Gamma \\ \sin\Gamma & \cos\Gamma \\ \cos\Gamma\{-E_{RP}\cos\Lambda + N_{RP}\sin\Lambda\} - H_{RP}\sin\Gamma & -\sin\Gamma\{-E_{RP}\cos\Lambda + N_{RP}\sin\Lambda\} - H_{RP}\cos\Gamma \end{bmatrix} \quad (4.21)$$

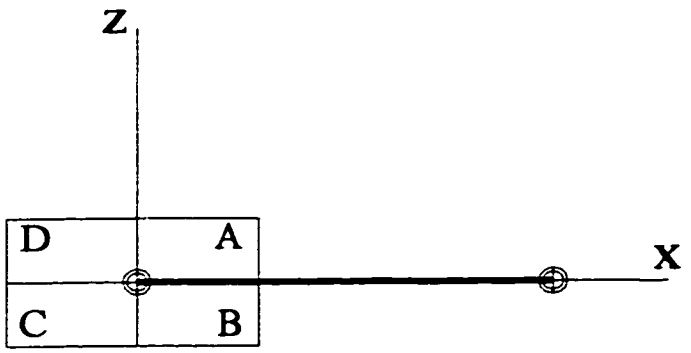

Figure 4.14 – Final transformation of a GAS

The craft location with respect to the quadrants must now be found. Referring to *figure 4.14*, it is evident that because of the transformations, each quadrant in the transformed system has a unique sequence of X and Z values which is dependant solely upon the sign of the two variables. Positive X and Z components of the transformed UAV position means that the UAV is located in quadrant A, whereas a positive X and a negative Z means that the craft is located in quadrant B. The full story is illustrated in *figure 4.14*. This brings to an end the analysis of the transformed system as all the information it can give has been drawn.

With the discussion of the transformed system complete, the idea behind the supplemental equations is turned to. To reiterate, by referring back to *figure 4.12*, when the ideal system is overlaid upon this GAS, there are regions in the quadrants represented by C and D which are split by the ideal system. These split quadrants will also have split philosophies as to where the craft will intercept the GS. For example, the majority of quadrant C is below the RP while the top section of the quadrant is above the RP. This means that even though the UAV may lie in this quadrant, its exact location within the quadrant determines which method of intercept calculation is undertaken. In this

instance, the height of the craft when compared with the RP, before any transformation has been made, determines its location and solves the problem for quadrant C.

The second such example is quadrant D. For the most part, the area lies above the RP and behind the GS. This is not the case in the small segment furthest forward. This area which extends ahead of the RP does not correspond to the philosophy for the rest of the region as described by the ideal system. Thus provisions must be made to rectify the discrepancy. This is performed by using a combination of the transformed and non-transformed UAV coordinate and data. The angle made between the plane which perpendicularly intersects the GS and the vertical is the absolute value of the descent angle ($|\gamma_{GS}|$) as shown in *figure 4.12*. Now, by using the transformed values to determine the angle between the UAV and this same plane, it can be verified whether the UAV lies ahead or behind the vertical section of the GS. In the transformed system, the plane which the angle is being taken from is the Z-axis, so it goes that the values required to determine the angle are the transformed X and Z values. The angle made by the vector containing the transformed UAV point and the RP with the plane perpendicular to the GS is described by *eqn 4.22*. It must be kept in mind that this is entirely a two dimensional analysis. Then the logic used to determine on which side of the ideal plane the craft lies is given by *eqn. 4.23*.

$$\phi = \tan^{-1}\frac{X}{Z} \qquad (4.22)$$

$$\textit{if } \phi > \gamma_{GS} \Rightarrow \textit{craft lies behind RP}$$
$$\textit{else craft lies ahead of RP} \qquad (4.23)$$

where,

ϕ = Angle between UAV and the plane perpendicular to GS

X = X component of transformed UAV location

Z = Z component of transformed UAV location

With these last two conditions, the system is fully developed. Six quadrants and two supplemental conditions are required to determine which ideal quadrant the craft lies within when using the GAS as a base. This solution is quite involved and complicated. The concatenated matrix, even the reduced one, demonstrates this. There is however the second system which is to be explored before a definitive decision is made as to which arrangement will be implemented.

4.5.2 Horizon Aligned System

The horizon aligned system (HAS), shown in *figure 4.15*, differs from the GAS by the location of the second and third planes. This means that the CP is again used, but that the second plane is perpendicular to the CP and parallel to the ground. The third plane is again perpendicular to the first two planes and passes through the RP.
As with the GAS, the starting point in craft location is to utilize transformations. Again the goal of the transformations, similar to those for the GAS is to translate and rotate the system so it lines up with the real life north, east, and height axes. The first transformation is to translate the RP to the origin of the X, Y, and Z axes. This transformation is identical to that described in the GAS and therefore the translation matrix described in *eqn. 4.17* holds true here. The next transformation is a rotation about

the Z-axis to align the GS with the X-axis. As before with the GAS, the angle of rotation is such to counter α. Again, this manipulation is identical to that one done for the

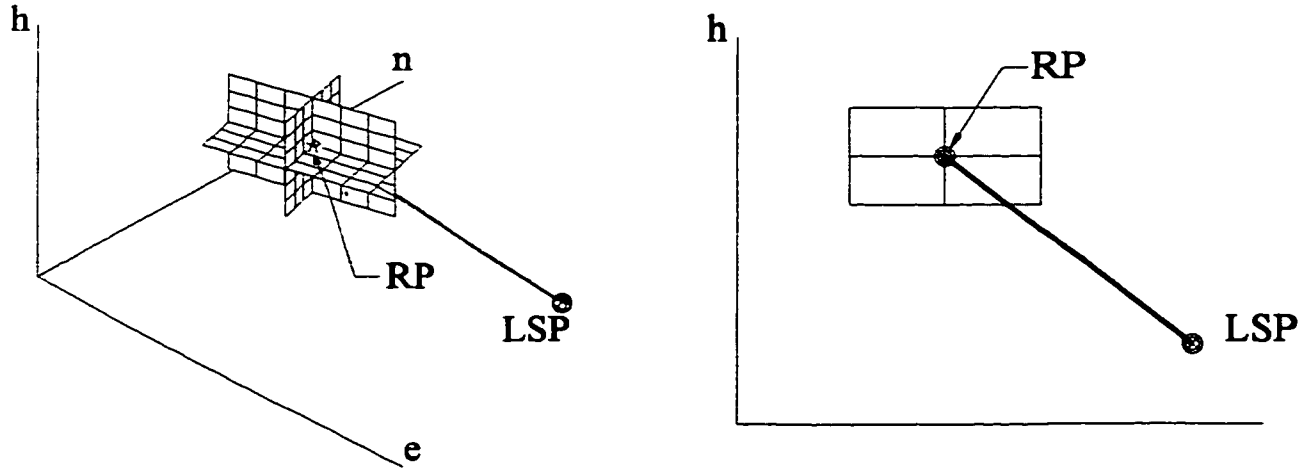

(a) (b)

Figure 4.15 – HAS

previous system so therefore the transformation shown in *eqn. 4.18* is true here. These are the only transformations required to align the quadrants to the X, Y, and Z axis system. This is a reduction of one transformation as opposed to the GAS. The concatenated transformation matrix for the HAS is shown in *eqn. 4.24*.

The reduced transformation matrix is given by *eqn. 4.25* and shows a marked simplification over the one derived for the GAS given by *eqn. 4.21*. As with the first quadrant arrangement, the signs of the transformed UAV position values are all that is required to determine the quadrant of the craft. This is all the information which could be garnered from the transformed system. This gives the preliminary location of the craft.

Now with the basic transformations complete, the last step is to provide contingencies for regions whose quadrants are split as to their function. To verify this the

$$T_{TOTAL}^{HAS} = \begin{bmatrix} \cos\Lambda & \sin\Lambda & 0 & 0 \\ -\sin\Lambda & \cos\Lambda & 0 & 0 \\ 0 & 0 & 1 & 0 \\ -E_{RP}\cos\Lambda + N_{RP}\sin\Lambda & -E_{RP}\sin\Lambda - N_{RP}\cos\Lambda & -H_{RP} & 1 \end{bmatrix} \tag{4.24}$$

where,

$$\Lambda = -\alpha_{GS}$$

$$\Gamma = -\gamma_{GS}$$

$$T_{TOTAL,RED}^{HAS} = \begin{bmatrix} \cos\Lambda & 0 \\ -\sin\Lambda & 0 \\ 0 & 1 \\ -E_{RP}\cos\Lambda + N_{RP}\sin\Lambda & -H_{RP} \end{bmatrix} \tag{4.25}$$

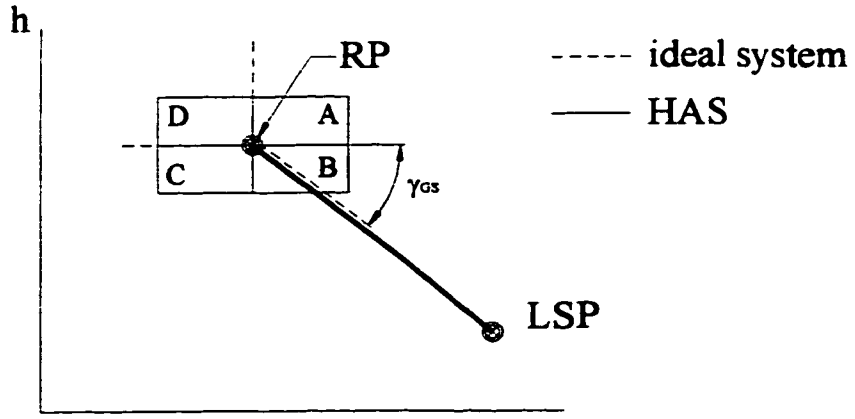

Figure 4.16 – Ideal system superimposed over HAS

ideal system diagram is overlaid on the HAS as shown in *figure 4.16*. This shows that the only region split by the ideal system is quadrant B. It contains space which is both ahead and behind the GS. This problem can be remedied the same as was done for quadrant C for the GAS. The line which dictates whether the craft lies ahead or behind the GS is the GS itself. Therefore the angle which in this case is the critical angle is the descent angle. When looking perpendicular to the CP, the angle composed of the UAV position, the RP and the horizon is found using the transformed coordinates using *eqn. 4.26*. Then according to *eqn. 4.27*, the craft can be placed ahead or behind the GS. This system can now fully represent the ideal system

$$\phi = \tan^{-1}\frac{Z}{X} \qquad (4.26)$$

$$\begin{aligned} &\textit{if } \phi > \gamma \Rightarrow \textit{craft lies behind GS} \\ &\textit{else craft lies ahead of GS} \end{aligned} \qquad (4.27)$$

When comparing the two methods, the GAS and the HAS, there is an obvious choice. The HAS requires one less transformation than its counterpart. Because of this fact, *eqns. 4.20* and 4.25 shows the distinct difference and evident simplicity of the HAS's simplified concatenated matrix as opposed to that of the GAS. In addition to this, the basic HAS, without any supplemental conditions, approaches the ideal system more closely than the GAS. It has only one quadrant which is split between two of the ideal quadrants. In fact, there is no point where the GAS shows a marked improvement over the HAS. For these reasons, the HAS is the system of choice for UAV pin pointing.

4.6 Simplified Version

The methods described in section 4.3 are very specific and give exact results. No matter where the craft lies, the most proximal intercept point is found. This approach can be used if the utmost accuracy is required. For some situations however, this rigidly precise approach to intercept calculation is not necessary. Simplifications can be made which will alter the path somewhat, yet continue to ensure craft safety. The idea is to have only two possible intercept to chose from, the RP and where the GS intersects the SVB. The RP represents the first available point on the GS to intersect while the intersection between the GS and the SVB represents the furthest most point allowed. Thus the methods disregarded would be numbers 1 and 3, which choose intercepts between these two points. A typical scenario with the GS and the SV to scale is illustrated in *figure 4.17*. The reduction in distance traveled due to the simplification is minor as compared to the length of path that the GS covers. The simplification in no way causes any increased risk to the vehicle as it always connects with a point which is within the SV and thus is protected.

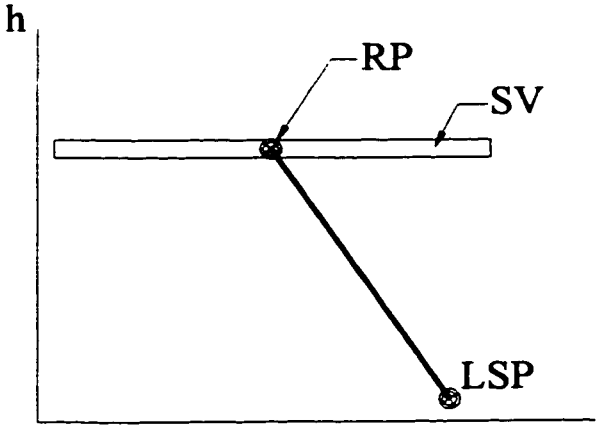

Figure 4.17 – Scale drawing of flight profile including SV

The major cause for simplification is for reduced calculations. The various methods which were devised were respectful towards this issue and at every turn during their development. This simplification goes one step further in reducing the number of calculations and moreover, those methods which remain do not require UAV position information and so can be performed at any time during the flight. Thus reducing the load on the microprocessor during the switchover procedure.

These reductions are not limited only to the intercept coordinate calculation portion. Rather the reduction in calculations are most prominent in the craft locating stage. With the reduction of the intercept options, the ideal system can be modified accordingly. *Figure 4.18* shows the new ideal system layout. If the craft lies above and behind, then the intercept is the RP. For a craft found in any other location, the intersection between the GS and the SVB is the place the craft will be sent. Thus, if after the UAV coordinates have been transformed they read $Z>0$ and $X<0$, then the RP is the intercept. For all other cases, the SVB is where it is to head to. It is a very simple system as the HAS corresponds exactly to that of the ideal system and so supplemental

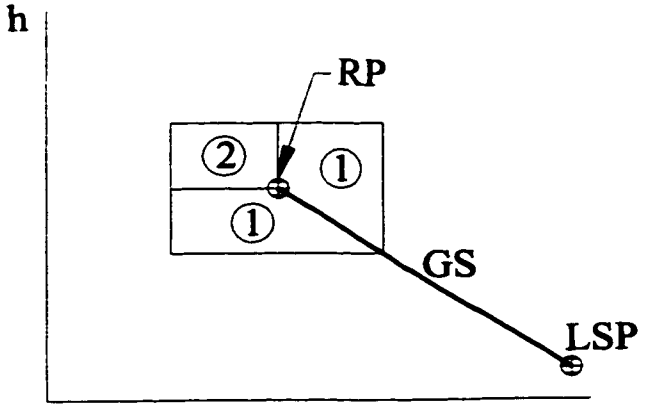

Figure 4.18 – Ideal system for simplified approach

calculations are not required.

The GS intercept algorithm is an effective tool in the autoland program. It reorients the AV away from the RP and towards a more suitable point in which to meet up with the GS. It does this ensuring complete safety of the craft through flight within the confines of the SV. It also performs the task with very few operations in order not to burden the microprocessor. This algorithm gives the craft a target point, but has told the craft nothing of how to get there. The straight-line path between where the craft lies and the intercept seems simple enough to negotiate, but the manner in which the AV is to get there must be implicitly described. To this end, the next chapter on trajectory generation gives specific directions to the craft of how to get between the two points.

5.0 Trajectory Generation Algorithm

With the location of the intercept point known, the next step is getting the craft to the intercept from where it was originally found after the switchover from GPS to DGPS. This is an involved topic which represents the larger issue of determining an appropriate method in which to lure the craft from one point to another. The method must be respective of the various criteria for flight which are required. The criteria includes those set out to provide safety limits, enhance performance while maintaining stability and handling, and, like that of the intercept algorithm, those concerning the free-ranging geometry of the path. Using the criteria for flight between two arbitrary points as a foundation, the reasoning behind the trajectory generator for the autoland process is developed.

The generator takes the known distance between the two points and creates a profile to determine where the craft should be at a given instant in time. This outlines the basic working theory behind the device, but how to go about doing it is where the questions begin. How will this path be created? What makes one path better than another? How long will it take the craft to travel between the points? How will the descent angle and bearing angle of the path effect the trajectory? How are the criteria for flight to be respected at the same time? These are all issues which will be addressed in order to select the best method to generate a trajectory for this application.

Reference is being made to devise this logic for two points rather than uniquely for the intercept portion of the autoland process. This is due to the desire for a universal trajectory generator. It will be capable of guiding the unit between any two points in

space. This makes it useful for the intercept portion , the glideslope descent portion, and any other situation which is similar.

5.1 Required Criteria

The conditions for the path in general and more specifically the trajectory generator itself are that which are at the heart of the design. They exist for various reasons, craft safety and stability concerns, those pressing for optimum performance and those addressing flexibility of path geometry. Together they lay a groundwork from which to start.

5.1.1 Safety and Stability

The criteria required of the algorithm grouped under the safety and stability banner exist to provide limits. These limits exist in order that the craft doesn't push itself so far that it subsequently will not be able to regain control of itself, hence their close ties with stability [29]. The three limits which must be respected during these maneuvers are those which effect the peak velocity, the vertical velocity, and the limit associated with the rate of change of lateral velocity or more specifically, a limit to the rate at which the craft can tilt or pitch over.

The first limit pertains to the maximum peak velocity ($V_{P,max}$) of the unit. The peak velocity is the highest combination of vertical and horizontal velocity the craft obtains when travelling between the two points. This peak velocity is given a maximum value to limit the speed of the craft as it comes through the landing maneuver. With the craft's proximity to ground and other obstacles during this phase, any sort of overshoot could result in a catastrophic event. The slower the combined velocity, the less the

chance of overshoot or worse yet, a situation where the craft becomes unstable. This limiting of the overall speed greatly reduces the chance of this occurring.

The limit to the vertical velocity ($V_{V,max}$) goes one step further than the limitation of the peak velocity and limits the vertical component of the combined velocity. This is again a case of reducing the chance of overshoot or runaway in the final moments of the mission. Even though the craft's response in the vertical significantly outperforms that in the horizontal, it is a measure which adds an additional level of safety.

The final limiter which is required is the one effecting the rate of tilt of the craft. This limiter is put in place so that when commanding a large lateral deceleration, the craft doesn't pitch itself aft so quickly that it over-rotates and produces a cartwheeling motion fueled by its own momentum. The limiter allows for a free range of tilt of a given number of degrees for a given time period. After this number of degrees has been rotated, the limiter activates itself and allows for a maximum of a certain number of degrees of rotation per second thereafter until the desired input is fulfilled. An example of how the limiter works is shown in *figure 5.1*. The difference between this limiter and the ones described previously, is that the one in question is already built into the system. Rather than incorporating it into the algorithm, similar to those previously discussed, the idea is to be aware and formulate an ideal path with the limiter in mind. It must be respected since in the vast majority of the cases where the limiter was tripped, the limited response of the craft instigates a loss of stability. It therefore goes that the point where the limiter becomes active is not to be approached as it represents the threshold zone between stability and instability. Consequently, sudden accelerations and decelerations are to be avoided at all costs. This is a very significant point to keep in mind.

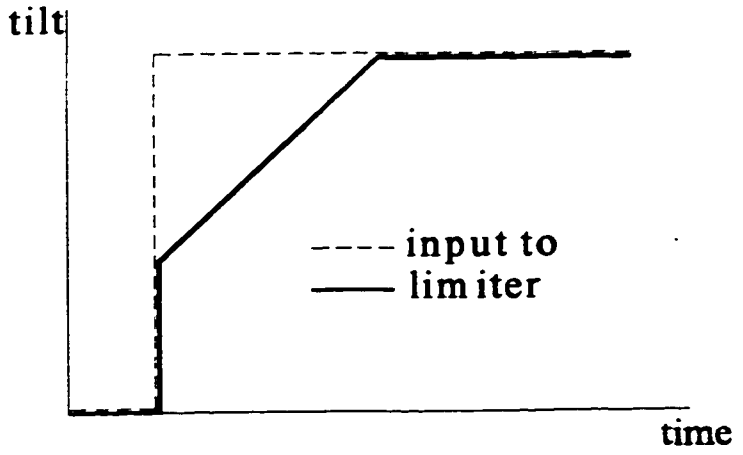

Figure 5.1 – How tilt limiter alters desired tilt command to the craft

5.1.2 Performance Considerations

The next group of conditions stresses the need to achieve the best performance possible. The logic must allow for the craft to perform all that it must and to do it in an expedient manner with good accuracy. This increased performance always comes at a price of reducing the overall stability of the unit. It comes as no surprise that a compromise must be found between the two. The areas of primary concern are the total time which the process takes to complete, the ability of the craft to adhere with the prescribed path, and its ability to deal with disturbances such as signal noise and winds. These when combined with the controller, will dictate the success of the algorithm. They must compliment one another to provide a total package.

The total time required to travel between the two points is crucial. This is one of the most obvious methods of evaluation of craft performance. Seeing as there is a peak combined velocity (V_P) which exists and the craft is limited to this value, once the craft reaches this speed, its performance cannot be altered. So it goes that the areas where time

can be economized is in the acceleration up to V_P and then the deceleration from V_P to rest. However, there exists a point where, in the pursuit of reduced operating time, if the acceleration is raised too much, problems with stability will be encountered.

The ability for the craft to adhere to a prescribed path in a smooth and flowing manner is also extremely important. A craft which jerks its way between points means that it is producing an error signal range which is too large. The error signal being referred to is the difference between the actual and desired craft position and its derivatives for the same instant in time. The range of this signal comprise the positive and negative maxima which are covered by the error signal. A large range creates a system who's controller must be detuned to allow for such range. This detuning of the controller and increase of the position error range is a recipe for instabilities.

The last area where performance gains must be realized is with the ability for the craft to deal with disturbances. Even though this does not speak of performance in the sense that has been dealt with previously in this section, it speaks of real world effects which the algorithm must be capable of overcoming. These disturbances are plenty, but the principle sources lie with the DGPS provided position and velocity data and with the winds. With the position and velocity data of the craft, inconsistencies can lead to the perception of sudden jumps and shifts. Similarly, wind can suddenly gust up and knock the craft off its desired heading and alter its velocity. It's evident that the end result between the two cases is similar. This is predominantly a problem for the controller, but the construction of a forgiving path generator can take some of the pressure off the controller to deal with this problem alone. For example, a smooth and flowing path means more natural movement without the necessity of fast reaction time. This allows

the craft to remain close to the ideal location under disturbance free conditions. This will allow for better accuracy under to adverse conditions when compared with a path which is not smooth. The overall error calculated by the controller due to signal noise will be reduced, thus if the craft is already very close to where it should be, a wind which blows the craft off course will trigger a reduced response compared to a craft which was not as close to its desired position to begin with.

5.1.3 Flexibility of Path Geometry

The final criteria governing the generic path between two points in space concerns the algorithm's flexibility. More specifically its flexibility with respect to path geometry. The requirements here are similar to those specified previously for the intercept algorithm's path geometry capabilities. The algorithm to guide the craft between the two points must be capable of dealing with any length of path at any bearing angle or descent angle. Moreover, it must comply with all previously set out conditions. This flexibility will ensure a product whose ability to deal with points anywhere in space and henceforth accommodate any situation which arises.

5.2 Advantages of a Trajectory Generator

The overall requirement is to move from one point in space to another. The unit must do this smoothly and quickly. Auspiciously enough, the path has been deemed clear of obstacles and the conditions to be met and respected have been set out previously. The idea is to use a trajectory generator to accomplish the task, but is it required? What will it lend to the process as a whole? The use of a trajectory generator will vastly simplify the overall task by working in conjunction with the controller to give the craft bearing [29].

In general, the trajectory generator will provide improvements in three major categories. The first revolves around its sole variable, time. It will provide much information on specifics of craft location and exact conditions for craft performance for a given instant [29] [32]. It will also permit implementation of the required limiters, discussed in the previous section. Lastly, it will help in reducing the overall error signal determined by the controller.

A path denotes a locus of points in space. On the other hand, a trajectory is a path on which a temporal law is specified [29]. This can manifest itself in terms of velocities, accelerations, and further derivatives of displacement. The use of time also has several secondary advantages. Firstly, the problems created by the craft's disturbances have no bearing on this variable. These manifest themselves in the actual position and velocity of the unit which have no bearing if the trajectory is being created or referenced using time. The time variable is a very precise variable which is independent of disturbances. The knowledge of time or rather the time which has elapsed since the beginning of the process can give the exact position, velocity, and acceleration of the unit which is not only of great importance for control purposes, but is pertinent information to ground crew. The elapsed time can also be studied to determine exactly how the time was spent and how much was allocated to each segment. This allows for easy modifications and tuning of the procedure [4].

The trajectory generator can also implement the required criteria specified previously. It can easily create the velocity profile of the trajectory while being mindful of the limits given to the vertical and combined velocities [29]. With these in place, and a good controller conducting the process, the chance of the unit exceeding the limits by

anything except a small fraction is removed. The generator will also endeavor to smooth the profiles to avoid the tilt-rate-limiter from being triggered. To reiterate, this occurs when sharp and sudden lateral movements are commanded or if the craft is reacting to large unavoidable disturbances. Lastly, the criteria concerning the range of path geometry can be addressed prior to the craft actually moving from its initial position. Any extremes in the path, be them bearing angle or descent angle, can be adjusted for in the trajectory planning stage, thus removing any glitches before they may occur.

Where the trajectory generator really shines is in its ability to reduce the position error between the ideal and actual craft locations for a given instant in time [2] [31]. This is where its partnership with the controller comes into form. It can use the data produced by the trajectory generator to drive the unit independent of outside disturbances. This provides tighter control of the unit as a whole which in turn can lead to finer tuning of the controller. This will produce increased stability, especially under harsh conditions. Difficult conditions is where an appropriately configured trajectory generator makes its presence felt the most. Lateral or vertical winds can come up suddenly and push the craft off course. Conversely they can die just as quickly and the craft can overshoot its prescribed position. Noise contained in the actual craft position and velocity can have an equal or even worse effect and are equally as difficult to predict. Consequently, preparing for them is paramount to good vehicle control. The trajectory generator will keep the craft closer to the desired position thereby reducing tilt reaction to position and velocity errors.

In the end, the trajectory generator will provide benefits all round, ranging from reduced position error to better knowledge of mission planning to implementation of

conditions. It is a very useful tool, but the decision on what it shall consist of must be addressed. Topics such as what the overall plan for the trajectory will be, which profile is best suited, and what are the optimum profiles of the displacement derivatives are all topics which will be covered. The next section addresses the terminology associated with the various stages of the motion while the craft is under the control of the trajectory generator.

5.3 Segment Labels

To further examine trajectory generation, the process itself will be broken down into individual segments which can then be analyzed individually. In general, there will be four segments which in the order they occur are acceleration, cruise, deceleration, and station keeping. For simplicity's sake, these will be labeled segments A through D respectively (*figure 5.2*). Doing this allows for distinction between the segments. Each is to be a separate entity with a defined purpose and will spell out exactly what the craft will be doing when under its control. Seeing as the craft is traveling through segment after segment, it is of no surprise that they will be interdependent. The final conditions of one would be the initial conditions of the next. However, the variables which all segments are based upon are few. They are the total distance covered (D_T), the peak velocity (V_P), and the amount of time required to complete segment A (t_A) and segment C (t_C).

The first action performed is acceleration and is labeled segment A. The craft begins at the initial point in space and accelerates along the ideal path. Traditionally it will be accelerating from rest and will continue until it reaches V_P. As is evident by

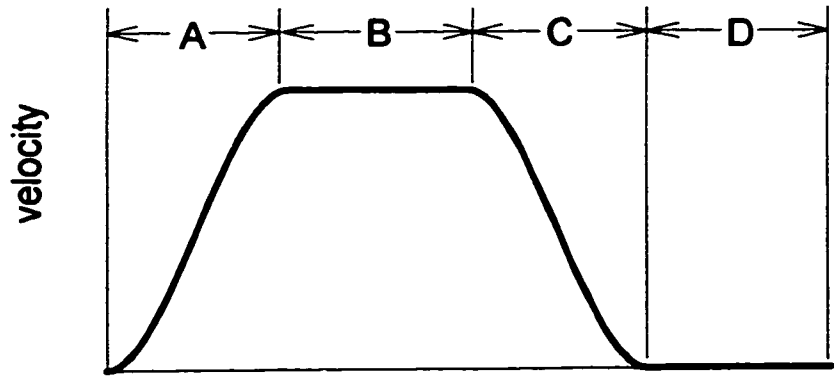

Figure 5.2 – Trajectory profile breakdown

figure 5.2, the segment is governed by the time that it takes to complete the segment. Though this segment is defined as that for acceleration, this is not the variable which it is planned around. The limit for this segment is defined as V_P as this is the velocity which is not to be surpassed. Therefore the acceleration is merely dependant on this value and the duration of the segment.

After the acceleration segment the craft embarks on a constant velocity portion. This portion is designated the cruise segment or segment B. The craft maintains the final velocity which was produced from the acceleration segment. The time which elapses during this segment is dependant on D_T. Segments A and C are considered primary regions while B is given secondary status. The distances which are covered in A and C are subtracted from D_T. The distance which remains, if any, is that which is allotted to B.

The final segment which commands motion is labeled segment C, the deceleration phase. The end of this segment is the second of the two points in space which make up the ideal path. The craft is to be rendered motionless by the end of the segment from its initial velocity of V_P. As for how it goes about this, it is very much the same as segment

A. The only difference is that t_A is not required to be the same as t_C. This then allows the profile for this segment to change as much as the user or customer so desires or requires.

The final segment is station keeping and is entitled segment D. This segment requires no movement as the craft is to maintain its position about the final point defined as the second of the two points in space. This segment exists to work simultaneously and in harmony with a target attainment algorithm. This segment does not have a time limit associated with it as a target attainment algorithm determines at what point the segment terminates which is a signal that the craft is to move on to the next portion of the autoland process. This signals the termination of this run of the trajectory generator.

The trajectory generator is to be a generic tool and is not to be specific to any one algorithm. It is to allow the program to be applied whenever navigation between two points is required. Thus the generalization of terms and procedures in this section. Similarly, segments A through C are to be flexible thereby allowing for the generator to be configured to any path.

The *figure 5.2*, used to illustrate the various segments in the trajectory generator, is a plot of velocity against time. This style of plot was used to illustrate the velocity tendencies for the various segments. However, from this point forth, the plot of choice will be that of acceleration against time. The acceleration plots will be used to detail why one system of trajectory profiles is more suited to this application than another. The next section details why the acceleration plot is employed as opposed to that of the displacement or velocity plots.

5.4 Profile Illustration

The acceleration profile, which will be the plot primarily used from this point forth, is a very versatile tool. Briefly, the various reasons why this plot was chosen to demonstrate and evaluate the basis for the trajectory generator, will be explained. Reasons given will cover the plot's recognizability, how it lends itself to easy implementation of the conditions, its relation to the tilt rate limiter, and how it allows for visual evaluation of jerk for the various profiles.

The acceleration plot tends to be a much more specific tool than those of velocity and position. In fact, when evaluating various trajectory profiles, it is difficult to discern between the various choices when their respective velocities are plotted. The obscurities are further concealed with the displacement plots. *Figure 5.3* gives light to this fact. The three plots use the same time scale and their respective subjects are all to scale. It can be seen that there is little difference when it comes down to the displacement traces of the three acceleration profiles. Even the velocity plots are similar. The same cannot be said of the acceleration plots. They are very different and easily recognizable from one another.

The acceleration plots are very useful in implementing the craft safety and stability concerns set out in *section 5.1.1*. Firstly, the peak velocity can be determined by finding the area under the curve for either the acceleration or deceleration sections. This is done simply by integrating the plots. The second factor is that the acceleration plot gives easy evaluation on how close the craft comes to approaching the tilt-rate-limiter activation threshold. Seeing as tilt for a helicopter describes lateral velocity, then the rate at which tilt changes would be analogous to a rate of velocity or, more commonly put,

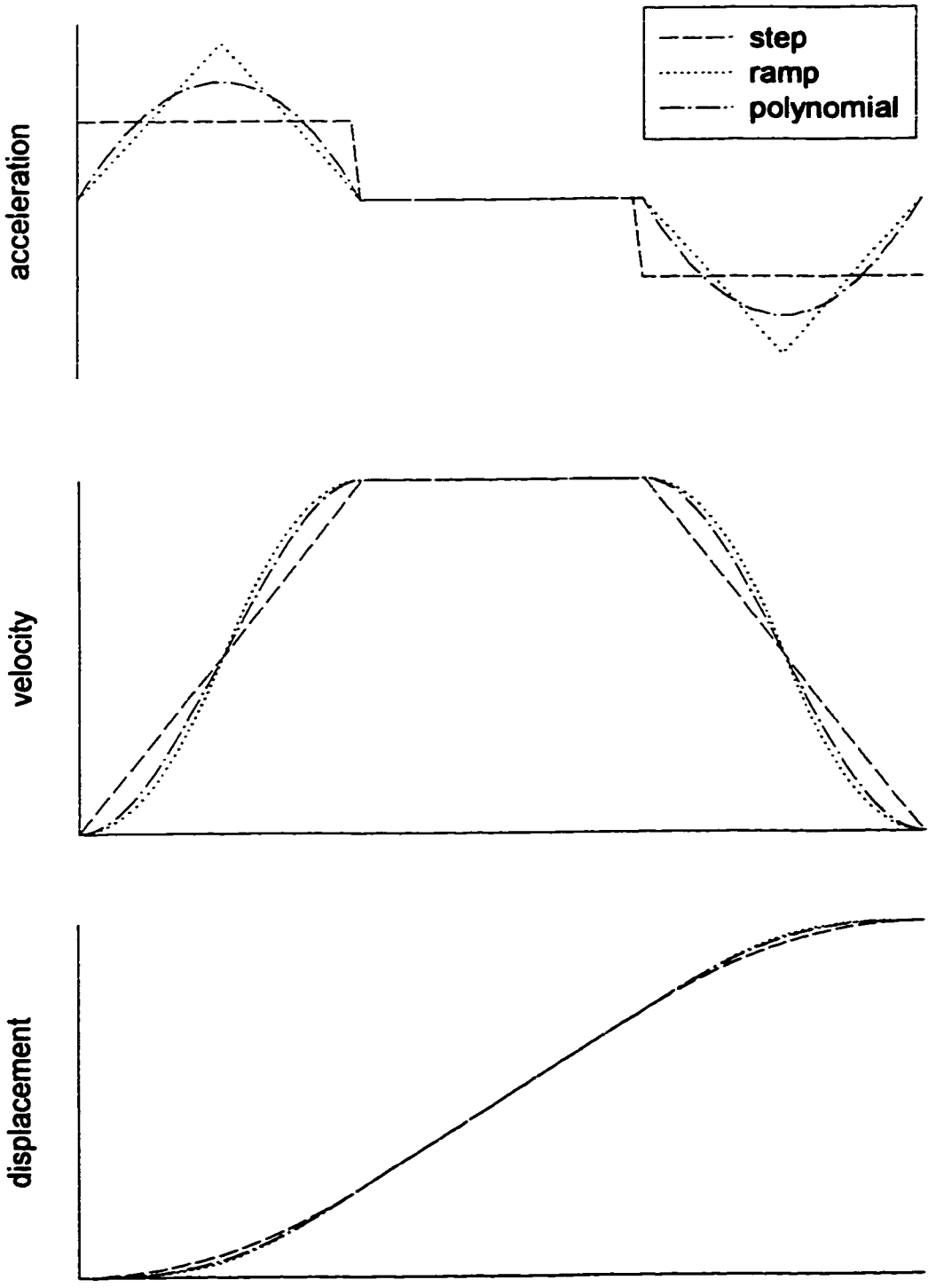

Figure 5.3 – Profile illustrations for various acceleration profiles and their respective integrations

acceleration [16] [27]. The difference between the craft's peak acceleration and the highest value associated with the unbridled region of the tilt-rate-limiter gives a good indication of how close the craft comes to activating the limiter. One must be conscious that as the craft is pushed off course, its tilts and consequently tilt-rates will increase and decrease rapidly in order to recapture the prescribed path. Therefore, a buffer region between the peak acceleration and that of the tilt-limiter threshold must be built-in to allow for disturbances.

The final reason behind using acceleration plots to evaluate the various trajectory profiles lies in the ease in which the potential for jerk can be evaluated. Jerk is a very informative aspect of motion and seeing as it's the rate of change of acceleration, it's easy to evaluate it from the acceleration plots. Jerk becomes an issue if its plots contain sudden changes, or worse yet asymptotes [19] [33]. These appear on acceleration plots as discontinuities. In reality, sudden jumps in jerk create large error signals over a short time span. Using acceleration plots to evaluate various profiles, discontinuities can be verified at a glance. Though jerk is an important tool in profile selection, to use the jerk plot as the primary evaluation tool would be a step back as far as overall insight is concerned.

The acceleration plot is the best of all choices available. It gives a simplified representation as compared to the position and velocity plots, but doesn't go so far as being over specific as the jerk plot does. It also helps in implementing or avoiding limits and limiters as the case may be. It is without a doubt the optimum of the plots available. The task now is to choose the correct acceleration profile to best perform the trajectory planning.

5.5 Acceleration Profiles

The acceleration profile is critical in the development of a well rounded autoland process. It is perhaps the key factor in obtaining a system which will work well under all conditions. The object is to obtain a combination of trajectory profile and controller which secures the best accuracy. The closer the craft can follow the ideal path described by the trajectory generator, the more disturbances the craft can withstand, which makes the system more robust as a whole. Craft acceleration is seen only in segments A and C as described in section 5.3 and depicted in *figure 5.3*. Both segments B and D are at constant velocity and therefore have no acceleration to speak of. It is important to realize that for the evaluation of the various profiles, both the acceleration and deceleration segments will be of the same duration, amplitude, and they will consist of the same profile. This is done to make the evaluation a more straightforward process. This may or may not be the case when the selected profile is implemented. In total, four profiles will be evaluated. They comprise some of the most widely used profiles in robotic control. They will be compared using their pros and cons and will be evaluated specifically with the autoland algorithm in mind. The approaches which will be evaluated are the step or bang-bang profile, the ramp, the polynomial and the cosine profile.

5.5.1 Step / Bang-Bang Profile

This method is the most simple and most commonly seen robotic acceleration trajectory profile [33] [34]. It is used in many instances and is often found to have acceptable results. The profile in question is illustrated in *figure 5.4*. It shows standard step acceleration responses for segments A and C, with its corresponding velocity profile to the right.

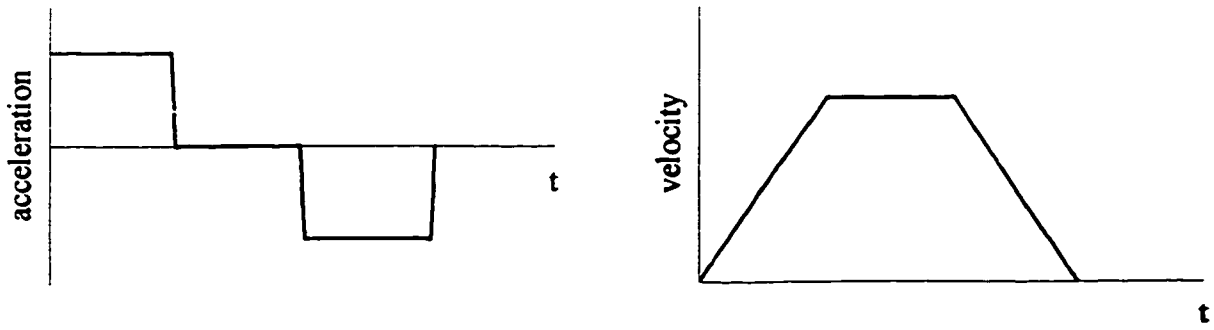

Figure 5.4 – Bang-bang acceleration and velocity profiles

There are may advantages to using this profile for the ideal profile. As was stated earlier, it is the most common profile used in robotics. It has been used for many years and has a proven track record in many different areas. It has been used so often as it is without a doubt the simplest method to understand, configure, and apply. It requires only the two values, acceleration and deceleration values to describe the entire system. With these, the peak velocity can be easily found by calculating the area under the curve. Moreover, since the acceleration is constant throughout, the traditional equations of motion can be employed to figure out the distance covered in the segments A through C.

With all the aspects of simplicity which this profile lends to the calculations, they are also the same sources for the problems which arise. The fact that the acceleration comes in sudden bursts is the problem. This provides a profile which is not smooth. Smooth transitions give the craft time to respond to these changes in commands. If the derivative of the bang-bang profile was taken, it would show four occasions where it would reach infinity. With the step approach, the craft, which in the horizontal requires time to shift its momentum, has no time to react to the changes. This leads to large differences between the ideal path and the actual path, which in turn causes the craft to

pitch radically to make up for lost ground. This is a scenario which lends itself to the activation of the tilt-rate-limiter, which, as described previously, is the effective onset for unstable conditions. Moreover, this happens on four separate occasions when this profile is used. To compound matters, the topic of disturbances has not been approached yet. Winds and noise would only degrade the situation.

The trajectory generation for the autoland process is very specific. It needs very accurate results for the system to function. Even though this is a very easy method to create the acceleration profiles, it is evident that the drawbacks outweigh the advantages. Consequently another solution must be found to provide the acceleration profile.

5.5.2 Ramp Profile

The ramp profile is the next method to be evaluated for possible implementation with the trajectory generator. It differs from the bang-bang profile in that it has varying values for acceleration and deceleration in both the segments A and C [34]. The profile is linear and proportional to time. The acceleration and velocity profiles are depicted in *figure 5.5*. It shows an acceleration profile, which is of the form of a pyramid, for the two segments in question and its associated velocity profile.

The pros associated with this segment revolve around the achievement of a smoother profile than described for the bang-bang profile. Most everything in nature happens in a gradual manner, at least on a relative scale. This smoother curve allows closer approximation to real world conditions by creating a more gradual acceleration and deceleration. As with the first option, the equations required to calculate the profile are also quite simple to come by. They are composed of straight lines aligned one after the

other. The integration of the various components of the profile would also be not difficult to come by as the initial and final conditions would prove easy to evaluate.

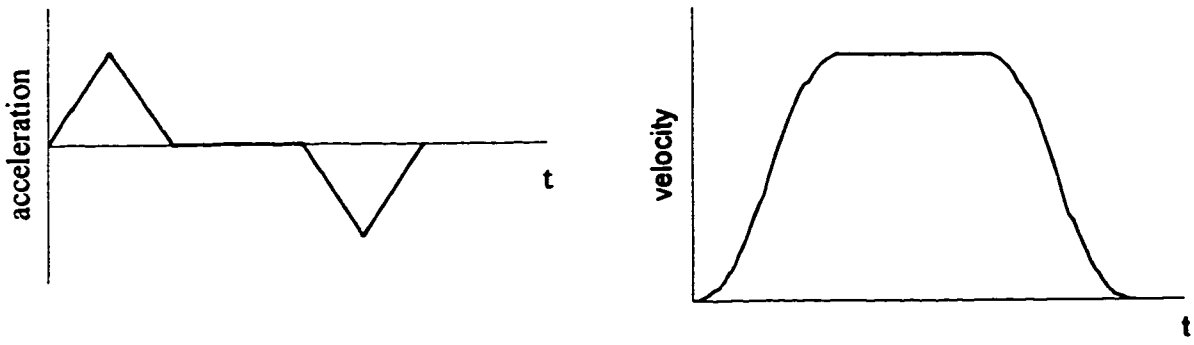

Figure 5.5 - Ramp acceleration and velocity profiles

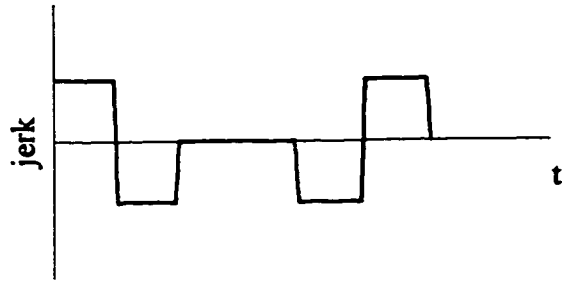

Figure 5.6 – Illustration of discontinuities in ramp profile using jerk plot

With all the advantages discussed, there are some significant drawbacks to the ramp acceleration profile. Most apparent is its increased number of segments. Both segments A and C are split into two additional regions, where each region contains a distinct equation to describe the slope. Seeing as the system is to be designed with as many capabilities as possible, the equations for the same segment need not be the same. Thus more complications and calculations are required to produce the full profile. This profile was deemed to be a more natural profile than the first. To this there is no dispute. This does not say that it is perfect. In fact, though this profile does not demonstrate

asymptotic tendencies in its first derivative, it does contain discontinuities. It contains six separate discontinuities, with three in each segment as shown in *figure 5.6*. These discontinuities, though not as harmful as asymptotes, produce abrupt changes in acceleration which produce sudden decreases in accuracy. As described previously, these are to be avoided for fear that an excessive tilt-rate could trigger the respective limiter. Lastly, there's the issue that the peak acceleration for this profile is greater than that for the first for a path of the same length and for acceleration and deceleration of the same duration. This can be seen by referring back to *figure 5.3*. These plots represent three of the four profiles considered and are plotted for equivalent duration and path length. It can be seen that the ramp profile has a peak acceleration twice that of the bang-bang approach.

It can be seen that though the ramp acceleration profile is worse than the bang-bang approach for peak acceleration values, it has one overwhelming virtue which the other approach does not possess. The profile is much smoother than the first. This is important as it will mean that the difference between ideal and actual craft position will be reduced which allows for finer tuning of the controller. This in turn allows for reduced position error again. The discontinuities however limit the reduction in position error. A subsequent reduction of these position errors means a further upgrade of the system as a whole.

5.5.3 Polynomial Profile

The third of the four types of acceleration profiles is the polynomial version. It is shown in *figure 5.7* with the acceleration and velocity profiles. The polynomial profile

shows a well contoured form throughout each segment [34] [35]. It differs from the ramp profile in that each segment is one piece.

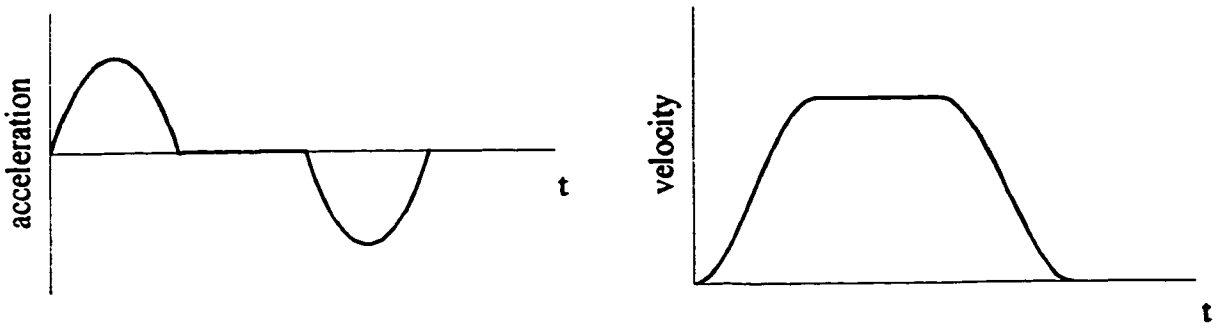

Figure 5.7 -Polynomial acceleration and velocity profiles

There are several advantages associated with this type of profile. Each segment is comprised of a single function. This simplifies the method as a whole and reduces the number of calculations required to formulate the equation describing constants. The profile itself also has a reduced maximum acceleration compared to that for the ramp profile. This provides an increased buffer region to allow for response to disturbances before the tilt-rate limiter is activated. On the whole, this profile is smoother than those examined previously which allows for increased accuracy. It also requires only a four term expression to produce the given results.

With the important advantages this profile lends to the trajectory generation as a whole, it also contains drawbacks. As was the case previously, the maximum acceleration for this profile is still greater than that for a bang-bang profile given a similar length of path and time to complete the task. The greater of the drawbacks however, rests with the complexity of the calculations to determine the profile. To obtain a smooth polynomial of sufficient accuracy, the polynomial must be of at least the 3rd order. Thus four constants must be created. Then this 3rd order equation must be used for each

iteration which is a marked increase in the number of calculations required to find the optimal position. Also, the polynomial constants consists of a group of numbers, both positive and negative, which give no indication as to profile dimensions upon quick inspection. With all that was said concerning smoothness, the profile still contains discontinuities at the beginning and at the end of each segment in question, therefore creating a total of four for the profile as a whole. These will cause errors which is the primary nemesis of this craft.

This method is the most calculation intensive of those evaluated so far. It first must evaluate a relatively increased number of constants, then use them over and over again to figure out the position of the ideal point for each iteration. In addition, this method still does not eliminate the errors grown out of discontinuities in the acceleration profile. However, the smoothness issue and the reduction of peak acceleration values is very promising. There are significant steps forward and in many instances, this would provide adequate results. The autoland requires excellent results with respect to accuracy. The primary method of obtaining these ends being the eradication of discontinuities in the acceleration profile.

5.5.4 Cosine Profile

The final profile which will be evaluated is the cosine profile. Its closest relation of those covered previously is the polynomial profile. The cosine profile represents the ultra-smooth solution [35] [36] [37]. The curve is by no means linear, but rather, as its name suggests, trigonometric. The profile itself is depicted in *figure 5.8*.

This method has many advantages to promote its use. For example, it does not require as many calculations to determine the equation describing constants for the

acceleration profile. In fact there are only two of these constants. These constants are the amplitude and frequency of the cosine wave. These, as opposed to those previously

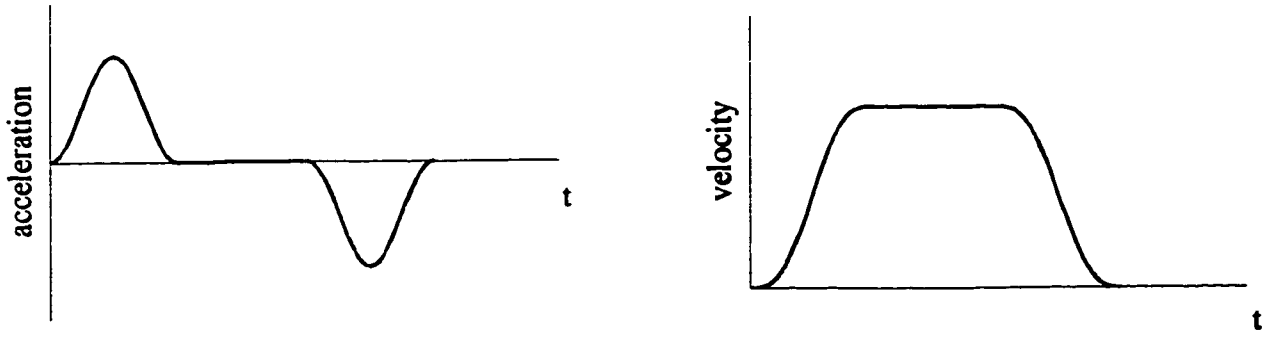

Figure 5.8 – Cosine acceleration and velocity profiles

described, mean something in real life. The amplitude and frequency describes everything about the shape of the profile. However, quite probably the profile's greatest attribute is that it is perfectly smooth. It describes the closest thing to the natural or ideal profile without requiring an infinite number of points. If the first derivative of the acceleration profile was taken, it would contain no discontinuities. In fact, it is continuous to the n^{th} derivative. The absence of discontinuities means no sudden jerking movements which drives down the possibility for position error. For a computer to evaluate the cosine function, simple series theory is all that must be used. The MacLaurin series for cosines is described as follows (*eqn. 5.1*) [38]. For most applications, four terms is all that is required to achieve a sufficiently accurate result.

$$\cos x = \sum_{n=0}^{\infty} (-1)^n \frac{x^{2n}}{(2n)!} = 1 - \frac{x^2}{2!} + \frac{x^4}{4!} - \frac{x^6}{6!} \qquad (5.1)$$

As for disadvantages associated with this method, they are substantial, yet few. Probably the greatest drawback is the number of calculations required to produce the ideal points. Not only is the microprocessor responsible for the evaluation of a four term expression to solve the value for cosine, but is then required to use the response in further calculations. This method also produces the highest peak acceleration. In fact it is tied with the ramp method for the highest peak.

As has been just described, the cosine profile has some major deficiencies. The highest peak acceleration and the greatest number of calculations to produce an individual trajectory point are significant drawbacks. This is then directly related to high load on the microprocessor. These are by no means minor issues. Yet when all is weighed, advantages led by the promise of low errors prevail. This was in fact the ultimate goal of the trajectory generation algorithm. The fact that the microprocessor in the craft is capable of accepting the workload is the deciding factor. If this was not the case, perhaps a polynomial profile would have been the method of choice. To deal with the higher peak acceleration issue, the duration of the acceleration is to be increased. Though this increase in time does represent an autoland performance downgrade, the extra amount of time which is required is a matter of a few seconds. This represents a negligible increase in mission time, yet allows for the use of a method with low potential for error.

5.6 Cosine Profile Calculations

The cosine profile is a very powerful tool. Its smoothness is its greatest attribute. Though the profile has this discernable benefit, for the vast majority of applications, it is not required. This case is an exception. For the autoland, the profiles for both segments

A and C will be cosine profiles. This is not to say that they must have equal duration. In fact, calculations are performed assuming that different periods are used, thus allowing for a general case. The method by which the profile is generated is not a difficult one. A thorough explanation of how the method is calculated will follow. It will start with the formation of the basic equations and values associated with the profile. These will then be used to define the trajectory itself from which the profiles will be generated. The method itself will be reduced to a matter of a few variables from which the curve is derived. The remaining sections will examine how these variables will be determined for various scenarios which the algorithm may encounter.

5.6.1 Generation of Basic Equations

The first matter to consider is that the cosine function, as it is found traditionally, is not of the form required to produce the profile. Modifications must be made to the base function for the profile to resemble the one required for the creation of a trajectory. The progression is depicted in *figure 5.9* as the base function is transformed from its conventional form (*figure 5.9a*) to that which can be applied by the algorithm. For positive acceleration, the negative of the function must be used (*figure 5.9b*). This function now must be shifted such that it will start with zero, so making the whole function positive. This means a unity addition of the amplitude to the function (*figure 5.9c*). Consequently, these modifications produce the near perfect profile. The beginning and end of the profile reaches zero in a smooth and well controlled fashion. It requires one full cycle to accomplish the form of profile so desired in segments A and C. The equation which describes the desired acceleration and its respective integrals are shown in eqns. 5.2-5.4.

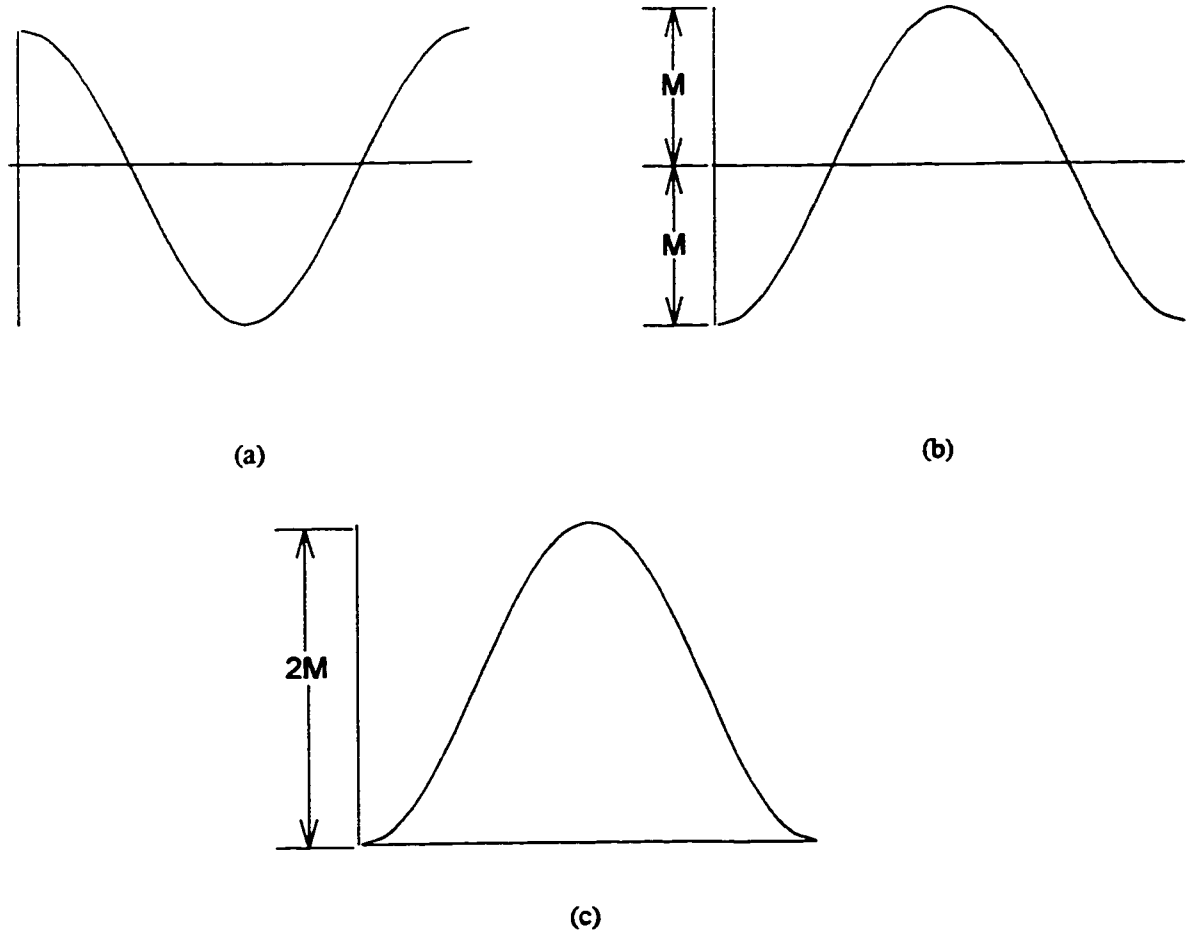

Figure 5.9 – Progression of Cosine profile

$$a = 2M[1 - \cos(\omega t)] \tag{5.2}$$

$$v = 2M\left[t - \tfrac{1}{\omega}\sin(\omega t)\right] \tag{5.3}$$

$$d = 2M\left[\frac{t^2}{2} + \tfrac{1}{\omega^2}\{1 - \cos(\omega t)\}\right] \tag{5.4}$$

where,

a = Ideal acceleration of craft

M = Amplitude of trigonometric function

ω = Frequency of trigonometric function

t = Instantaneous time since trajectory generation began

v = Ideal velocity of craft

d = Ideal displacement of craft

As per *figure 5.9*, it is known that the time to complete segment A is equal to the period (*eqn. 5.5*). Then from the convention given in *eqn. 5.6*, we get the frequency for segment A as *eqn. 5.7*. Similarly, the frequency for segment C is found. In the vast majority of cases, the calculations used for segment A can be used to calculate the same variable for segment C. For the sake of avoiding redundancy, the equations will not be duplicated for segment C. This is not to say that any dissimilarities between the segments will be duly noted.

$$t_A = T \tag{5.5}$$

$$\omega = \frac{2\pi}{T} \tag{5.6}$$

$$\omega_A = \frac{2\pi}{t_A} \tag{5.7}$$

where,

t_A = Amount of time allotted to perform segment A

T = Period of trigonometric function

ω_A = Frequency of profile for segment A

By convention the peak velocity is reached when the end of segment A is reached. This occurs exactly at time $t=t_A$. This means that at this instant, $v=V_P$ Using these two

revelations, *eqn. 5.7*, and substituting them into *eqn. 5.3*, the general form of the amplitude expressed in terms of the time to complete segment A and the peak velocity is found (*eqn. 5.8*). The amplitude for segment C is found in the same manner.

$$M_A = \frac{V_P}{2t_A} \tag{5.8}$$

where,

M_A = Amplitude of acceleration profile for segment A

V_P = The peak ideal, combined velocity during trajectory algorithm

The peak acceleration for segment A is found in a method similar to that of the previous derivation. The peak acceleration is known to occur at $t = {}^{t_A}/_2$ and by combining this and *eqn. 5.7* into *eqn. 5.2*, *eqn. 5.9* is the result. It is interesting to note that if the same derivation was performed for segment C, *eqn. 5.10* would be produced. Combining *eqns. 5.9* and *5.10* gives an interesting result (*eqn. 5.11*). It shows the relation between the two segments in terms of their appropriate boundaries.

$$a_{P,A} = 4M_A = \frac{2V_P}{t_A} \tag{5.9}$$

$$a_{P,C} = -4M_C = -\frac{2V_P}{t_C} \tag{5.10}$$

$$a_{P,A}t_A = -a_{P,C}t_C \tag{5.11}$$

where,

$a_{P,A}$ = Peak acceleration reached in segment A

$a_{P,C}$ = Peak acceleration reached in segment C

M_C = Amplitude of acceleration profile for segment C

t_C = Amount of time allotted to perform segment C

By letting $t=t_A$, and employing *eqn. 5.7* and *eqn. 5.8* in the framework of *eqn. 5.4*, the amount of distance traveled in the first segment is found to be that described by *eqn. 5.12*. The method in which the distance traveled in the segment C is very similar to that outlined above (*eqn. 5.13*).

$$D_A = \frac{V_P t_A}{2} \qquad (5.12)$$

$$D_C = \frac{V_P t_C}{2} \qquad (5.13)$$

where,

D_A = Distance covered during segment A

D_C = Distance covered during segment C

Seeing as the distance between the two points in space is the factor which the trajectory generation is primarily based upon, the total distance between the points is of paramount interest (eqn. 5.14). Seeing as the distance covered in segments A and C are known, the amount of distance to be covered by the constant velocity portion is easily found using these values and the total distance (eqn. 5.15). As segment B is traveled at constant velocity, then the time required to complete the segment is found using the distance required to travel and the velocity in this segment (eqn. 5.16).

$$D_T = \sqrt{(N_i - N_f)^2 + (E_i - E_f)^2 + (H_i - H_f)^2} \quad (5.14)$$

$$D_B = D_T - D_A - D_C \quad (5.15)$$

$$t_B = \frac{D_B}{V_P} \quad (5.16)$$

where,

D_T = Total distance between two points in space

N_i = North position of initial point in space

N_f = North position of final point in space

E_i = East position of initial point in space

E_f = East position of final point in space

H_i = Height of initial point in space

H_f = Height of final point in space

D_B = Distance covered during segment B

t_B = Amount of time allotted to perform segment B

5.6.2 Profile Generation

Using the aforementioned variables and equations, the acceleration profile can now be described. Though the acceleration profile gives the most useful information regarding the advantages of one profile over another, it is not required that acceleration be the information created by the algorithm. In fact, the velocity profile is the most important as far as usability of the information is concerned. The reasons for this will be given in the section describing controller selection. The manner in which the profiles

will be called is segmental. If the time falls within a certain range, one equation will be used as opposed to another. These are given in *eqns. 5.17-5.20.*

Segment A:

$$t_{s,A} \le t < t_{s,B} \qquad v = 2M_A\left(t - {}^{1}\!/\!_{\omega_A}\sin(\omega_A t)\right) \qquad (5.17)$$

$$where,\ t = t - t_{s,A}$$

Segment B:

$$t_{s,B} \le t < t_{s,C} \qquad v = V_P \qquad (5.18)$$

Segment C:

$$t_{s,C} \le t < t_{s,D} \qquad v = V_P - \left[2M_C\left(t - {}^{1}\!/\!_{\omega_C}\sin(\omega_C t)\right)\right] \qquad (5.19)$$

$$where,\ t = t - t_{s,C}$$

Segment D:

$$t_{s,D} \le t \qquad v = 0 \qquad (5.20)$$

where,

$t_{s,A}$ = Time at which segment A begins.

$t_{s,B}$ = Time at which segment B begins.

$t_{s,C}$ = Time at which segment C begins.

$t_{s,D}$ = Time at which segment D begins.

To find the displacement plot for the ideal path, the path for velocity need just be integrated. This can be done numerically by the microprocessor. Thus the exact

displacement (d_i) from the onset of the trajectory generation can be found for any instant in time.

To determine the position for the craft at any instant, all that need be known is the displacement for that time instant and path geometry, namely the bearing and descent angle. There exists two places where the trajectory algorithm is employed during the autoland process, the glideslope descent and the intercept portions, so contingencies must be made to discern between the two. Though differences in terminology exist, there should be no difference in which these cases are handled by the program. To solve the problem, the two geometrical components of descent and bearing angle will be written in general terms. Specific calculations for the two applications are given and then substituted where appropriate. If the intercept portion is the process in question, the values are determined as shown in *eqns. 5.21-5.26.*

$$nor_{CPT} = N_f - N_i \tag{5.21}$$

$$est_{CPT} = E_f - E_i \tag{5.22}$$

$$\gamma_{CPT} = \tan^{-1}\left(\frac{H_f - H_i}{\sqrt{nor_{CPT}^2 + est_{CPT}^2}}\right) \tag{5.23}$$

$$\alpha_{CPT} = \tan^{-1}\left(\frac{nor}{est}\right) \tag{5.24}$$

then,

$$\gamma = \gamma_{CPT} \tag{5.25}$$

$$\alpha = \alpha_{CPT} \tag{5.26}$$

where,

nor_{CPT} = North displacement of intercept path

est_{CPT} = East displacement of intercept path

γ_{CPT} = Descent angle of path between initial point and intercept point

α_{CPT} = Bearing angle of path between initial point and intercept point

γ = Generalized descent angle

α = Generalized bearing angle

Otherwise if the trajectory generator is being used for the glideslope portion, the variables for the generalized path geometrics are given in *eqns. 5.27* and *5.28*.

$$\gamma = \gamma_{GS} \tag{5.27}$$

$$\alpha = \alpha_{GS} \tag{5.28}$$

where,

γ_{GS} = Descent angle of GS

α_{GS} = Bearing angle of GS

With the exact geometry for a given path known, the business of calculating the exact position of the craft in space can be performed. The instantaneous position of the craft for a given point in time is much like that calculated previously in section 4.3.1 (intercept chapter). For a detailed explanation of the calculations, refer to that section. The calculations are as follows *eqns. 5.29-5.32*.

$$H_{IP} = H_i + d_i \sin(\gamma) \tag{5.29}$$

$$N_{IP} = N_i + h_i \sin(\gamma) \tag{5.30}$$

$$E_{IP} = E_i + h_i \cos(\gamma) \tag{5.31}$$

$$h_i = d_i \cos(\gamma) \tag{5.32}$$

where,

H_{IP} = Height of ideal point produced by trajectory generator

d_i = Ideal total displacement of craft since trajectory generation began

N_{IP} = North coordinate of ideal point produced by trajectory generator

h_i = Ideal horizontal displacement of craft since trajectory generation began

E_{IP} =East coordinate of ideal point produced by trajectory generator

There are a significant number of calculations which have been presented thus far. This being said, the previous calculations rely on the knowledge of only three fundamental variables. These are t_a, t_c, and V_P. From these, the profile can be found. The values for these variables depend on the specific case being faced.

5.6.3 Specialized Cases

5.6.3.1 Case 1 : Long Path and $V_V \leq V_{V,max}$

The three variables which are required to complete the calculations for the trajectory generation are the focus of the next three sections. With these variables, the range of calculations explained in the previous section can be undertaken. These variables are initially declared to be their maximum allowable values as given by *eqns. 5.33-5.35*.

$$t_A = t_{A,\max} \tag{5.33}$$

$$t_C = t_{C,\max} \tag{5.34}$$

$$V_P = V_{P,\max} \tag{5.35}$$

where,

$t_{A,max}$ = Maximum time allotted to complete segment A

$t_{C,max}$ = Maximum time allotted to complete segment C

$V_{P,max}$ = The maximum peak total velocity commanded by trajectory generator

The specific values associated with these maxima have been arrived at either through testing or by being declared. The two variables describing the time allowed for segments A and C were found through tuning of the vehicle. They allow for an optimum balance between speed of reaction and system stability. They are especially important when disturbances are considered. The other variable $V_{P,max}$ was declared at the outset. It is the limit which describes the maximum total peak velocity which is prescribed by the craft's trajectory system. It is put in place primarily for the sake of craft safety and was one of the primary features the algorithm was required to incorporate. It is important to note that even though it is considered a limit, the craft can, under adverse conditions, exceed the value. This occurs when the craft is traveling at its peak velocity and a disturbance brings it off course. In order to recapture the ideal points being produced, the vehicle will have to exceed the limit velocity by a small margin. If this is not the case, the craft will never catch up to the generated ideal points until sometime in segment C. This would lead to the creation of instabilities.

With these variables declared, the critical path distance can be determined. The critical path distance is the distance covered in segments A and C combined, when the three fundamental variables are set at their respective maxima. Using *eqns. 5.12* and *5.13* and setting the fundamental variables at their respective maximums, *eqn. 5.36* is produced. If the total distance (*eqn. 5.14*) is greater than the critical distance, then the path is considered long and the maximum values can be used. Not only that, but the distance of segment B will be greater than or equal to zero. The fact that the path is considered long is the first condition of this case.

$$\begin{aligned} D_{crit} &= D_A + D_C \\ &= \frac{V_P}{2}\left(t_A + t_C\right) \end{aligned} \qquad (5.36)$$

where,

D_{crit} = Critical path distance

With the path distance calculated and verified as being long, the next major step is to confirm that the vertical component of the ideal velocity does not exceed the limited value. By definition, the peak velocity can be described by *eqn. 5.37*.

$$V_P = \sqrt{V_V^2 + V_H^2} \qquad (5.37)$$

where,

V_V = Vertical component of peak velocity

V_H = Horizontal component of peak velocity

The path descent angle can also be described using the craft's velocity components just as it was using the distances between the two points (*eqn. 5.23*). Manipulation of the equation provides an equation for the horizontal velocity (*eqn. 5.38*).

$$V_H = \frac{V_V}{\tan(\gamma)} \tag{5.38}$$

Then by combining *eqns. 5.37* and *5.38*, through subsequent manipulations, an equation describing the vertical component of the velocity is produced, dependent solely on the peak velocity and the path descent angle (*eqn. 5.39*).

$$V_V = \frac{V_P}{\sqrt{1 + 1/\tan^2(\gamma)}} \tag{5.39}$$

Recall that the peak velocity has already been set to that described by its maximum allowable value. The path descent angle is known, so therefore the vertical component of the ideal velocity can be found. For this case, it will be assumed that the vertical component of the ideal velocity is less than that set out by the maximum value (*eqn. 5.40*). This maximum value is the limit set out for the vertical velocity. It is the second of the two limits which required implementation by the trajectory generator.

$$V_V \leq V_{V,\max} \tag{5.40}$$

where,

$V_{V,max}$ = Maximum value for the vertical component of the peak velocity

This case has depicted what is possible for the trajectory generator fundamental variables if all is ideal. This means the distance between the two points in question is considered long by the presented criteria and the maximum vertical velocity of the craft is not exceeded. Because of this, the maximum values for the fundamental variables V_P, t_A, and t_C may be used. It will occur that either one or both of these conditions will be violated. This is to be recognized and corrected by altering the fundamental variables. The next section will describe the first of the two non-ideal cases, where the critical distance exceeds the path distance.

5.6.3.2 Case 2 : Short Path

A short path is one which is described according to *eqn. 5.41*. Not only does it mean that there is no segment B to speak of, but moreover, segments A and C are too long assuming that the maximum values for the fundamental variables are used. It is therefore evident that appropriate reductions to the fundamental variables are required.

$$D_T \leq D_{crit} \tag{5.41}$$

Using *eqn. 5.9*, the peak maximum acceleration can be found using the maximum values for the peak velocity and the time allocated to perform segment A (*eqn. 5.42*). The case is similar for that of segment C.

$$a_{P,A,\max} = \frac{2V_{P,\max}}{t_{A,\max}} \qquad (5.42)$$

where,

$a_{P,A,max}$ = Maximum peak combined acceleration for segment A

For the total distance to be reduced, the fundamental variables must be reduced proportionally. If the reduction is proportional, this process will be linear and the task as a whole will subsequently be much simpler. As was demonstrated previously with *eqns. 5.9* and *5.42*, the peak velocity is a function of the time allotted for a segment and the peak acceleration for that same segment. By reducing these variables, the peak velocity and then the distance covered during the respective segment will be reduced accordingly. Recalling *eqn. 5.36* and by using *eqn. 5.9* and the maximum values for the respective variables, a new expression for the critical distance is created (*eqn. 5.43*).

$$D_{crit} = \frac{a_{P,A,\max} t_{A,\max}}{4}\left(t_{A,\max} + t_{C,\max}\right) \qquad (5.43)$$

Imagine that the acceleration profile as a whole was scaled by n (*figure 5.10*). Both the peak combined acceleration and the time allotted to perform the two dynamic segments are multiplied by the factor n. This is shown as a_2 and t_2 are half that of a_1 and t_1 respectively. Applying this scaling factor to *eqn. 5.43* results in *eqn. 5.44*. As n is reduced below unity, the expression describes a smaller and smaller distance. Thus if n=1, the resulting expression will describe the critical distance while if n=0, the expression describes no distance.

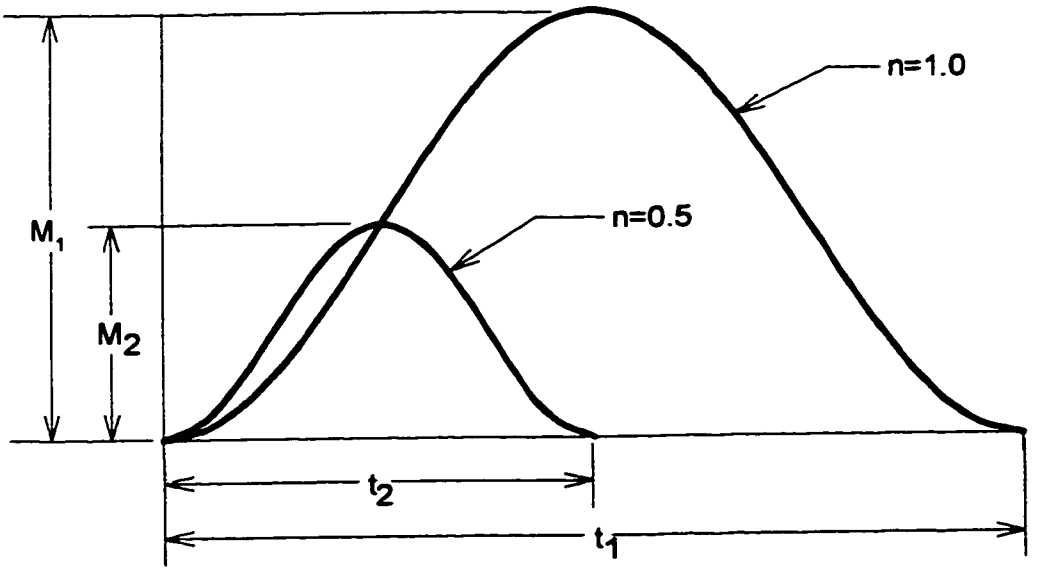

Figure 5.10 – How scaling equally effects both amplitude and duration of acceleration

$$\begin{aligned} D_T &= \frac{na_{P,A,\max} nt_{A,\max}}{4}\left(nt_{A,\max} + nt_{C,\max}\right) \\ &= n^3\left[\frac{a_{P,A,\max} t_{A,\max}}{4}\left(t_{A,\max} + t_{C,\max}\right)\right] \\ &= n^3 D_{crit} \end{aligned} \qquad (5.44)$$

where,

n = Scaling factor

Eqn. 5.44 can be rearranged to produce a more useful form of *eqn. 5.45*.

$$n = \sqrt[3]{\frac{D_T}{D_{crit}}} \qquad (5.45)$$

A similar procedure is performed to arrive at an expression which describes the scaling coefficient in terms of velocity (*eqn. 5.46*) and of course acceleration (*eqn. 5.47*).

$$n = \sqrt{\frac{V_P}{V_{P,\max}}} \tag{5.46}$$

$$n = \frac{a_{P,A}}{a_{P,A,\max}} \tag{5.47}$$

The stumbling block in this section was that the distance between the two point was less than that described by the critical distance. By using *eqn. 5.45*, an appropriate scaling factor can be found. Use of the scaling factor, along with maximum time allotted for the two segments, gives the correct time duration for both segments A (*eqn. 5.48*) and C (*eqn. 5.49*). The corrected peak velocity can be found using the newly determined scaling factor and *eqn. 5.42* to produce *eqn. 5.50*.

$$t_A = nt_{A,\max} \tag{5.48}$$

$$t_C = nt_{C,\max} \tag{5.49}$$

$$V_P = \frac{n^2 a_{P,A,\max} t_{A,\max}}{2} \tag{5.50}$$

So it goes that the three fundamental variables are recalculated to produce a trajectory which can adjust to any length. It must be pointed out that the length of the combination of segments A and C are exactly equal to that of the path between the two points in question. In other words, there is no segment B to speak of if scaling takes place. This allows for the quickest run between the two points.

5.6.3.3 Case 3 : $V_V > V_{V,max}$

The second and final condition is that where the vertical component of the ideal velocity exceeds that of the limit value. This occurs when γ is large relative to V_P. One way to understand when this occurs is supposing that V_P and V_V are set at values described by their respective maximums. By using *eqn. 5.39* and solving for γ, the critical descent angle (γ_{crit}) for the given path is found (*figure 5.11*). For descent angles less than this amount, the peak velocity is the limiting factor. For a descent angle greater than that described by the critical angle, the vertical component of the peak velocity has grown so much that it now becomes the limiting factor. It is to be noted that all this is being described for a path which is considered long. If the path is shorter than that described by D_{crit}, then V_P is reduced from $V_{P,max}$, so therefore γ_{crit} increases accordingly.

To determine if the vertical component of the ideal velocity exceeds the specified limit, *eqn. 5.39* with the maximum peak velocity is used in conjunction with the descent angle of the path in question. If the vertical component exceeds its respective maximum, a revised peak velocity can be found by again using *eqn. 5.39* and by substituting in the maximum value for the vertical component (*eqn. 5.51*). Thus the vertical component becomes the factor limiting the velocity and produces a reduced value for V_P.

$$V_P = V_{V,max}\sqrt{1 + {}^{1}\!/\!_{\tan^2(\gamma)}} \qquad (5.51)$$

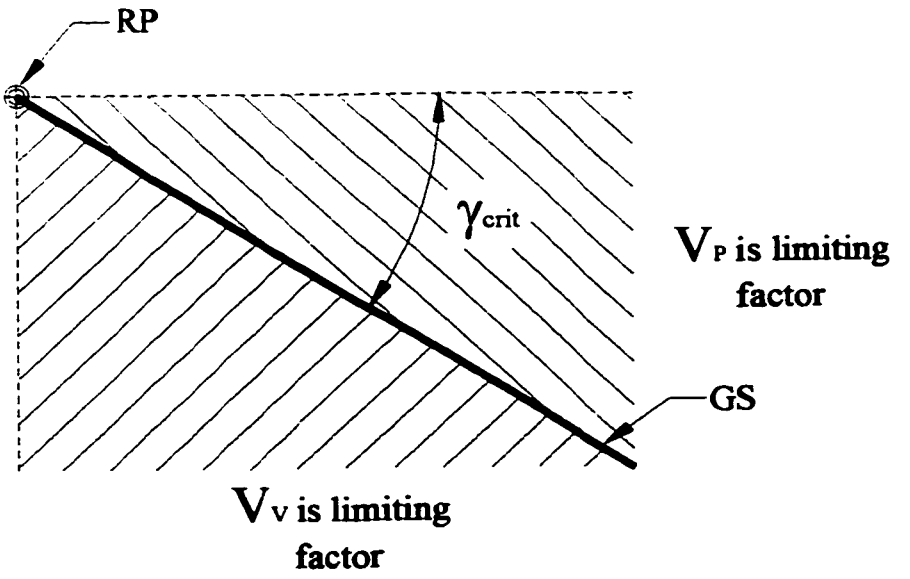

Figure 5.11 – GS critical descent angle and the velocities which depend on it

In the event of a new peak velocity, the profile of the acceleration curve must be modified to represent this. In order for the profile to correspond, the idea of the scaling factor must be revisited. The scaling factor itself can be found using *eqn. 5.46*. The time allotted to the segments A and C can then be recalculated according to *eqns. 5.48* and *5.49*.

The trajectory generator effectively manages to produce a locus of points based on a time law which can then be used to draw the craft from one point in space to another. It does this with the smoothest possible profile and can accommodate any length or orientation of path. Also built-in are the user defined safety limits on velocity to protect the craft. The change of only two variables can vary the strain which the craft feels in order to match the speed at which the ideal points are moving. To this end, the algorithm is easily reconfigurable. The trajectory generator supplies the set of ideal

points to the controller to drive the vehicle. Thus the two work in conjunction with one another and so the controller is the final piece of the autoland puzzle.

6.0 Controller Design

Ever since Ktesibios first designed a float regulator to feed a water clock back in 270 BC, man has been intent on finding ways of making life easier for himself through the use of feedback control. Fundamentally, feedback control is the basic mechanism by which systems maintain equilibrium or homeostasis. Feedback control may be defined as the use of difference signals, determined by comparing actual values of system variables with their desired values, as a means of controlling the system [39]. In the case for the autoland procedure, the difference signals available to monitor and drive the system are position and velocity. The ideal and actual values for each could be provided by the trajectory generator and the navigation unit respectively. This being said, the primary goal of this exercise is positional accuracy of the vehicle and so position feedback will be given primary importance. In general, the reasons for feedback is twofold. Firstly, it is to reduce sensitivity of performance from parameter variations of the plant and imperfections of the plant model used for design. Secondly, feedback reduces the sensitivity to noise and disturbance [7] [28]. This last benefit is especially important for the AV. The disturbances which the craft will encounter will come from many sources and will at times be of sizeable magnitude.

The fact that feedback will be used is only the first step in coordinating the AV. The requirements for the craft are very strict as was seen in *section 3.3* and so chances are, a simple proportional controller will not be enough. A controller will need to be developed and to this end, a proportional plus integral plus differential (PID) controller will be used. The virtues associated with this approach are many, one of which is its

proven track record for controlling plants which are complex and non-linear such as those of the CL-327. The PID will monitor the error signal and prevent the craft from approaching unstable conditions and increase the unit's stability envelope. The PID has three explicit terms which all have their respective characteristics which are lent to the system as a whole. These will be overviewed and explained how they relate to the autoland.

By this point it should be understood that the performance in the vertical is significantly different than that in the horizontal. For this reason, the controller for each plane will be dealt with separately, thereby allowing for a full explanation for each. But first an explanation of the individual components of a PID will be undertaken. These points will then be put into context as to what are the general advantages of using a controller and more specifically how and why this system is best for the craft.

6.1 Why use a PID?

The first autopilots were built for ships and subsequently those for aircraft followed. Elmer Sperry, was a leader in the design of such devices when the field was still in its infancy. He built his autonomous systems to mimic the behavior of a human pilot. The greatest problem he and others were faced with at the time was the fact that as the topic of controls was so new, there was no overseeing body or organization to unite the researchers. It went so far as there was no common language of control systems and the concept of block diagrams hadn't come about yet [40]. It wasn't until the 1920's that order began to come about. It was in 1922 that Nicholas Minorsky presented a very clear analysis of the control actions necessary to provide effective control of a system who's exact dynamics were unknown. It involved the sum of three terms, a proportional gain

times the magnitude of the feedback error, an integral gain times the integral of the feedback error, and a derivative gain times the derivative of the feedback error [40]. The acronym which describes this process is PID. The error being referred to here is short for the tracking error. Recall that this refers to the difference between the desired input to the plant and the plant's output. The goal of the PID controller, and for that matter the feedback design in general, is to reduce steady state errors of the system while improving the transient response [28]. A generalized form of a plant employing a PID controller is given in *figure 6.1*. The basic proportional, integral, and derivative actions are fundamental to many dynamic compensators so a good understanding of their actions is important. An overview of the physical contributions which each of the three (P, I, D) components bring to a system follows.

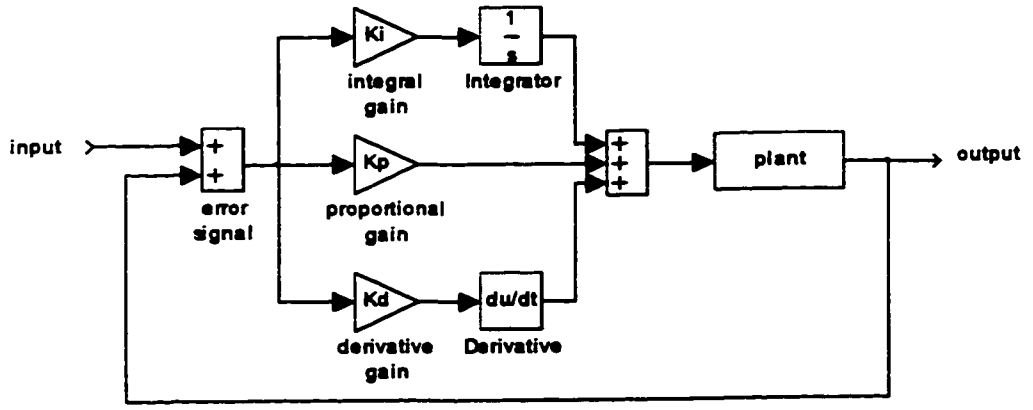

Figure 6.1 – Plant using PID control and position feedback

6.1.1 Performance of PID

Proportional control action is the simplest of the three options available and therefore the most common. It alters the system response by adjusting the loop gain of the system [41]. It's effect on system response is dependant on the amount of corrective

effort provided, but generally results in a decrease in rise time, an increase in overshoot, a negligible change in settling time, and a decrease in steady-state error [42].

The prime requirement of many control systems is that there should be no error or at worst a very small error in the steady state. To accommodate this requirement, a signal proportional to the time integral of the error is added to the existing proportional term. Since the error signal is integrated within the controller, even the smallest error eventually produces a corrective signal of sufficient magnitude to actuate the system to eliminate the error. The system will, theoretically, only come to rest when the error has been reduced to zero [41]. In addition to its effect on steady state error, integral control decreases the rise time, but has a tendency to destabilize the system [42]. In some instances, integral action is referred to as a "reset action" as it has a characteristic of resetting the plant to the desired condition [43].

Derivative control is the last of the three fundamental types of control which will be covered here. It is a form of control action which can increase the effective damping of the system. It modifies the output when the error is changing rapidly, thus anticipating a large overshoot and making some corrective action before it occurs. This is always a highly desirable feature in the design of a control system, since any change in the values of plant parameters over a period of time is less likely to cause the system to drift into instability [41]. As for tangible effects, derivative action in the forward path will significantly decrease the overshoot and settling time [42] [44].

A PID takes all the previously overviewed benefits and combines them into one controller. It calculates both the integral and derivative of the error. The proportional control is used to reduce the rise time and reduce the steady state error. The derivative

control is responsible for reduction of settling time and overshoot while the integral action eliminates the steady-state error.

6.1.2 Advantages to Using PID

PIDs are very useful controllers. Their performance is so good and so reliable that they have become the most commonly used standard form of dynamic compensation in practice [28]. They have a long history of being a simple yet very effective means to an end. Another major plus is the ease at which a PID can be adjusted. In fact, with the empirical response driven techniques such as the Ziegler-Nichols methods and others like it, PID tuning is an extremely simple task [28] [41] [43]. Another advantage is its universality. It can be used with all sorts of systems whether they are simple or complex, with known or unknown dynamics. These controllers also provide a very robust system. When a system is faced with disturbances, either external or internal, PID controllers are very good at maintaining system stability. The final advantage which the PID controller brings to any system is its ability to deal with systems which are linear or non-linear. When models are created for a real system, often they are linearized to reduce development time. A PID can be used and tested in a linear model then mated with the real system while undergoing only minor adjustments.

6.1.3 Transfer Functions and PIDs

Tuning PIDs can be done as described in the last section using existing empirical techniques. However a more exact method is to use a system describing transfer function and perform the tuning analytically using methods such as root locus diagrams [41]. Transfer functions are obtainable for simple systems, but can be difficult if not

impossible to be found for complex systems. Dynamics of the CL-327 are complex and non-linear unless grossly simplified. Thus derivation of a representative transfer function is not a simple task. A possible solution to this problem is to linearize the system about a typical operating point and work out a transfer function which is valid for this typical operating point. Though this approach could be used, it diverges from the scope and purpose of the project. The task was to conceptualize and devise an automatic landing process. This assignment spans many different fields and is comprised of several different concepts. The controller is not the focus of this work, but rather a component of the overall package. The object is not to apply true synthesis and produce a unique solution or to employ cutting edge controllers, but rather use existing ideas to complete the package. A PID controller will accomplish this with ease and considering its many distinguished features, is a fine tool for the job.

6.2 Controller for Horizontal Plane

The control of the craft in the horizontal is provided in a physical sense by the tilting the vehicle towards where it needs to go. The actual mechanism which is responsible for this task is the swashplate which creates a cyclic pitch of the rotor blades to perform the feat [27] [45] [46]. Commands must be sent to the actuators which act on the swashplate to perform these tasks. These commands are formulated within the FCS by the controller [16]. The controller for the horizontal is very involved due to the complexity of the craft's dynamics in the horizontal plane. The focus for the remainder of this section will be the process which was undertaken to create the controller for the horizontal.

One of the most important challenges faced was the decision of which inputs were to be used by the controller. Some choices existed as to which inputs to include as two sources were available, position and velocity. Given that positional accuracy was such a high priority during this portion of the mission, it was a logical starting point. Since the contingencies existed, the position input to the controller would actually be in the form of position feedback. The position error for the craft would be calculated from the ideal position provided from the trajectory generator and from the actual position supplied by the navigation unit. Seeing as this controller will be activated during the landing of the craft, after the switchover to DGPS has already occurred, it is assured that the quality of the position feedback signal would be high. In the interest of keeping the controller as simple as possible [42], only position feedback was used. The velocity signal was omitted initially.

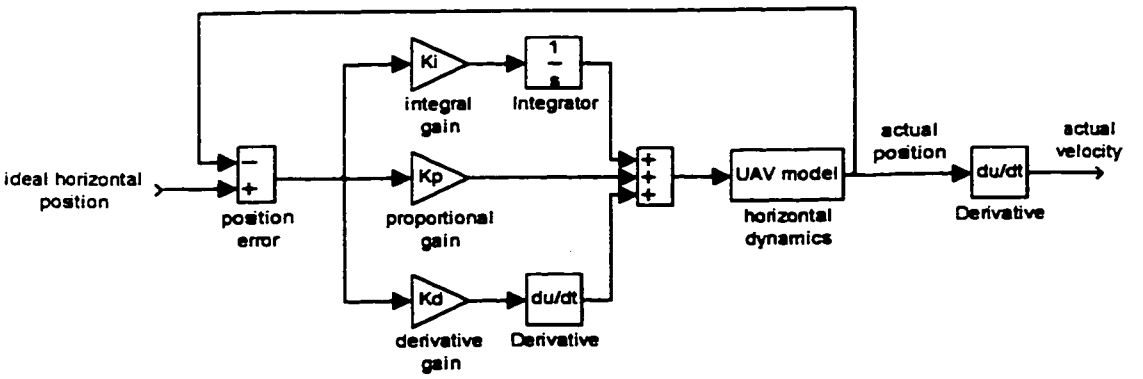

Figure 6.2 – Position feedback horizontal controller

The controller itself consisted of a PID and was responding to position feedback described previously (*figure 6.2*). This was the simplest system available and was made the initial choice for this reason. The system required tuning to see if it was capable of controlling the vehicle. For the initial stage, no disturbances of any sort were included.

The flight profile for the test regime was horizontal which allowed for attainment of the maximum peak velocity in the horizontal ($V_{P,max}$). *Figure 6.3* shows the ideal velocity profile used while tuning the horizontal controller. When the velocity profile was integrated, it supplied the ideal position information and when used as is, it gave the ideal velocity for the tests. As is evident by *figure 6.3*, the maximum speed reached in the horizontal during the tests was indeed the maximum allowed total speed of the craft

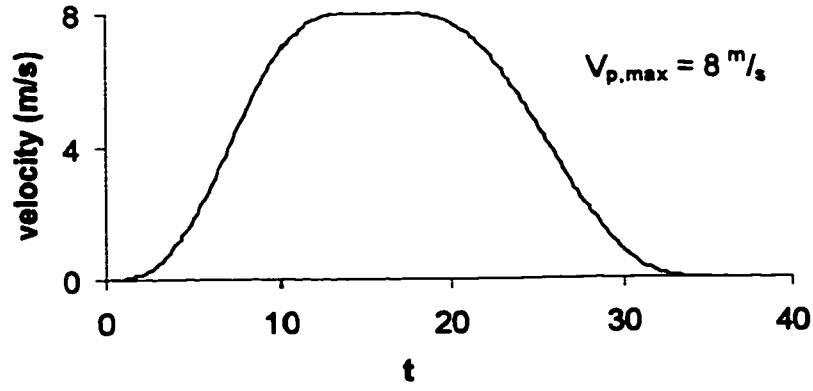

Figure 6.3 – Ideal horizontal velocity profile used for tuning horizontal controller

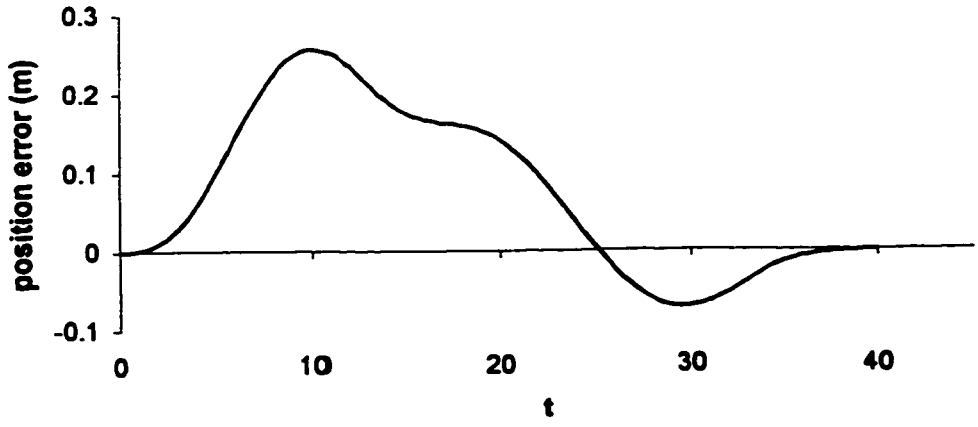

Figure 6.4 – Horizontal position error response using position feedback controller (ideal conditions)

(8 $^{m}/_{s}$). The method devised by Ziegler and Nichols was the tuning method of choice for the PID [28] [41] [43]. However, the fundamental criteria for this method is to tune the system to maintain the stability limit using only proportional control [41]. This was not possible. The craft was unstable at all times when proportional action was the only compensation used. Thus the only manner in which the controller could be tuned was by using intuitive methods and modern simulation techniques. Using these methods, the AV response was made stable. *Figure 6.4* shows the response for position feedback in the horizontal. Note that the error magnitude reaches a maximum of 0.27 m or 27 cm.

The ideal world is a good place to begin the tuning. However, the next phase was to test the system under real world conditions. This meant the inclusion of disturbances. There are two types of disturbances which the system was tested against, external and internal. For the case of the AV, external disturbances usually come from wind gusts while internal sources are predominantly found in the area of signal noise from the navigation unit. For this phase of controller tuning, these were the sources for disturbances effecting the craft. *Figure 6.5* shows the disturbance inputs, where *figure 6.5a* represents the wind gusts which span a range from ±15 $^{m}/_{s}$ at a frequency of 10 Hz and *figure 6.5b* represents position signal noise which covers a range of ±0.15 m and occurs at 25 Hz. These noise signals were decided upon after conversations with Bombardier staff and represent higher than normal values [47]. These noise signals are those which are referred to throughout for the horizontal.

When the position feedback supplied PID controller was faced with only the winds, the response of the AV remained stable and accurate, but jumpy (*figure 6.6*). When the actual position error noise was included along with the winds, the system went

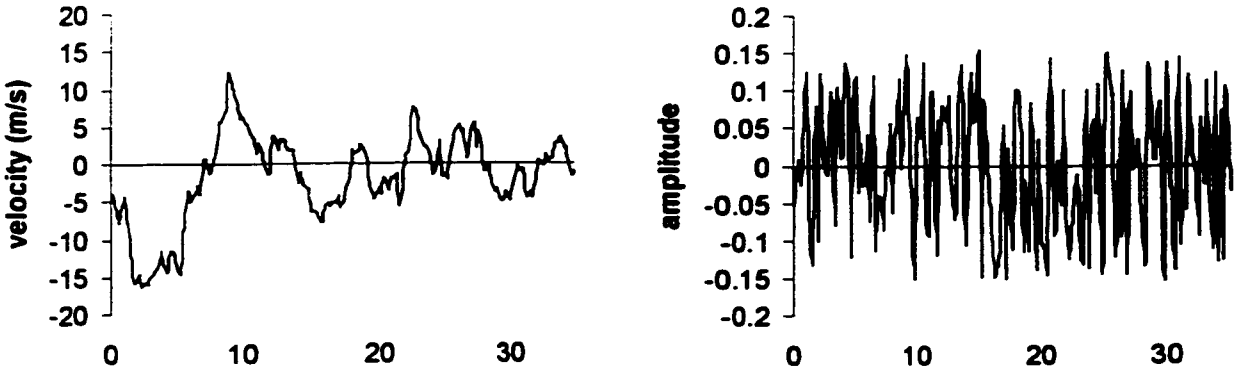

(a) Winds (b) Navigation unit signal noise

Figure 6.5 – External and internal disturbances

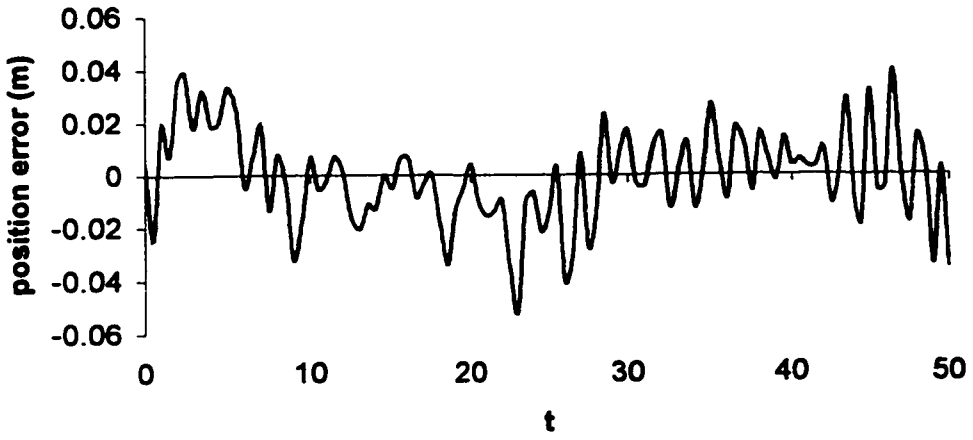

Figure 6.6 – Position error response for position feedback with internal and external disturbances included

unstable. This inability to suppress internal disturbances describes a controller which was not adequately prepared to handle the demanding regime which the AV operates within. Its stability envelope was not large enough to provide for safe operation. The controller had to be modified to allow for these conditions.

To avoid these problems with degraded response due to disturbances, additional control action had to be introduced. A classic method to achieve this goal is to initiate an action similar to that of proportional-plus-derivative control by incorporating within the

control loop, a minor feedback path with introduces control action known as velocity feedback. A signal proportional to the derivative of the output is used and is generally arranged as depicted in *figure 6.7*. The result of such an action will reduce the overshoot, add damping, and quiet the response to allow for AV operation under noisy conditions. Another method uses the velocity error signal [47] in the form of an additional major feedback loop (*figure 6.8*). The concept of the control input is similar to that used for

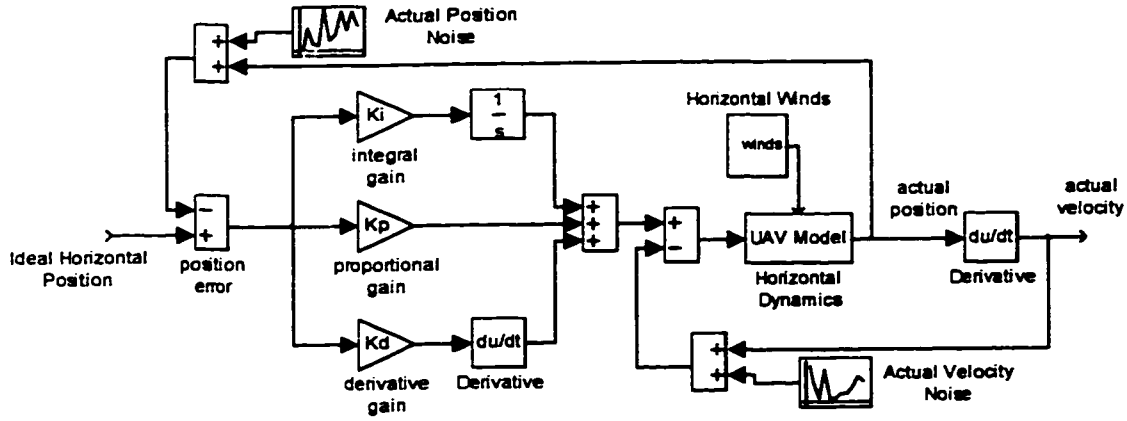

Figure 6.7 – Horizontal minor loop velocity feedback schematic

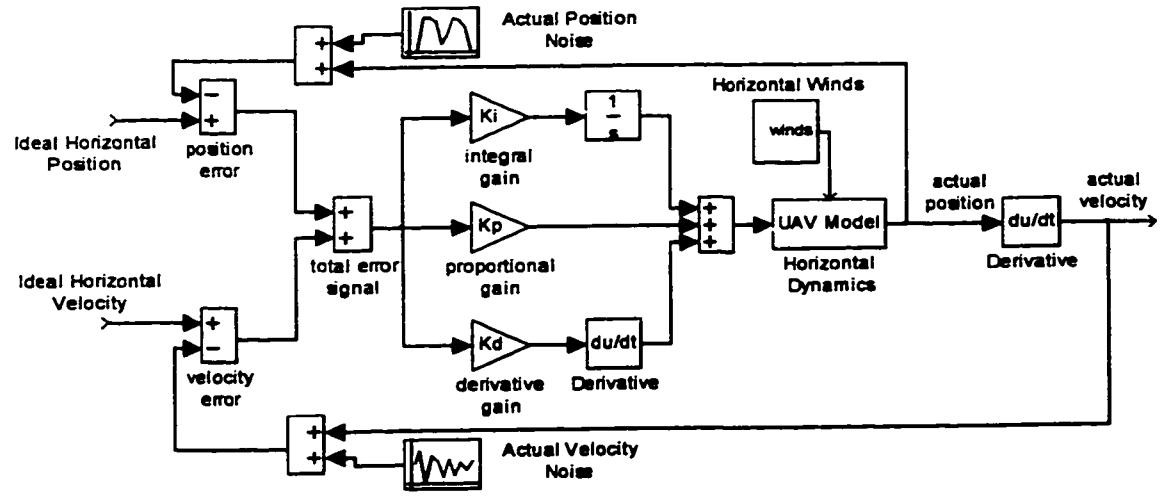

Figure 6.8 – Horizontal major loop velocity error feedback schematic

position feedback. The sources for the ideal and actual data are the trajectory generator and the navigation unit respectively, similar to the sources for the position feedback. At this point in the mission, the navigation unit comprises its values for actual velocity from DGPS provided information. The benefits rendered by using this method are similar to those using velocity feedback in reduction of overshoot, addition of damping, and quieting of the response.

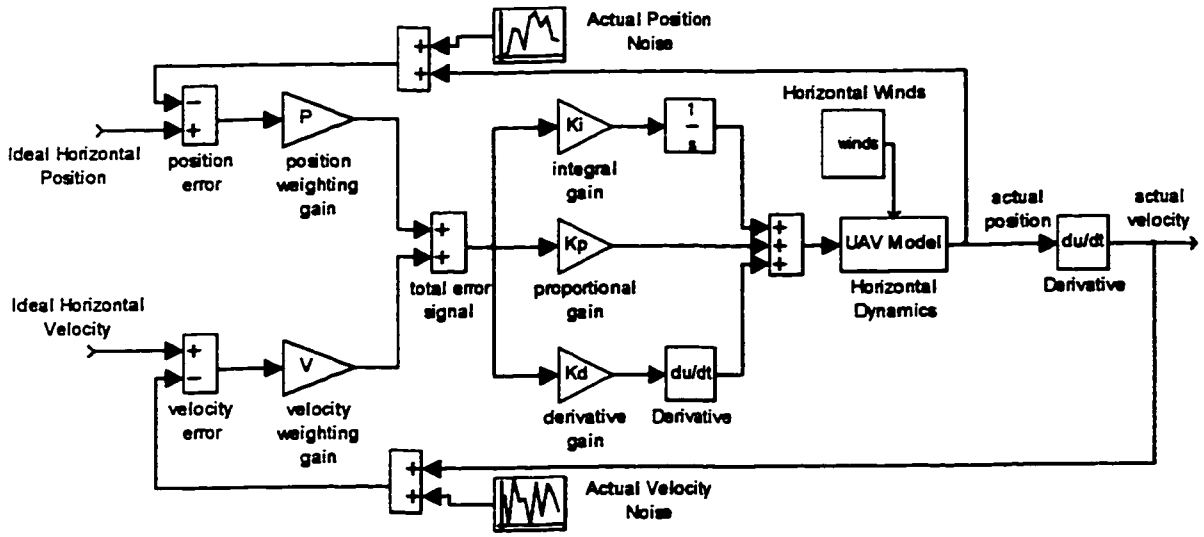

Figure 6.9 –Horizontal position and major loop velocity feedback schematic with individual signal weighting

The task was to find which variety of position time rate of change signal would best stabilize the craft. Tests showed that the minor loop velocity feedback was not effective in achieving system stability even with repeated attempts at PID retuning. The outcome was much brighter when major velocity feedback loop was employed. It provided system stability with very little PID adjustment from the original values found from tuning using only the position feedback. With wind disturbances and feedback signal noise (both in terms of position and velocity), the controller handled the system

well. As a final task, the weights of the position and velocity feedback signals were adjusted prior to their being fed into the controller. *Figure 6.9* shows the schematic for individual signal weighting. It was noticed that when the amplitude for the actual velocity signal noise from the navigation unit was increased, an effective countermeasure was to increase the weighting of the velocity feedback signal. To illustrate the difference

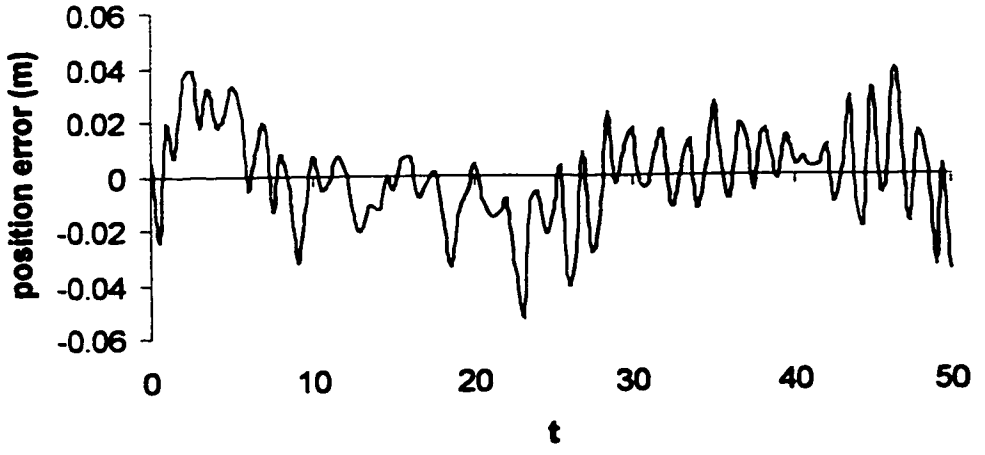

(a) Only position feedback

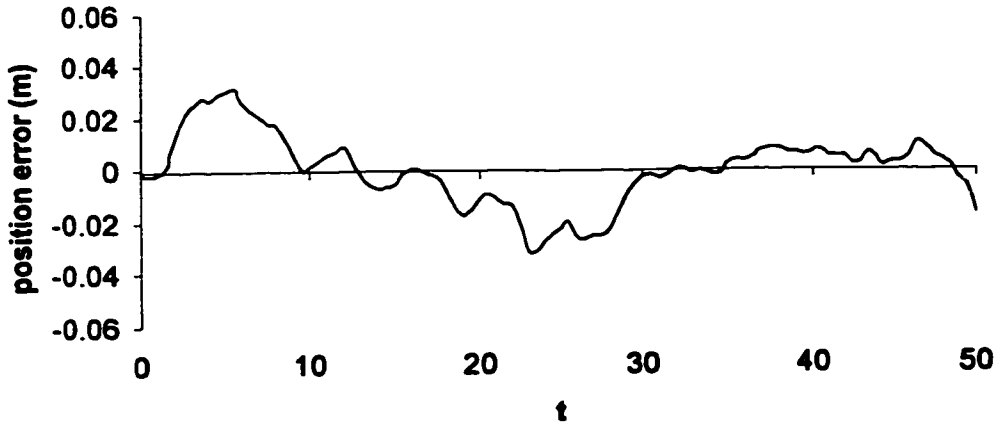

(b) Position and velocity feedback

Figure 6.10 – Position error plots comparing system using only position feedback and system using position and major loop velocity feedback (external disturbances only)

with the addition of the major loop velocity feedback signal as opposed to the original system using only the position feedback, *figure 6.10* shows position error plots when the same wind is used with each system. Recall that the system using only position feedback was not capable of remaining stable after winds and signal noise was added (*figure 6.5*). *Figure 6.11* shows the position error response for the system using the combination position and velocity feedback when both winds and noise (on both the actual position and actual velocity) signals are included.

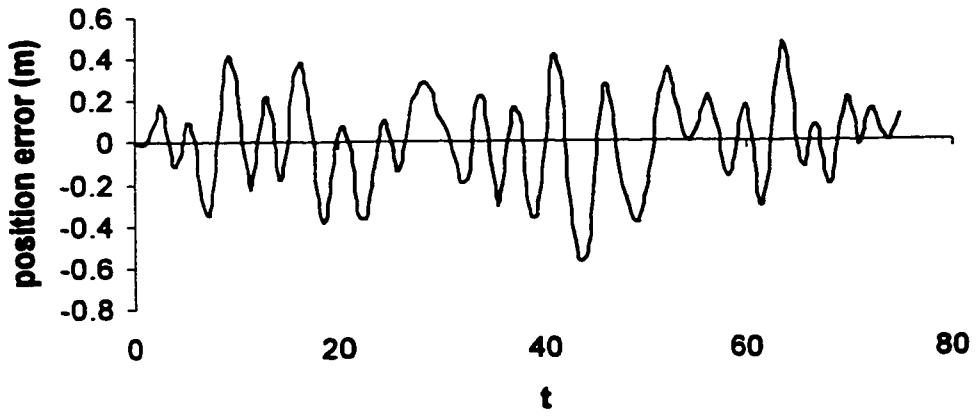

Figure 6.11 – Horizontal position error plot for system using combination position and major loop velocity feedback with both internal and external disturbances

One important observation was made as to when the craft became unstable in the horizontal. If the navigation signal noise was removed and the winds were increased, due to position error spikes at the end of segment A and start of segment C, the craft would become unstable shortly after these points. Upon further investigation, it was found that it was at these points where the tilt-rate-limiter would be activated and the system would subsequently become unstable. If the tilt-rate-limiter was not activated, the response would remain stable. This revelation allows foreknowledge of when the craft will become unstable. This could allow for actions to be taken to prevent such an occurrence.

6.3 Controller for the Vertical Plane

For a helicopter to move in the vertical, the collective pitch or the pitch of all rotor blades must be altered. For this to occur, the swashplate must be repositioned using various actuators [27] [45] [46]. Similar to the horizontal, the commands for these swashplate actuators are provided by the FCS within which resides the vertical controller. The vertical dynamics of the system are very different from those of the horizontal and so a thorough analysis must once again be undertaken.

As with the horizontal, the initial version of the vertical controller was kept as simple as possible. Positional accuracy was again of great importance and to this end the position feedback was the sole source for error to be passed on to the controller. The ideal vertical position was to be obtained from the trajectory generator while the actual vertical position was provided by the navigation co-processor (NCP) through the navigation unit. Even with DGPS information available, the NCP deduces the vertical position of the craft after verifying a number of vertical data providing systems. The velocity signal would not be employed unless it was required.

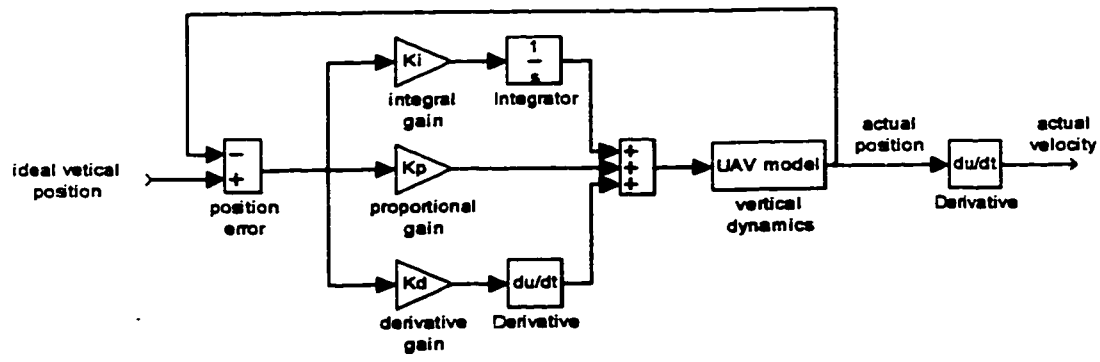

Figure 6.12 - Position feedback vertical controller

The vertical controller, at this point, consisted of a position feedback supplied PID (*figure 6.12*). In order to tune the PID, a few considerations were taken into account. Simulations were designed so that no disturbances were present and that the flight profile itself was vertical. Since there is a maximum vertical descent rate allowed by the trajectory generation algorithm of -5 $^{m}/_{s}$, a vertical profile allowed for the ideal vertical velocity to be brought to its limit (*figure 6.13*). This information was then integrated to provide the ideal position information. The first phase was to tune the PID using the

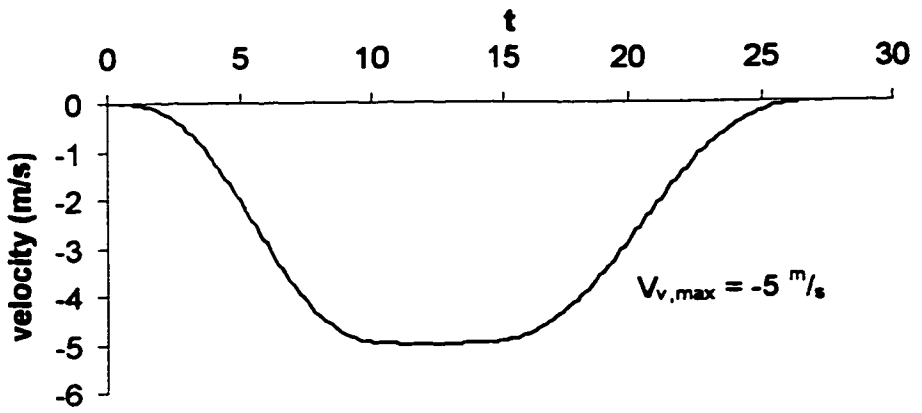

Figure 6.13 – Ideal vertical velocity profile used for tuning vertical controller

Ziegler-Nichols criteria referred to previously. As with the horizontal, the system could not be brought to the condition of marginal stability using only proportional action and so the method of intuitive trial and error was reverted to. Using a well tuned PID, the system using only a position feedback signal was stabilized. The response was very accurate (*figure 6.14*), but surprisingly enough, not as accurate as the response in the horizontal as can be verified by comparing *figure 6.4* and *6.14*. This was contrary to the result expected seeing that the open loop step response for the vertical system was much quicker than that for the horizontal (*figure 2.6*).

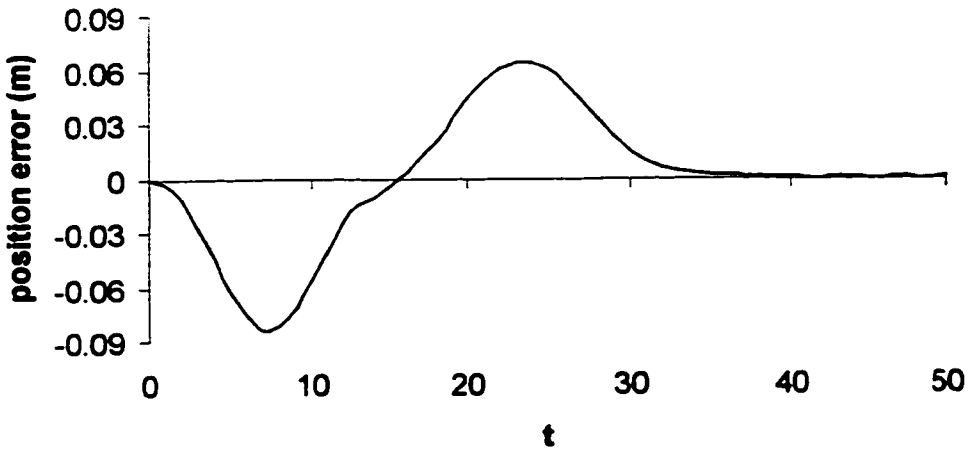

Figure 6.14 – Vertical position error response using position feedback controller (ideal conditions)

With the ideal system configured, disturbances were added. Both internal and external disturbances were applied with navigation signal noise and winds used for internal and external disturbances respectively. The navigation signal noise amplitude and frequency was no different than that used for the horizontal system (*figure 6.5b*) while the wind model was unique to the vertical with a range from +15 to -10 $^{m}/_{s}$ at a frequency of 0.25 Hz (*figure 6.15*). This wind model was provided by Bombardier staff and again represents above average wind conditions [47]. With the addition of only the winds, the controller was not capable of maintaining stability in the vertical. This was not acceptable performance as the system had become unstable even before the internal disturbances had been tested.

As with the horizontal, the solution was to turn to velocity feedback of one form or another. The minor loop velocity feedback (*figure 6.16*), using information provided

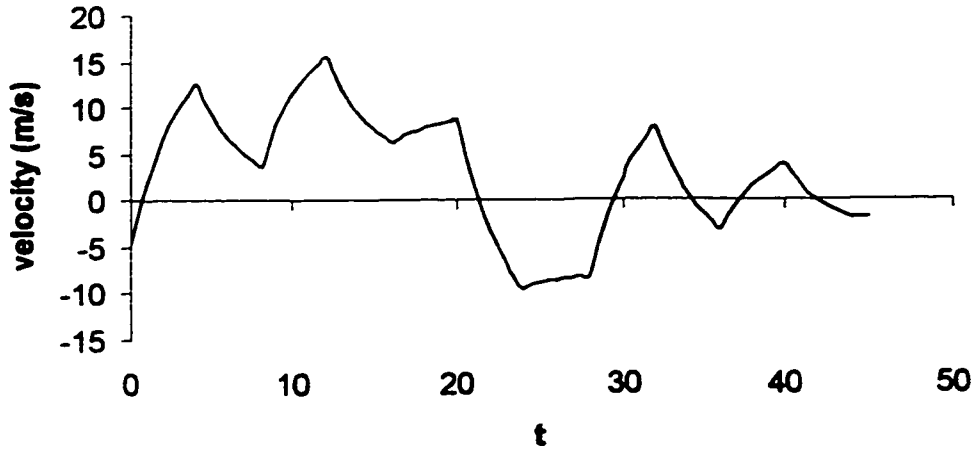

Figure 6.15 – Wind model for vertical

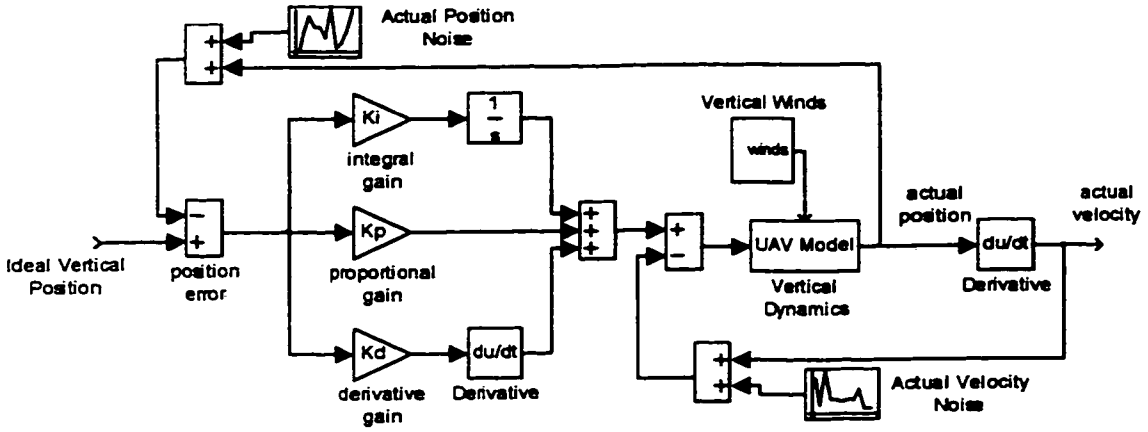

Figure 6.16 – Vertical minor loop velocity feedback schematic

by the NCP, was not controllable even with repeated adjustments of the PID. On the other hand, major loop velocity feedback (*figure 6.17*) worked well from its inception before the PID gains were adjusted from their settings when only the position feedback was used. The velocity error is provided to the craft by the trajectory generator and the NCP. Slight gain adjustments were required when the major loop velocity feedback was added before optimum results were found. The last step in tuning of the controller was to

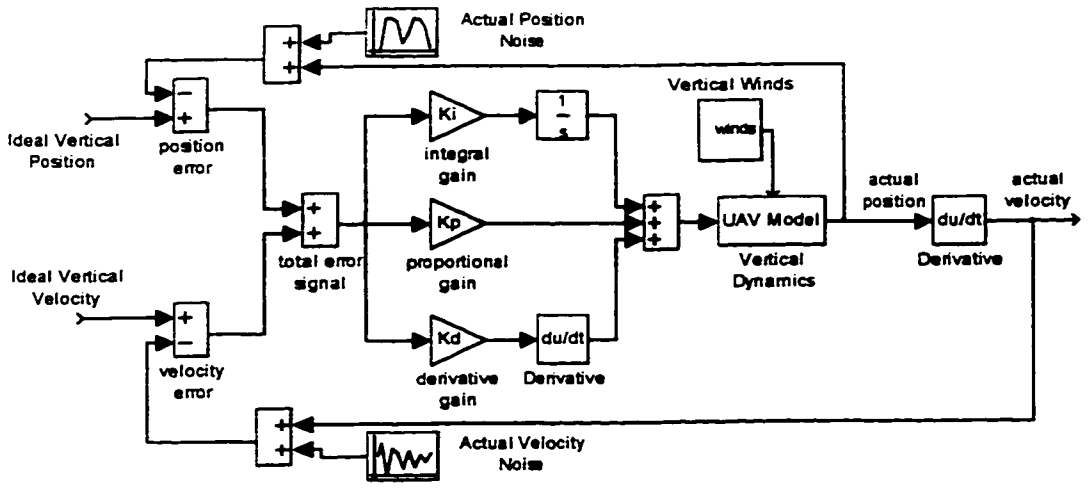

Figure 6.17 -Vertical major loop velocity error feedback schematic

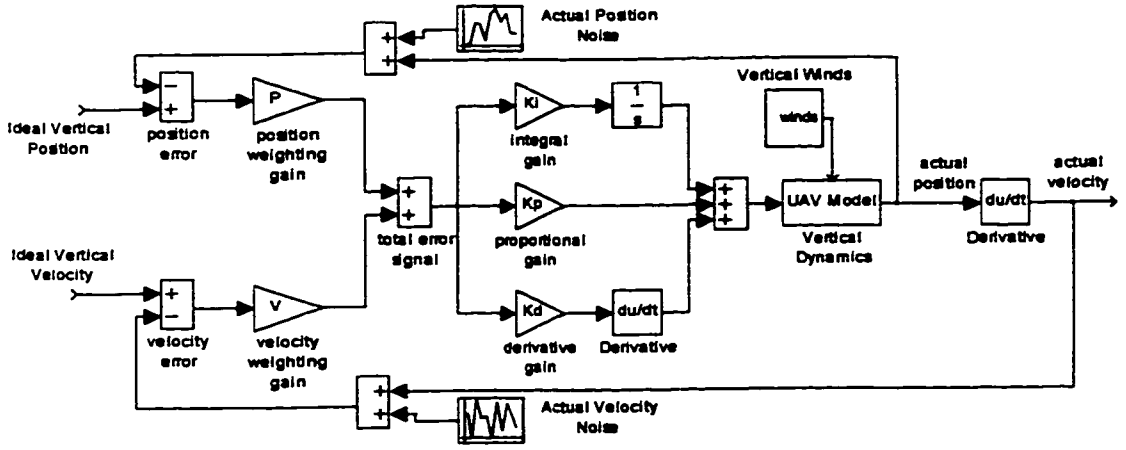

Figure 6.18 – Vertical position and major loop velocity error feedback schematic with individual signal weighting

adjust the weight of the two feedback signals against one another (*figure 6.18*). The trend was similar to that for the horizontal. As the navigation velocity signal error was increased, an increase in weight of the velocity feedback was the solution. This seems surprising as it would make sense that the increasing of the value for this error would in effect amplify the noise, but through simulations, it was shown to stabilize the system.

Figure 6.19 shows the position error plot for the system using weighted position and velocity feedback signals, with internal and external disturbances included.

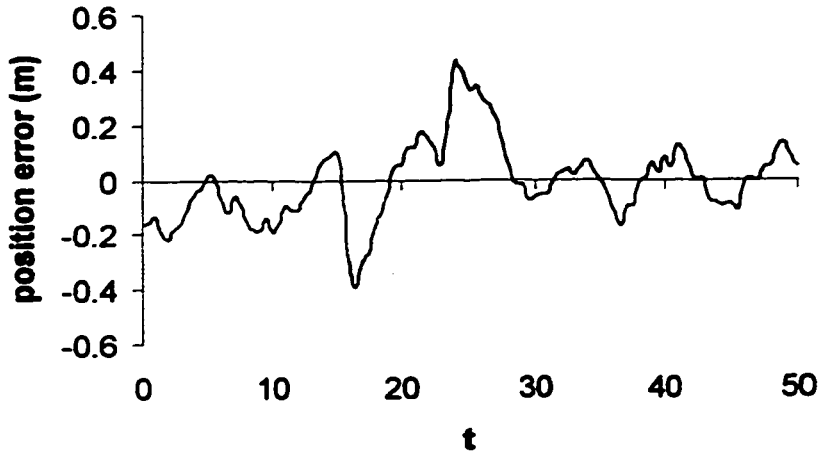

Figure 6.19 - Vertical position error plot for system using combination position and major loop velocity feedback with both internal and external disturbances

6.4 Effects of the Trajectory Generator

It was said in the chapter describing the trajectory generator and should be clear at this point that the trajectory generator and the controller work in unison to provide stable conditions for the craft. When the trajectory for a given path was calculated, apart from the limited velocities, there were only two other variables which the profile depended on, the time to accelerate (t_A) and the time to decelerate (t_C). These values were selected to provide a balance between well controlled flight and quick response. Through tests, it was found that on average, t_C should be about 30% longer than t_A to provide similar maximum position error jumps for their respective segments. Another finding was how a system which was not being strained by quick accelerations and decelerations was able to withstand higher amounts of disturbances before instability occurred. Tests were done to

confirm this using only external disturbances. For the same amplitude and frequency of wind, if t_A and t_C were reduced proportionally, the craft would become unstable. Conversely, if large winds were present and these two variables were increased, the system would become stable. This concept is understandable as if the controller is less strained in keeping up with the ideal points being provided by the trajectory generator, the controller has more ability to be able to deal with disturbances.

6.5 A Final Comment

The craft's controllers were designed and various traits were uncovered concerning the response and the manner in which these responses were produced in both the horizontal and vertical. Prior to the topic being wrapped up, there are some issues which must be discussed. Firstly, there is the fact that neither the horizontal nor the vertical systems could be brought to the brink of instability and so it was not possible to use the Ziegler-Nichols criteria to tune the PID. In this event, the system was tuned through intuitive means. This is not the most accurate method to produce such results and it is noted that this is a point where there is a great chance improvements can be made. Also, it is important to understand that all these the tests performed to achieve the PID gains were simulations with a model. A model by definition is an approximation of reality at the best of times [48]. Moreover, the model which these tests were performed on was a simplified version of the true model. So it goes that the controller gains which were used to produce the information for the previous sections, are only estimations for the values required on the real vehicle. The values themselves will undoubtedly have to be found using testing on the full model and on the flying hardware before the controller is labeled as proven. However these observations do not take away from the general

findings of this chapter concerning the use of velocity feedback, the effects of trajectory generation variables on the craft's ability to suppress disturbances, and the manner in which to predict the onset of instabilities in the horizontal and vertical planes.

7.0 Conclusions, Recommendations, and Future Work

7.1 Conclusions

The objective of this thesis was to develop a novel automatic landing system for Bombardier's CL-327. An issue of importance is that the system was to work using predominantly DGPS information. This was a new feature on the redesigned Bombardier VTOL UAV offering. The system was to be designed via simulations using the Bombardier supplied simplified model of the AV. It was then to undergo small adjustments and finally be mated with the flying hardware. The project itself was based on three key topics, the design of GS intercept and trajectory generation algorithms, and the selection of a controller.

The GS intercept logically determines where the craft should go after navigation system switchover from GPS to DGPS. It evaluates where the craft lies about the flight profile and selects an efficient target point where the craft should intercept the GS. By this, it avoids the obvious, but not necessarily best choice of sending the AV to the RP. The intercept decision making process maintains flight within the SV and thereby ensures craft safety. The algorithm works for all path lengths and orientations. It determines which target point selection method is to be used by dividing up the space around the flight profile and calculating where the craft lies. It determines AV position about the profile using the established method of homogeneous transformations. Various regimes of target point selection methods are established to allow for varying degrees of precision with respect to target point selection along the GS.

The trajectory generator algorithm provides an ideal path between two arbitrary points in space. This path involves temporal laws and thereby represents velocity and acceleration as well. This algorithm works in conjunction with the controller and therefore is a component of the guidance system. It is easily reconfigurable to user defined limitations on maximum peak velocity and maximum vertical velocity. In addition to this, it was designed to respect the tilt-rate-limiter. It provides a large stability envelope while providing quick overall response. It also accomplishes this while having the ability to adjust for any length or orientation of path. Though the acceleration path for the chosen cosine profile gave the highest peak value for those tested and was the most calculation intensive, its smooth profile with the absence of jerk was unattainable by the other profiles evaluated. The calculations for the path require the knowledge of very few variables with the time allotted to perform segments A and C being the only ones which can be tuned without altering the craft velocity limits. To achieve the infinitely variable path length and geometry, the algorithm accommodates with automatic proportional scaling of time and magnitude of the acceleration.

The object for the controller was to select one which was capable of withstanding large disturbances, was well-known with a proven track record, and was easy to tune. To this end, the PID controller was the ideal candidate. To tune the PID precisely, a transfer function is required. This was problematic as it could not be found directly and though linearization of the model was contemplated, this seemed beyond the scope of the project. The horizontal controller was, for the sake of simplicity, originally designed using only position feedback. When it became apparent that this controller was not capable of withstanding the various disturbances, major loop velocity feedback was added. The

system using this arrangement was responsive, stable, and accurate. Tests showed that in the horizontal, the threshold of instability and the activation of the tilt-rate-limiter were one and the same. Knowing this proved instrumental in trajectory parameter adjustment. The vertical plane controller also began with only position feedback, but graduated to a combination of position and major loop velocity feedback due to controller inability to accommodate disturbances. This system then became stable and responsive through not as accurate as that for the horizontal. For both the horizontal and vertical, PID controllers were used. Though they are an effective approach as evidenced by the results, there exists potential for the synthesis of a unique controller

7.2 Recommendations and Future Work

The project was thorough and complete, but still questions exist. The following are recommendations which this researcher believes would be beneficial to the autoland system. As was just mentioned, the PID is a very capable controller, but one which is generic by nature. Development of specific controllers for both the vertical and horizontal have the potential to further extend the bounds of the current stability envelope. A possible manner in which this could be done is by the incorporation of non-linear controllers.

Another area of interest is the curves used for trajectory generation. The cosine profile was chosen even though it was calculation intensive. Investigations could be undertaken to reduce the number of calculations required to provide cosine trajectory data. Further, employment of composite curves could be looked into where half of an acceleration profile is comprised of a polynomial profile and the other half is a cosine profile. This would save travel time if designed correctly.

For future work, as the scope of the project is so broad, there exists no shortage of opportunities for continued progress. With the revelation of how the craft becomes unstable in the horizontal, methods can be devised to adjust for and avoid instabilities. One way is to actively monitor the aircraft tilt and just prior to the activation of the tilt-rate-limiter and subsequent instabilities, the vehicle could relax the trajectory generation parameters t_A or t_C to reduce strain on the system thereby reducing the risk of unstable flight. The work could even go so far as redesigning the tilt-rate-limiter so this wouldn't be a problem.

Another area is the management of the actual switchover process between navigation modes. Logic must be developed so the AV knows to hover on station while the DGPS information is uploaded and the controller itself to be switched for that of the autoland. Throughout all this preparation for next phase, the craft must remain stable.

A final topic for continuing interest is the development of an algorithm to transition between the various segments of the landing profile. As it stands at the moment, the craft must fully capture the intercept point before the GS descent may begin. The idea is that the transition between the two portions should be smooth and flowing. This system development would save time and is traditionally associated with high level UAV offerings, included in which is the Bombardier CL-327.

References

1 http://bris.ac.uk/Depts/Union/BUHABS/first.html

2 Englebert, H.P.; Schröder, J., "Landing of an Unmanned Helicopter on a Moving Platform," *AGARD: Pointing and Tracking Systems* (N94-36616 12-18), pp. 5.1-5.9.

3 Meyers, M.J.; Magee, J.P., "Flight Testing the Eagle Eye Tiltrotor Unmanned Air Vehicle," *IN: Vertical Lift Aircraft Design Conference*, Jan. 18-20, 1995, pp. 6.7-1-6.7-14.

4 Thronberg, C.; Cycon, J.P., "Sikorsky Aircraft's Unmanned Aerial Vehicle, Cypher: System Description and Program Accomplishments," *AHS Annual Forum*, May 9-11, 1995, pp. 804-11.

5 Schrage, D.P. et al., "The Autonomous Scout Rotorcraft Testbed as an Integrated System," *AHS Annual Forum*, Apr.29-May 1, 1997, pp. 906-14.

6 http://www.aerospace.bombardier.com/htmen/H4A.htm

7 Potter, K.J.; Rawnsley, B.W., "Helicopter Automatic flight Control Systems for All Weather Operations: EH101 and Beyond," *Proceedings of the Fixed and Rotary Wing All Weather Operations Conference*, United Kingdom, Apr. 23, 24, 1991, pp. 13.1-13.14.

8 Sherman, D. et al., "University of Central Florida Technical Report: AUVS International Aerial Robotics Competition," *IN: AUVSI '96*, July 15-19, 1996, pp. 955-64.

9 Black, K.M. e al., "The UTA Autonomous Aerial Vehicle – Automatic Control and Navigation," *NAECON 92, Proceedings of the IEEE*, May 18-22, 1992, pp. 489-96.

10 http://www.auvsi.org/auvsicc/learning.htm

11 Weidel, M.; Alles, W., "Automatic Flight Control System for an Unmanned Helicopter System Design and Flight Test Results," *AGARD, Active Control Technology: Applications and Lessons Learned* (N95-31989 11-08), pp. 15.1-15.10.

12 http://www.sikorsky.com/programs/cypher/index.html

13 Tharp, W. et al., "Design of a Tiltrotor Unmanned Air Vehicle for Maritime Applications," *AHS Aerospace Design Conference*, Feb. 16-19, 1993, pp. 1-11.

14 Upton, B. et al., "The Design, Development, and Flight Testing of the CL-227 Unmanned Air Vehicle (Sentinel and Sea Sentinel)," *AHS: Annual Forum*, May 9-11, 1995, pp. 47-56.

15 Bokos, G.; Ferrier, B., "Development, Integration, and Test of an Automatic UAV Recovery System for the CL-227 VTOL-UAV," *AHS: Annual Forum*, May 9-11, 1995, pp. 812-19.

16 Pelletier, M. et al., "Autonomous Navigation and Control Functions of the CL-327 VTOL UAV," *AGARD Symposium on System Design Considerations for Unmanned Tactical Aircraft*, Oct. 7-9, 1997, pp. 18-1-18-10.

17 http://www.services.bombardier.com/htmen/pr_5_42.htm

19 Denton, R.V. et al., "Autonomous Flight and Remote Site Landing Guidance Research for Helicopters," NASA-CR-177478.

20 McDonald-Gibson, N.C., "All Weather Operations," *Proceedings of the Fixed and Rotary Wing All Weather Operations Conference*, United Kingdom, Apr. 23, 24, 1991, pp. 3.1-7.

21 Downes, M; Brown Lt. Cdr. C., "Helicopter Approaches in Low Visibility Using RGPS and EFIS," *Proceedings of the Fixed and Rotary Wing All Weather Operations Conference*, United Kingdom, Apr. 23, 24, 1991, pp. 12.1-12.

22 Petruszka, A.; Stentz, A., "Stereo Vision Automatic Landing of VTOL UAVs," *IN: AUVSI '96*, July 15-19, 1996, pp. 245-263.

23 Kaminer, I. et al., "Trajectory Tracking for Autonomous Vehicles: An Integrated Approach to Guidance and Control," *Journal of Guidance, Control, and Dynamics*, Vol. 21, No. 1, 1998, pp. 29-38.

24 Conversation with Louise Cléroux, Eng., Ph.D., Robotics and Systems Engineer, UAV Engineering, Bombardier Services: Defense.

25 Wacker, U.; Both, A., "DGPS Multichannel Autoland System Performance," *IN: National Technical Meeting*, Jan 22-24, 1996, pp. 35-42.

26 "ARINC-429 Reference Manual Version 2.0, " *SBS Technologies Incorporated*, 1998.

28 Van de Vegte, J., *Feedback Control Systems*, Prentice Hall, New Jersy, 1994, pp. 97-146.

29 Sciavicco, L.; Siciliano, B, *Modeling and Control of Robot Manipulators*, McGraw-Hill, New York, 1996, pp. 169-96.

27 Coyle, S., *The Art and Science of Flying Helicopters*, Iowa State University Press, Iowa, 1997.

30 Egerton, P.A.; Hall, W.S., *Computer Graphics: Mathematical First Steps*, Prentice Hall, Toronto, 1998, pp. 174-6.

31 Klafter, R.D. et al., *Robotic Engineering: An Integrated Approach*, Prentice Hall, New Jersey, 1989, pp. 571-6.

32 Craig, J.J., *Introduction to Robotics: Mechanics and Control*, Addison-Wesley, Don Mills, Ontario, 1989, pp. 227-46.

33 Andersson, R.L., *A Robot Ping-Pong Player: Experiment in Real-Time Intelligent Control*, IT Press, Massachusetts, 1988, pp. 87-94.

34 Mujtaba, M.S., "Discussion of Trajectory Calculation Methods," in *Exploratory study of computer integrated assembly systems*, Binford T.O. et al., Stanford University Artificial Intelligence Laboratory, AIM 285.4, 1977.

35 Parkin, R.E., *Applied Robotic Analysis*, Prentice Hall, New Jersey, 1991, pp. 242-4.

36 Wilson, C.E.; Sadler, J.P., *Kinematics and Dynamics of Machinery*, Harper Collins, New York, 1993, pp. 341-4.

37 Brady, M. et al., *Robot Motion: Planning and Control*, MIT Press, Massachusetts, 1983, pp. 221-30

38 Kreyszig, E, *Advanced Engineering Mathematics Ed. 7*, Wiley and Sons, 1993, pp. 803.

39 Lewis F.L., *Applied Optimal Control and Estimation*, Prentice-Hall, New Jersey, 1992, pp. 1-19.

40 Bennett, S. "Development of the PID Controller," *IEEE Control Systems*, Vol. 13, No. 5, 1993, pp. 58-65.

41 Schwarzenbach, J.; Gill, K.F., *System Modeling and Control*, Edward Arnold, London, 1979, pp. 171-81.

42 http://www.engin.umich.edu/group/ctm/PID/PID.html

43 Foster, K., *An Introductory Guide to the Control of Machinery*, Professional Engineering Publishing Limited, London, 1998, pp. 167-9.

44 Nice, N.S., *Control Systems Engineering 2nd Ed.*, Benjamin Cummings, California, 1995, pp. 459.

45 Newman, S., *The Foundations of Helicopter Flight*, Wiley and Sons, London, 1994.

46 Fay, J., *The Helicopter: History, Piloting, and How it Flies*, David and Charles, Vermont, 1976.

47 Conversation with Keith S. Monk, Senior Systems Engineer, Bombardier Services: Defense.

48 Tierno, J.E. et al., "Numerically efficient Robustness Analysis of Tracking for Nonlinear Systems," *Journal of Guidance, Control, and Dynamics*, Vol. 20, No. 4, 1997, pp. 640-7.

49 http://www.cmtinc.com (Introduction to GPS)

50 http://www.avweb.com/toc/avionics.html (GPS Explained)

Appendix A : GPS Background

The global positioning system (GPS) is a location system based on a constellation of 24 satellites orbiting the Earth at altitudes of approximately 17,500 km (10,900 mi.). GPS was developed by the United States Department of Defense (DOD), for its tremendous application as a military locating utility. The DOD's investment in GPS is immense. Billions and billions of dollars have been invested in creating this technology for military use. However, over the past several years, GPS has proven to be a useful tool for non-military applications as well.

GPS satellites are orbiting high enough to avoid the problems associated with land based systems, yet can provide accurate positioning 24 hours a day, anywhere in the world. Uncorrected positions determined from satellite signals produce accuracy in the range of 50 m to 100 m. When using a techniques called differential calculation, users can positions accurate to within 5 meters or less.

In a nutshell, GPS is based on satellite ranging – calculating the distances between the receiver and 3 or more satellites (4 if elevation is desired) and then using mathematics to calculate the position. Assuming the position of the satellites is known, the location of the receiver can be calculated by determining the distance from each of the satellites to the receiver. GPS takes these 3 or more known references and distances and "triangulates" an additional position.

The DOD can predict the paths of the satellites vs. time with great accuracy. Therefore, the orbits and thus the locations of the satellites are known in advance. Today's GPS receivers store this orbit information for all the GPS satellites in what is

known as an almanac. Each GPS satellite continuously broadcasts the almanac. GPS receivers will automatically collect this information and store it for future reference.

The DOD constantly monitors the orbit of the satellites looking for deviations from predicted values. Any deviations (caused by natural atmospheric phenomenon such as gravity), are known as ephemeris errors. When ephemeris errors are determined to exist for a satellite, the errors are sent back up to the satellite, which in turn broadcasts the errors as part of the standard message, supplying this information to the GPS receivers.

GPS determines distance between a GPS satellite and a GPS receiver by measuring the amount of time it takes a radio signal (the GPS signal) to travel from the satellite to the receiver. Radio waves travel at the speed of light, which is about 300,000 $^{km}/_{s}$ (186,000 $^{mi}/_{s}$). So if the amount of time it takes for the signal to travel from the satellite to the receiver is known, the distance from the satellite to the receiver can be determined. If the exact time when the signal was transmitted and the exact time when it was received are known, the signal's travel time can be determined.

In order to do this, the satellites and the receivers use very accurate clocks which are synchronized so that they generate the same code at the same time. The magnitude of accuracy which is being referred to is such that an average GPS atomic frequency standard has to maintain frequency of ±1second over 30,000 years and all satellites are synchronized to within 176 nanoseconds of UTC. The code received from the satellite can be compared with the code generated by the receiver. By comparing the codes, the time difference between when the satellite generated the code and when the receiver generated the code can be determined. This interval is the travel time of the code.

Multiplying this travel time, in seconds by 300,000 $^{km}/_{s}$ gives the distance from the receiver position to the satellite in kilometers. So if a satellite was located directly above a receiver, the time required for the signal to travel from the satellite to the receiver would be $^{1}/_{17}^{th}$ of a second. This would mean that an error of a mere $^{1}/_{1000}^{th}$ of a second would result in a 290 km deviation.

Receiver clocks are not of atomic quality (cesium) so a way around that was to develop receiver clocks that are consistently accurate over relatively short periods of time so long as they're reset often. Though only 3 satellites are required to determine a position, a fourth is used to validate this value calculated using the other 3 satellites. If the fourth line of position doesn't pass through the other three, the receiver knows something is wrong. It is geometrically impossible for four intersecting spheres to merge at the same point unless the clock is exact. If the fourth doesn't match with the other three, the receiver's internal clock is assumed out of sync with the satellites. The receiver then runs a simple routine to adjust the clock until all four lines of position intersect at the same point. This is known as correcting clock bias and it's how the receiver resets its clock.

The GPS system has been designed to be as accurate as possible. However, there are still errors. These originate from atmospheric conditions, inaccuracies in satellite orbital position, and signal reflection, amongst others.

A technique called differential correction (DGPS) is necessary to get accuracy within 1-5m, or even better with advanced equipment. Differential correction requires a second GPS receiver, a base station, collecting data at a stationary position on a precisely known point. Because the physical location of the base station is known, a correction

factor can be computed by comparing the known location with the GPS location determined by using the satellites.

The differential correction process takes this correction factor and applies it to the GPS data collected by a GPS receiver in the field. Differential correction eliminates most of the errors found in GPS.

References:

http://www.cmtinc.com (Introduction to GPS)

http://www.avweb.com/toc/avionics.html (GPS Explained)

Appendix B : Transformations

With the ideal system and its base method of implementation known, it must be explained how the craft will be located within the given system. One method is to evaluate the UAV position against that of the Cartesian system by calculating the equations for the three planes in space and calculating the UAV position amongst them. However an opportunity arises when a Cartesian system is being used to describe the ideal system. This is because the inertial coordinate system being used is also Cartesian (north, east, and height). By manipulating the ideal system originating at the RP to the origin of the ground based system, equations for pin-pointing the craft within the RP based system will be extremely simple. The manipulations required to produce these results are described by homogeneous matrix transformations. Transformations are well documented, so only a brief description will follow.

Transformations are matrix operations performed on homogeneous coordinates. Homogeneous coordinates represent a coordinate being described with four terms instead of the traditional three terms. The fourth term is designated the scaling term. For this application, no scaling will be required, but the matrix operations which follow demand that that the fourth term be present. Therefore a coordinate that was given as *eqn. A.1* would be written as *eqn. A.2* in its homogeneous form.

$$q = (x, y, z) \qquad (A.1)$$

$$Q = \begin{bmatrix} x & y & z & 1 \end{bmatrix} \qquad (A.2)$$

Translation of coordinates is a simple task. It changes the position of a point by adding or subtracting values from the original coordinate. Contrary to the nature of addition or subtraction, the operation is performed via matrix multiplication. This is the importance of the homogeneous coordinate configuration. Both coordinate summation and multiplication actions are performed by matrix multiplication if a coordinate of this form is used. Imagine that the coordinate q was to be relocated to by the displacement vector defined by q' (*eqn. A.3*). The transformation matrix describing the translation would take on the form of *eqn A.4*. Thus *eqn. A.5* is the transformed coordinate in the homogeneous form.

$$q' = (x', y', z') \tag{A.3}$$

$$T(x', y', z') = \begin{bmatrix} 1 & 0 & 0 & 0 \\ 0 & 1 & 0 & 0 \\ 0 & 0 & 1 & 0 \\ x' & y' & z' & 1 \end{bmatrix} \tag{A.4}$$

$$QT = \begin{bmatrix} x + x' & y + y' & z + z' & 1 \end{bmatrix} \tag{A.5}$$

The next series of transformations are rotations. With these rotations and the previously described method of translation, a point or any number of points can be reoriented anywhere in space. All the rotations are of similar form though each is specific to a rotation about a given axis. For example the rotation described by *eqn. A.6* describes a rotation of angle ψ about the x-axis. The transformation matrices about the three axes are as shown below (*eqns. A.6-A.8*). It is important to note that the positive

direction of rotation corresponds to the right hand rule. For more detailed description of this topic, see reference.

$$R_x^\theta = \begin{bmatrix} 1 & 0 & 0 & 0 \\ 0 & \cos\psi & \sin\psi & 0 \\ 0 & -\sin\psi & \cos\psi & 0 \\ 0 & 0 & 0 & 1 \end{bmatrix} \qquad (A.6)$$

$$R_y^\theta = \begin{bmatrix} \cos\psi & 0 & -\sin\psi & 0 \\ 0 & 1 & 0 & 0 \\ \sin\psi & 0 & \cos\psi & 0 \\ 0 & 0 & 0 & 1 \end{bmatrix} \qquad (A.7)$$

$$R_z^\theta = \begin{bmatrix} \cos\psi & \sin\psi & 0 & 0 \\ -\sin\psi & \cos\psi & 0 & 0 \\ 0 & 0 & 1 & 0 \\ 0 & 0 & 0 & 1 \end{bmatrix} \qquad (A.8)$$

A Cartesian based system has been chosen to represent the foundation for the ideal quadrant system. Reasons for using the Cartesian system, even though it didn't exactly replicate the ideal system, range from ease of use to the fact that it corresponded exactly to that of the inertial reference frame. The latter reason allows for the use of homogeneous matrix transformations to determine craft location within the RP centered system.

References:

Egerton, P.A.; Hall, W.S., *Computer Graphics: Mathematical First Steps*, Prentice Hall, Toronto, 1998.

Klafter, R.D. et al., *Robotic Engineering: An Integrated Approach*, Prentice Hall, New Jersey, 1989.